University of Southern Queensland

Faculty of Health, Engineering and Sciences

Determining the Effectiveness of Vortex Generators with regards to Automotive Applications

A dissertation submitted by

Luke Greenbank

In fulfilment of the requirements of

ENG4111 and 4112 Research Project

towards the degree of

Bachelor of Engineering (Honours) - Mechanical

Submitted October, 2019

Abstract

Engineers are continuously looking at ways of redesigning vehicles to reduce aerodynamic drag as this is the major contributor to the total resistive force at highway speeds. Any reduction in the drag coefficient of a vehicle will improve the fuel economy for a standard commuter car and increase the top speed of a performance car. In the past, vortex generators have been investigated for use on aircraft with once classified studies dating back to the 1950's, however since this time there has been infrequent testing on vehicles.

In 2004, Mitsubishi released the Lancer Evolution 8 MR, amongst numerous performance upgrades it included vortex generators into the design (in the form of a row attached to the trailing edge of the roofline). Not only was this a bold statement fifteen years ago, but there has only been one other vehicle since this time (released in 2017) to include these devices from the factory. The press release stated that the inclusion of vortex generators was an innovation in aerodynamics technology. However, there was no quantifiable data included to go along with these claims. This study investigates the question of whether vortex generators can reduce aerodynamic drag of a vehicle and whether lift forces are impacted as well.

This research project included experimental and computational data collection. The experiments were separated into full-scale and small-scale testing. For the full-scale tests a row of vortex generators was positioned on the trailing edge of roofline of a test vehicle that also had a multitude of twine pieces attached all over the rear windscreen. Three speeds were tested, up to and including 100 km/h in an attempt to gain a variety of data. It was discovered that due to the high aerodynamic efficiency of the test vehicle the boundary layer did not noticeably separate from the surface, even in the control test where no vortex generators were installed. Therefore, this made identifying benefits of the vortex generators difficult. An additional test was undertaken where the devices were setup at a 25° incident angle to the oncoming airflow, based on a previous study that stated this angle was the most effective. However, for this situation there was no discernible difference from the original tests and it did not reveal any supplementary information that could be discussed.

The small-scale tests used 1:24 models in the wind tunnel to calculate the impact 3D printed vortex generators had on the drag and lift forces. It was discovered that drag slightly increased along with a decrease in lift. The reasoning behind this was due to the fact the scaled vortex generators were 1:12, which essentially made them twice the size of the original design for the vehicle. Due to 3D printing and handling limitations a matching scale was not practicable in this instance. From research compiled in the literature review it was discovered that there is an optimum height of the device, relating to the boundary layer thickness and if this is exceeded the form drag created outweighs the drag reduction

of the devices. This creates a situation where they become redundant and lead to greater drag forces and inefficiencies. Smoke visualisation was attempted via a machine but due to the relatively small size of the model any flow characteristics around the shape were not explicit in detail.

Computational fluid dynamics (CFD) software was used to collect the quantifiable data. The scale vehicle with and without vortex generators was tested over a range of scenarios involving airspeeds up to 50 m/s. From the initial low airspeeds it was found that there was a reduction in drag force for the model that had vortex generators and this trend continued throughout all data points up until the maximum airspeed, where this reduction reached 15%. Vector, contour and streamline plots were used in the study to visualise the air flow around the vehicle. These images added additional depth to the study along with the raw data that the wind tunnel smoke visualisation failed to provide. However, upon analysis the findings were not conclusive by way of displaying the benefits compared to the control tests.

This study relied on complex and highly detailed 3D models. It would not be recommended for future investigations to include 3D scanning into the process, as to help reduce the quantity of geometry errors encountered. Another consideration would be the scaling of the vehicle in the tests. As this differs from a full-sized vehicle the results can only be an indication and not conclusive in the findings.

In theory, vortex generators can reduce aerodynamic drag of a vehicle but ascertaining conclusive results via experimentation can be challenging. From the research completed it is likely that vortex generators need to be specifically designed for each application to determine the parameters leading to the greatest reduction in drag, thereby the optimal design. Aspects such as vortex generator height relative to boundary layer thickness, the positioning relative to each other, the quantity used and the shape of the device are to be studied. Mainstream adoption may not be viable due to the additional research and development (R&D) costs. Also, factors such as the effect on aesthetic appeal for a standard commuter car will need to be considered.

University of Southern Queensland

Faculty of Health, Engineering and Sciences

ENG4111 & ENG4112 Research Project

Limitations of Use

Certification of dissertation

I certify that the ideas, designs and experimental work, results, analyses and conclusions set out in this dissertation are entirely my own effort, except where otherwise indicated and acknowledged.

I further certify that the work is original and has not been previously submitted for assessment in any other course or institution, except where specifically stated.

Luke Greenbank

Student Number: [redacted]

[redacted]

____

Signature

[redacted]

____

Date

Acknowledgements

I would like to extend an acknowledgement to my supervisor, Dr Ahmad Sharifian-Barforoush for his patience in answering all my questions and help guiding me along my research path. The staff at the University of Southern Queensland (USQ) were very generous with their time and helped facilitate the efforts of my research project. It was much appreciated to be able to use the new wind tunnel in the hydraulics laboratory that is generally out of reach for undergraduate students. In no particular order I would also like to thank:

Stephanie Piper: for help with the three-dimensional (3D) scanning equipment and numerous suggestions relating to 3D mesh refinement via third-party software.

Dr Khalid Saleh: for the recorded lectures from USQ course MEC5100 – Computational Fluid Dynamics that taught me the basics of the ANSYS Fluent software. Also, for the suggested library text books regarding boundary layer effects on a scale model in a wind tunnel.

Mohan Trada: for help with understanding the basics of the TecQuipment AF1300 subsonic wind tunnel, the correct setup and what data could be collected from the electronic components.

Terry Byrne: for 3D printing of the 1:6 scale vortex generators and general suggestions on how to achieve the highest possible quality at small scales.

Adrian Blokland: for help with the revised 3D printing of the 1:12 scale vortex generators.

Brian Aston & Oliver Kinder: for the workshop fabrication that went into creating the rig to support the scale models in the wind tunnel.

Brian Lenske: for help with the smoke machine and technical information required for the propylene glycol procurement.

Finally I would like to extend my appreciation towards the USQ Residential Colleges for the 2019 Research Prize that helped facilitate my research and provided money for additional supplies.

Table of Contents

List of Figures

List of Tables

Table of Nomenclature

The following abbreviated terms have been throughout this dissertation

CPU	Central Processing Unit
C_D	Coefficient of drag
C_L	Coefficient of lift
CFD	Computational Fluid Dynamics
CAD	Computer Aided Design
CPD	Continuing Professional Development
F_D	Drag force
FPS	Frames per second
F_L	Lift force
MB	Megabyte
R&D	Research and Development
RMP	Risk Management Plan
SDS	Safety Data Sheet

Chapter 1: Introduction

1.1 Context

In 2004, Mitsubishi released a special edition of the Lancer Evolution (Evo) 8, entitled MR. This was the first car to include mainstream use of vortex generators. The press release stated that these devices were an innovation in aerodynamics technology. It was offered as a dealer-fitted accessory and created small vortices at the trailing end of the roof that helped to reduce drag and increase downforce generated by the rear-deck spoiler (Mitsubishi Motors 2004). There was however no quantifiable data included in the press release to go along with these claims and therefore has the potential to be a marketing gimmick. My research project will attempt to generate this missing data and answer the question of whether vortex generators positioned at the trailing end of the roof can result in a reduction in aerodynamic drag along with increasing the downforce generated by the rear wing.

Figure 1.1: Mitsubishi Lancer Evolution 8 MR (Mitsubishi Motors 2004)

Figure 1.2: Vortex generators along the trailing edge of the roof
(CT Auto Parts 2018)

1.2 Research Aim and Objectives

The intent of this research was to determine the effectiveness of vortex generators with regards to automotive applications. This will include investigating topics that relate to fluid flow, namely aerodynamics. It will focus on vortex generators as aerodynamic devices that can be used to induce vortices that help to delay the local boundary layer flow separation from the downward surface that the fluid is travelling along. The objectives of my study are to help ascertain via research:

- Background information relating to fluid mechanics, subsonic aerodynamics, lift and drag coefficients, boundary layer separation and vortices.
- What literature has been previously compiled that relates to the use of vortex generators on vehicles.
- How vortex generators alter airflow characteristics downstream of their positioning and whether it is beneficial via research, experiments and computational analysis.
- Full-scale and small-scale experiments that provide analysable data or visualise the airflow around the vehicle.
- CFD analysis that obtains quantifiable data to indicate whether there is a reduction in drag or lift forces on a vehicle fitted with vortex generators compared to the control.
- The most appropriate design of a vortex generator for a vehicle based on research and CFD studies.

1.3 Purpose of this Study

The motive for this study lies in ascertaining whether vortex generators used on cars can make a viable reduction in aerodynamic drag. This investigation mostly focuses on performance car aspects. In essence, reducing the lift at the rear section of the car can lead to better weight distribution whilst cornering and higher velocities can be achieved.

Not only are aerodynamics important for performance car applications but as engineers are constantly looking at ways to redesign cars in order to decrease drag, there is an untapped mainstream potential to be had as well. A reduction in the drag coefficient would lead to higher efficiencies and therefore lower fuel consumption.

The findings aim to determine the optimum vortex generator design that could also be implemented on mainstream cars to increase fuel economy. Which is the result of reducing the volume of turbulent air behind the car and therefore drag. It may be that vortex generators are a gimmick and have no place in vehicle design. This would be a similarly successful study as it concludes one way or the other. This study will not be life-changing or revolutionary. Nor does it aim to be. It merely investigates a topic of interest that has a solid foundation and can be the stepping stone for future studies.

There is however a potential business case for the inclusion of a product that reduces fuel economy. Many large automotive corporations have sustainability strategies that focus on decreasing the reliance on fossil fuels and this includes the fuel consumption of their model line-up. Prospectus new car buyers consider the fuel economy of a vehicle on a similar level to reliability and safety. The more fuel efficient the vehicle, the more appealing it becomes.

1.4 Ethical Concerns

Ethical standards are critical for all forms of research. They prevent false or misleading data from being published and encourage the truth to be shown in the research. The importance of ethics has spread to encompass many mission statements of well-known businesses. Some professional associations have adopted codes and policies that are used to reference the quality and sustainability of the work performed (Grand Canyon University).

Sustainability has become an ever more popular noun in the 21st century due to the wide-spread concern relating to the environment and increasing accountability for the actions of an individual and companies alike. Engineers Australia code of ethics make mention of sustainability as one of their core beliefs. This ensures that all engineering works practised incorporate an aspect that considers the health of the community and the environment.

A common theme of the prior 30 years is the ever-increasing gasoline efficiency of new vehicles. For example, over this time, the average fuel economy of a standard vehicle, automatic 4-cylinder Toyota Camry has gone from 21 miles per gallon (MPG) (11.2 L/100 km) in 1989 to 34 MPG (6.9 L/100 km) in 2019. This alone is a decrease of 61.8% fuel use and does not take into account the hybrid variants available at present. Also for reference the greenhouse gas emissions from the tailpipe of both vehicles is 423 g and 264 g respectively per mile (1.61 km) (United States Department of Energy 2018).

Every manufacturer aims to produce vehicles that have less of an environmental footprint with a decrease in emissions. With the rise of alternative renewable power sources along with electric vehicles the reliance on fossil fuels will become less frequent. As petrol prices steadily increase with time, it becomes advantageous to have a more fuel-efficient vehicle, which is sought after by the general public. Automotive engineers look for innovations to achieve this. Even small improvements in aerodynamics can have a significant impact on the power output required to reach or maintain a similar velocity.

This research investigates whether vortex generators have a benefit when positioned on the roofline of a car. If the findings ascertain that these aerodynamics devices alter the airflow over the car's rear section and lead to a reduction in drag then this will result in a decrease in fuel usage.

1.5 Dissertation Outline

This dissertation was intended to be structured in an orderly and easy to follow way. With progressive sections that where complete but flowed into the next. The focus of each of chapter is detailed below:

Chapter 1: Introduction - Presents the broad overview of the dissertation. It provides the basis of the study, identifies the gap in current research and why an investigation into this topic is required.

Chapter 2: Background Information – The vehicle selection of which the study is based on is explained, along with identifying the scale model to be used in the experiments. Supplementary background information on the topics of fluid mechanics and subsonic aerodynamics are included to provide the reader with some basic knowledge on the topic areas that are to follow in the succeeding chapter.

Chapter 3: Literature Review – An extensive look into the science of vortex generators, what their uses are and where they have been used in the past. Additional topics such as wind tunnel conditions, concerns of scale models, flow visualisation, boundary layer separation and control, along with lift and downforce are studied.

Chapter 4: Research Methodology – Details the experiments of this research project. As this project is not purely a desktop study each of the three experimental aspects are explained along with the methodology. The data collection phase of this research project will include two distinct elements experimental and computational.

Chapter 5: Results and Analysis - The results from each of the experimental and computational tests are provided in this chapter, along with an analysis into the findings and comments as to whether they are indicative or conclusive.

Chapter 6: Discussion - A detailed discussion into what was found and what could have been improved is detailed along with how this correlates with the findings of the literature review. A comparison to the original plan and how the results could be used by the industry or extended upon in further studies is included.

Chapter 7: Conclusion - The concluding chapter to this dissertation wraps up the major discoveries from the study into a concise yet detailed page.

Chapter 2: Background Information

2.1 Selection of performance car for study

The aforementioned Mitsubishi Lancer Evolution 8 MR was the basis for the study of vortex generators as this vehicle came with them from the factory (if optioned at the dealer). However, over the years several other performance cars have adopted vortex generators into their aftermarket options; mostly to increase the aesthetic appeal.

The relative sizing of the wind tunnel made the procurement of a model vehicle restricted to a maximum scale factor of 1:24. It was difficult to source a 2004 Evo 8 MR as it was by now an old vehicle and becoming more of a collector's car than a readily available design. Unfortunately, it was out of my grasp in order to attain this vehicle's scale model. This however made it more practical to allow the tests to include vortex generators of my own 3D printed design and not to be limited to the original design shape.

The next best vehicle that could match the Evo was its natural rival, the Subaru Impreza WRX STI. It competed alongside the Evo for many seasons of the World Rally Championship and even to this day is seen as its competitor. The external dimensions are very close with similar design philosophies of four doors, traditional sedan styling and a large rear wing. The specifications are compared in Table 2.1 to show the compatibility of the test model.

Table 2.1: Comparison of the dimensions of each vehicle (Motor Trend 2004)

Dimensions	2005 Lancer Evolution 8	2005 Subaru Impreza WRX STI	Difference to Evolution 8
Overall Length	4490 mm	4465 mm	-25 mm
Height	1450 mm	1440 mm	-10 mm
Width	1770 mm	1740 mm	-30 mm
Wheelbase	2625 mm	2525 mm	-100 mm
Kerb Weight	1470 kg	1495 kg	+25 kg

Figure 2.1: Comparison of Evo (left) and STI (right)
(Motor Trend 2004)

It can be seen in Figures 2.1 and 2.2 that the side profile of both cars is very similar and therefore the coefficient of drag and aerodynamic characteristics will also be alike. This means by using a scale model of either car the results should theoretically be directly correlatable.

Figure 2.2: Side profile of Evo (top) and STI (bottom)
(Motor Trend 2004)

There are a few minor differences in the profile of each car. Namely the location of the radio antenna on the Evo (positioned on the rear section of the roof) and the presence of a hood scoop on the STI (to direct air into the top-mount intercooler). For this study these features can be overlooked as the focus of this investigation will be on the rear section of the roof and adjacent area including the rear windscreen, boot and wing. Also, the scale model to be used in the experiments does not feature an antenna to alter the airflow characteristics.

If there was a major difference in the angle from the roofline to the rear windscreen then it would pose an issue as the resulting airflow would not be comparable, such as studying both a hatchback and a coupe. Figure 2.3 below visually indicates the angle from the roofline to the boot along the rear windscreen. As there were no examples of each vehicle available a rough estimate was taken from photos sourced online. It can be seen that the angle is 27° for the Evo and 26° for the STI.

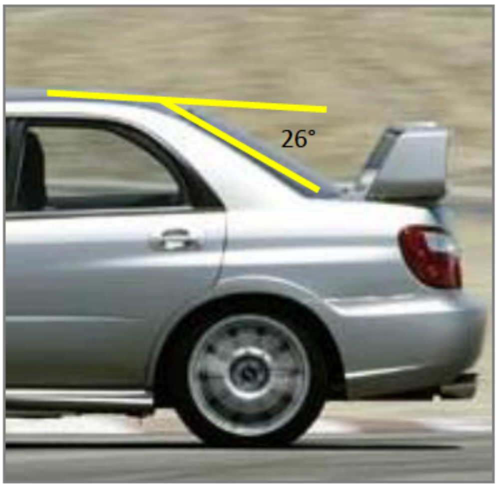

Figure 2.3: Rough indication of the angle for the sloping section of both sedans

2.2 Scale model sourced for the experiments

This scale model for use in the wind tunnel experiments was purchased from Supercheap Auto and is manufactured by Welly, a company who specialises in die-cast car models. The product is licensed by Subaru and is a very accurate recreation of the real vehicle. This model purchased was the aftermarket variant as it featured a large rear wing. The scale of the vehicle is 1:24.

Figure 2.4: 1:24 scale model used for wind tunnel experiments

2.3 Fluid mechanics

Fluid mechanics is the study of all fluids, either in static or dynamic situations. This branch of physics deals with the relationship between the forces, motions and conditions of a continuous material (Bar-Meir 2013). The significance of this science is how it defines fluid flow around a body and the perceived stability of that flow. Unsteady flow or turbulent in nature can have an impact of the resulting drag forces experienced by a moving vehicle. Viscosity is a key property of any fluid as it controls the rate of motion in response to applied forces. This in turn provides a link between load cases and the velocity distribution within the fluid (Evans 2012). These topics are of interest for this study as the relation of airflow to vehicle aerodynamics at varying speeds will be analysed.

2.4 Aerodynamics

Aerodynamics is defined as a sub-branch of fluid mechanics. It deals with the motion of air and the forces acting on the bodies as they pass through the fluid. It aims to explain the fundamentals that govern the flight of planes. Not only can it help to identify the principles of flight, but it can also be utilised within automobile design, or for ships and trains as they are moving through a fluid at high velocity. Even static objects such as large bridges or buildings need to be analysed due to their exposure to high wind speeds (Encyclopædia Britannica 1998). The forces that act on a body during motion are lift, weight (gravity), thrust and drag. Typically these are overlaid on an image of an airfoil but as this research focuses on automobiles the relevant forces are shown on a street car. Note the direction of motion is implied to be to the left.

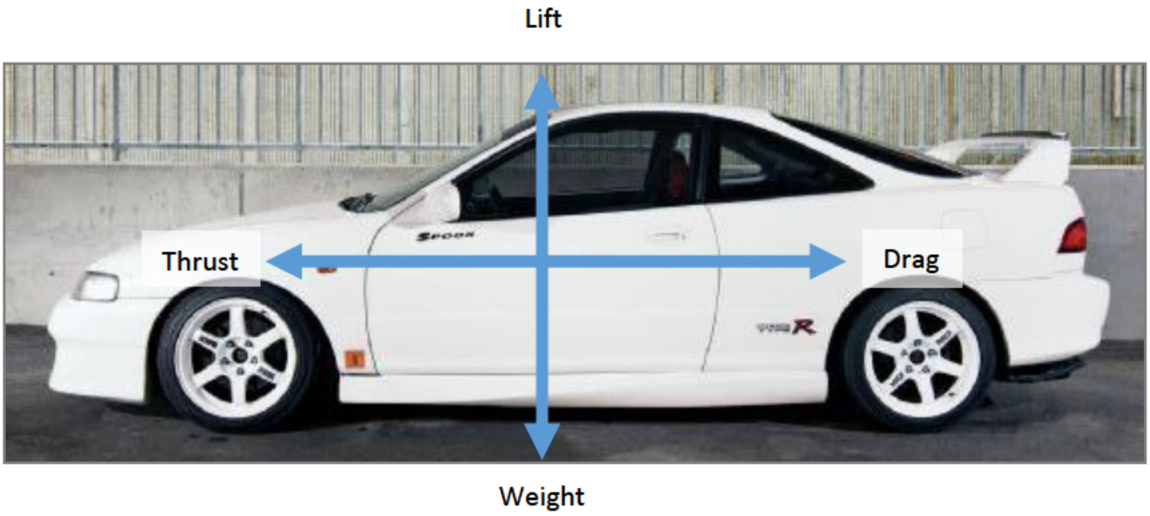

Figure 2.5: The aerodynamic forces on a car (Klingelhoefer 2011).

Aerodynamics are of interest for many aspects of vehicle operation. These include but are not limited to:

- Performance – Top speed, acceleration, fuel economy.
- Cooling – Engine, brakes, air conditioning (AC) condenser.
- Comfort – Wind noise, ventilation.
- Stability – Cross wind sensitivity, directional air flow (Solmaz 2018).

For the purpose of this study the focus will be on the force components of lift and drag as they contribute to the major findings of this study. The thrust contributes to both lift and drag as increasing the airflow velocity increases the forces exerted on the body. The weight of the car does not alter how much lift or drag is created, whereas its shape and size does.

2.5 Computational Fluid Dynamics

CFD is defined as a set of numerical methods used to approximate solutions of problems for fluid dynamics and heat transfer. The science of fluid flow along with heat and mass flow, feature an approach to describe the physical properties in a differing manner when compared to conventional methods. Bulk properties such as momentum, energy or entropy of a system are analysed with a focus on distributed properties. This can therefore ascertain entire fields such as temperature, velocity or density throughout or around an object. Even when integral forms are the final goal of analysis it can be derived from distributed fields. This method includes features that allow for internal processes of a fluid flow such as motion, rotation or deformation to be solved; creating a thorough analysis.

In general, there are three approaches to solve fluid flow problems, theoretical, experimental or numerical. The latter is used for CFD and makes use of high-level computing power to find a solution to complex questions. Almost any fluid flow can be described as a set of partial differential equations. Numerical methods used via a computational approach to solve problems surpasses the methods of analytical and experimental due to the aspects of flexibility, accuracy, cost and the universal nature of the study (Zikanov 2010).

CFD can be used to replace or supplement wind tunnel testing. It has several benefits over conventional methods including:

- Able to plot the flow path in and around the entire vehicle,
- Simulating non-linear flows, which is important for studying the cornering of vehicles as they travel in a circular path along with the air flow,
- Reliability of testing as it uses computer-based technology and there is no physical mechanical equipment that could fail,
- Optimisation techniques are easier to implement using feedback-controlled coding,
- CFD and Finite Element Analysis (FEA) software packages can operate in parallel, providing an in-depth look at the forces present on a vehicle,
- Cost effective solution and relatively quick method of testing depending on the problem (Aero Performance Engineering 2010).

One of the main benefits of CFD is the ability to revise designs and test multiple scenarios with ease.

Chapter 3: Literature Review

3.1 Airflow characteristics

3.1.1 Laminar and turbulent flow

Airflow can be defined as either laminar or turbulent. The segregation between these variants relates to the Osbourne Reynolds experiment in 1883. He visualised the flow within a tube by the help of introducing a dye at the entrance of the tube. At low velocities it was seen that the flow formed a thin straight thread flowing parallel to the tube's length. As the airspeed was slowly increased it was found that the flow changed character. Instead of the smooth flow it become frantic and the dye spread over the entire tube (Panaras 2012, p.13).

The transition from laminar to turbulent flow occurs over time as the streamlines flowing near of the edges of the body are offset by the wake of the flow at a distance. This transition is dependent on several variables such as surface roughness, flow velocity, geometry and viscosity of the fluid (Jonuskaite 2017, p.11). Turbulent flows are common and occur frequently around us in everyday life. Some common examples include internal combustion engine cylinder flow, the wakes behind moving vehicles or coffee flow in a cup. These flows are generated by different mechanisms but have one feature in common, the Reynolds number (Zikanov 2010). It is a ratio of inertia to viscous shear forces and distinguishes situations where viscous forces dominate (small Re) or momentum forces dominate (high Re). The generally adopted formula is:

$$Re = \frac{\rho D V}{\mu} \tag{1.1}$$

Where ρ = density of fluid (SI units: kg/m^3)

D = diameter or characteristic length of the geometry (m)

V = velocity of the free-stream fluid (m/s)

μ = dynamic viscosity (m^2/s)

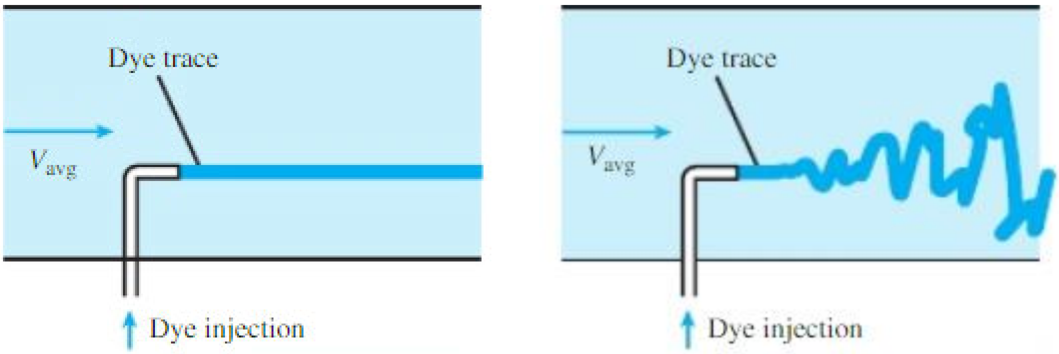

Figure 3.1: Laminar Flow (left) vs Turbulent Flow (right)
(Cengel & Ghajar 2015)

This dimensionless quantity is important in the classification of fluid flows. It helps to predict whether a particular flow is laminar or turbulent and determines the flow regime. At large Reynolds numbers, the inertia forces are much greater than the viscous forces and therefore the latter cannot prevent the random fluctuations of the fluid; leading to turbulent flow. There is a critical value of the Reynolds number that indicates this phenomenon and is aptly called the critical Reynolds number. Written as Re_{cr} this value differs for varying geometries and flow conditions. For the internal flow in a circular pipe the generally accepted values are:

- Laminar flow when Re ≤ 2300,
- Transitional flow when 2300 ≤ Re 4000,
- Turbulent flow when Re ≥ 4000 (Jonuskaite 2017, p.12).

This indicates a Re_{cr} = 2300. For the case of a flat plate or circular cylinder/sphere the commonly accepted values are 500 000 and 200 000 respectively; i.e. the boundary layer remains laminar up until this value. The general form equation can be written as:

$$Re_{cr} = \frac{\rho \, V \, x_{cr}}{\mu} \tag{1.2}$$

Note that x_{cr} is the distance from the leading edge of the plate at which the laminar to turbulent flow instigates (Cengel & Ghajar 2015). The airflow over a vehicle can undergo the same phenomenon by being laminar in one section and turbulent in others. The boundary layer thickness is a function of the Reynolds number. The above equation will be relevant when investigating the scale model in the wind tunnel.

3.1.2 Internal and external flow

Flows are classified based on the boundary conditions. The assumptions as to whether the flow has edges, walls or boundaries of a model. Internal flows are bounded by walls that induce friction and the flow velocity will reduce to zero upon contact, known as no-slip condition. A pipe containing a fluid is the most common example. External flows are ideally bounded by uniform external atmospheres at some distance away from the object. This could be a parachute, aerofoils, or wind load designs for buildings (Evans 2012). In general, a wind tunnel experiment creates an idealised environment of internal flow, however for my study as the cross sectional area is large enough to ensure the flow around the scale model will not be affected by the boundary layer, external flow will be assumed. Any internal flows such as through the engine compartment, air duct piping or past a diffuser are also characterised by dimensionless coefficients but will not be investigated in this research.

3.1.3 Incompressible and compressible flow

A fluid can be categorised as either incompressible or compressible based on a number of factors. If the fluid density differs significantly within the flow field it will be considered a compressible flow. Typically these variations can occur after the flow velocity exceeds Mach number 0.3 (Drela 2006, p.1). In general if the flow velocity is less than thirty percent of the speed of sound ($V < 0.3c$) it can then be treated as incompressible flow. At these velocities all testing is considered subsonic.

For a real world vehicle travelling on the road the air flow around the assembly would not exceed this value as 0.3 * 343 = 102.9 m/s = 370.44 km/h. There are only five production cars that can travel faster than this but for the purpose of this study the focus will be on speeds up to 180 km/h. Compressible flows become more complicated as they are governed by the ideal gas law, first and second laws of thermodynamics in addition to the conservation laws applicable to all fluids (Evans 2012). One area of interest for this study is how the air flows around the surface of a vehicle. This will be investigated as an incompressible flow and analysed in CFD.

3.2 Drag

When a solid object moves through a fluid it induces a mechanical force, called drag. This force is not generated similar to a gravitational or electromagnetic field but from a difference in velocity between a solid and a fluid. Drag can be considered as aerodynamic friction or air resistance. Therefore, drag only occurs to objects in motion. As drag is a force it is a vector quantity and has both a magnitude and direction. In general, drag acts in the direction to oppose motion (NASA 2015).

There are two components to this force, skin friction and form drag. Skin friction occurs because of the interaction between the solid object and the fluid. The level of resistance experienced relates to the properties of both entities. For example, a smooth surface produces less skin friction than a roughened surface. The viscosity of the fluid and its Reynolds number dictate the magnitude of forces that will be generated on the solid. The other component of drag relates to the shape of the object moving through the air. This is called form, or pressure drag. As air flows around a body the local pressure and velocities change which in turn creates a situation where pressure varies around the entire object (DOT 2012, p.2).

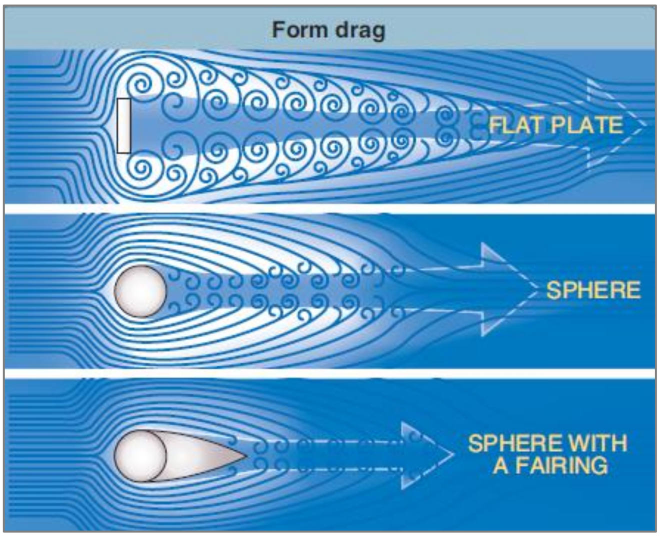

Figure 3.2: Visualisation of the form drag of various shapes. Note the benefit of reducing the frontal area via streamlining (DOT 2012, p.5)

The drag forces exerted by a fluid on a body are the combined effects of skin friction and form drag. For low Reynolds numbers ($Re < 10$) skin friction is the main factor in the total drag created whereas at higher Reynolds numbers ($Re > 5000$) form drag is the major contributor. The total drag coefficient can be found by adding both values (Cengel & Ghajar 2015).

3.2.1 Vehicular drag forces

Aerodynamic drag forces are of high attention due to making a significant proportion of the total resistance force whilst at highway speed. Lewington (2016, p.5) states that the resistive forces acting on a vehicle includes two components: aerodynamic drag and the tyre and chassis losses. The latter is constant and at low speeds contributes a large proportion of the total resistive force as aerodynamic drag is relatively low. However, as speeds increase the force required to overcome the aerodynamic component increases rapidly, and by 40 miles per hour (mi/h) (64.4 km/h) both forces are equal in magnitude. Above these speeds the aerodynamic component continues on an exponential trend and by 100 mi/h (160.9 km/h) it attributes close to 90% of the total resistance force. This of course, is dependent on the drag coefficient of the vehicle.

The aerodynamic drag force generated by a vehicle depends on a number of factors such as the:

- Air flow velocity,
- Frontal area and overall design shape that influences the flow on each side, undercarriage flow and amount of turbulent air behind the vehicle (wake),
- Coefficient of friction between the air and vehicle.

One study by Dumas (2008, p.2) found that the overall drag generated by a vehicle could be broken down into percentages based on the vehicle system. Table 3.1 displays the values that contribute to the overall drag coefficient number. However, these values will change with the design basis of the vehicle. It would be inaccurate to assume the upper surface of a Ford Ranger would have the same drag force as a streamlined Porsche 911. It is more of a baseline for a standard vehicle.

Table 3.1: Drag decomposition by major systems (Lewington 2016)

System	Percentage
Upper surface	40
Cooling	10
Lower surface	20
Tyres/wheel arches	30

At low Reynolds numbers most of the drag is created by the frictional component, especially on streamlined bodies. This friction drag is proportional to the surface area, meaning larger surfaces will experience a greater force. The form drag is proportional to the frontal area and the pressure differential between the front and back of the body. This leads to the understanding that blunt objects will experience a greater force than that of a streamlined one (Cengel & Ghajar 2015).

3.3 Lift

The forces experienced by a body are the same when it is moving through a fluid or if it is stationary and the fluid is flowing past. In both these cases the fluid will exert a tangential shear force on the body due to the no-slip condition brought about by the viscosity. The force that acts in the normal direction to the flow is known as lift. Technically speaking this interaction leads on a pressure differential between the upper and lower surfaces of the body. When the pressures are lower on the top surface than the underside it will create a situation whereby the body will want to move upwards to reach the area of lower pressure as this requires less energy (Cengel & Ghajar 2015). This concept forms the basis of how an airfoil generates positive lift. The most common place an airfoil is used is on the wings of an aeroplane.

However, for vehicles it is common to see designs by manufacturers that aim to reduce the lift generated as this can make for lateral instabilities at high speeds and cornering. It is possible to use an inverted wing design, such as a rear spoiler or wing to furthermore reduce the positive lift generated by the rear section of a vehicle. By introducing negative lift, known as downforce, this counteracts the positive lift and is very important to race car dynamics. Due to lift increasing with vehicle velocity it is possible to generate more negative than positive lift, yielding performance improvements (Katz 2006, p.27). Not only can these design changes be used on track cars, but mainstream street cars can benefit from an increase in high speed stability, especially if they are designed and driven in countries with unrestricted highways such as the German Autobahns.

3.3.1 Downforce

In a world of highly modified race cars such as Formula 1, it is possible that teams will compromise a mechanical system design in order to maximise the potential of aerodynamic performance. A vehicle with significant downforce can return faster track lap times, whilst maintaining a level of high-speed stability (Marchesin, Barbosa, Gadola, & Chindamo 2018, p. 1269-88).

Katz (2016, p.27) states that the overall performance of a race car depends on factors including engine, tyres, suspension and aerodynamics. However, in recent times the latter has gained increased attention due to the vast performance potential. An increase in aerodynamic force can lead to greater tyre adhesion on the road. Handling can be impacted by the level of downforce distribution between the front and rear, altering the stability and controllability of the vehicle. Over the past fifty years improvements to cornering have been largely attributed to aerodynamic downforce revisions. Figure 3.3 indicates these relative improvements in terms of lateral gravitational (g) forces.

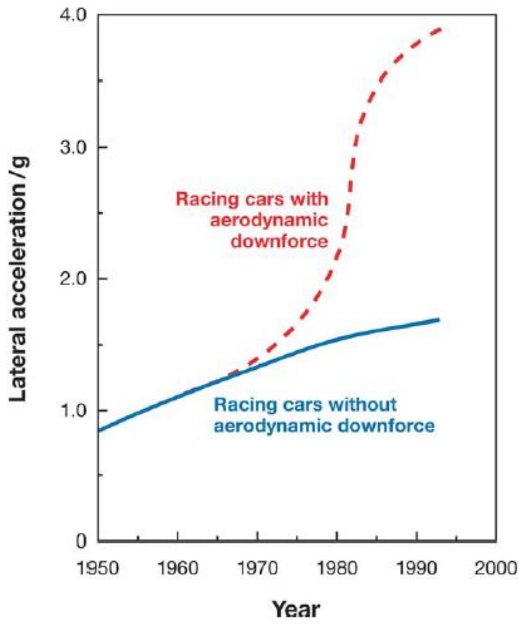

Figure 3.3: Improvements to cornering acceleration from aerodynamic revisions (Katz 2006, p.31).

An inverted airfoil is designed to provide a desired reaction force when in motion relative to the oncoming air. When used on a vehicle the large amounts of downforce can offset the positive lift and increase the amount of tyre grip available. This can result in much larger lateral grip and allow the vehicle to carry higher speeds through a corner and out of the exit. A higher velocity is critical to producing the lowest lap times especially when a corner accompanies a long straight. The amount of lift an airfoil can create is dependent on several factors including:

- Angle of attack, measured in degrees relative from the ground,
- Shape,
- Size,
- Position in the air stream (APR Performance, 2014).

It is this last factor that is of interest for this study. Free-stream airflow is less turbulent than the mixed air that normally encounters a vehicles rear wing when it is positioned below the roofline. If vortex generators help guide the free-stream airflow downwards it might contact the wing, making it more effective. Modern wings are designed based on CFD studies to find the most effective design, notably three-dimensional characteristics that allow for varying cross-sectional areas of the centre and outer sections. It is common to find high quality wings, produced by companies such as APR Performance or Voltex that feature outer sections that have a greater angle-of-attack than the centre portion. For example if the centre section is set at zero degrees, then the outer sections could be set at fifteen degrees, both with regards to the ground. This can be seen in Figure 3.4. The incorporation of both low and high angles of attack across the wing span allows for more downforce to be created when the wing is mounted below the roofline of the vehicle.

Figure 3.4: GTC-300 Adjustable Wing (APR Performance, 2014)

APR Performance (2014) detailed that the suitability of a rear wing changes with each vehicle application. Some racing categories have rules that must be followed to stay within the category. In general, from research it was seen that when height restrictions are enforced that limit the wing to below the roofline it was beneficial to use a three-dimensional airfoil. Whereas if there were no restrictions then a traditional two-dimensional airfoil could be used to intercept the free-stream airflow.

3.4 Vehicle coefficient of drag and lift

The total forces acting on a body whilst moving through a fluid consist of normal pressures and shear stresses acting on the surface. The force that acts parallel to the motion of the vehicle and 'free-stream' airflow is labelled as the drag force. Whereas the component that acts perpendicular is known as the lift force. These result in a value that defines a ratio of the predetermined drag or lift force to the total force produced by the dynamic pressure multiplied by the area. Both the dimensionless coefficients C_L and C_D relate to the fluid flow past a body such as an airfoil or a vehicle (Schlichting & Gersten 2017, p.8).

The coefficient of drag (C_D) for a vehicle is a dimensionless number that indicates the relative aerodynamic performance and shape efficiency. The higher the number, the more resistant the car is to move through the air. For example, a blunt body would tend to block the flow more than streamlined design and therefore acquire a larger drag coefficient. Typical C_D values for a car range from 0.25 – 0.40. Engineers design cars to have as low as C_D as possible; this improves general performance characteristics and fuel economy (Lewington 2016).

The coefficient of drag can be written as:

$$C_D = \frac{F_D}{\frac{1}{2}\rho V^2 A} \tag{1.3}$$

Where F_D = drag force, ρ = air density, A = cross sectional frontal area, V = velocity of the car/airflow

The coefficient of lift is very similar with the only difference being the drag force being replaced by the lift force:

$$C_L = \frac{F_L}{\frac{1}{2}\rho V^2 A} \tag{1.4}$$

These equations provide the major factors that engineers have to work with. It can be seen that the relative velocity of the air will dictate the magnitude of the drag that is created. As this value increases at a rate of the square of the velocity it indicates that substantial drag will be generated at high speeds of a vehicle. Lewington (2016) found that from speeds of 64 km/h the aerodynamic drag will contribute more than 50% of the overall resistive force. The other forces come from tyre and chassis losses and stay constant throughout the entire velocity range of a vehicle unlike aerodynamic drag which increases at an exponential rate.

Not only does the rate of motion determine the drag of the object but the inclination angle and overall size of the frontal area (NASA 2015). Figure 3.5 shows the relative trend in vehicle design up until 2000. Since this image is nearly twenty years old it is not as relevant anymore. It should be noted the majority of design changes since this time has been focused on elements with a technological nature such as advances in infotainment displays, Bluetooth integration, reversing cameras and electronically controlled driver assists. This is not to say there has not been aerodynamic improvements though, as the rise in CFD useability and capability has reduced the reliability on traditional wind tunnel testing and allowed for revisions to be taken into consideration quickly and efficiently. The inclusion of the streamlined forms, shown on the left-hand side of Figure 3.5, provide a visual look into what contributes to a low coefficient of drag value.

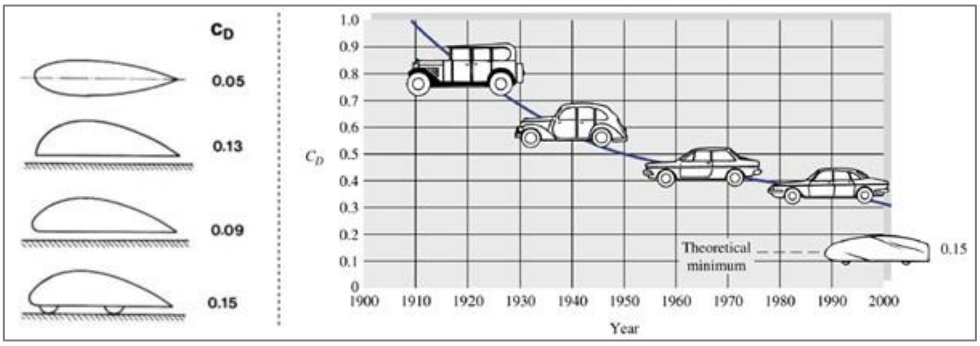

Figure 3.5: The progression of typical automobile drag coefficient through the years (Solmaz 2018)

3.5 Vortices

In order to understand how vortex generators work the concepts of what a vortex is must be understood. In general, a vortex relates to the motion of a fluid that is dominated by rotation about an isolated line in space. Everyday examples are seen in atmospheric events such as tornadoes, water spouts and tropical cyclones. These form when air/water fronts of varying temperatures and pressures combine. In aerodynamics, vortices are formed when airflow once confined within the boundary layer developed along the body's surface detaches (Panaras 2012, p.79).

A common example of where vortices are formed involves aeroplane design. The pressure differential on an airfoil helps to generate lift, it does however have a negative side effect. At the wing tips, the higher-pressure air travelling along the bottom surface of the wing spills up the wing tip into the lower-pressure region of air. The forward movement of the aeroplane spins this upward motion of air into a spiral that trails the wing tip. These vortices create form drag due to the energy requirement of creating turbulent airflow and is technically known as vortex drag (Flight Literacy 2015). It is common on modern aeroplanes to see winglets added into the design of the overall wing shape. This invention opposes the drag created by the wingtip vortices by utilising the airflow over the end section to help modify the characteristics of the wing tip and generate forward lift which counteracts the drag component. (Udris 2018).

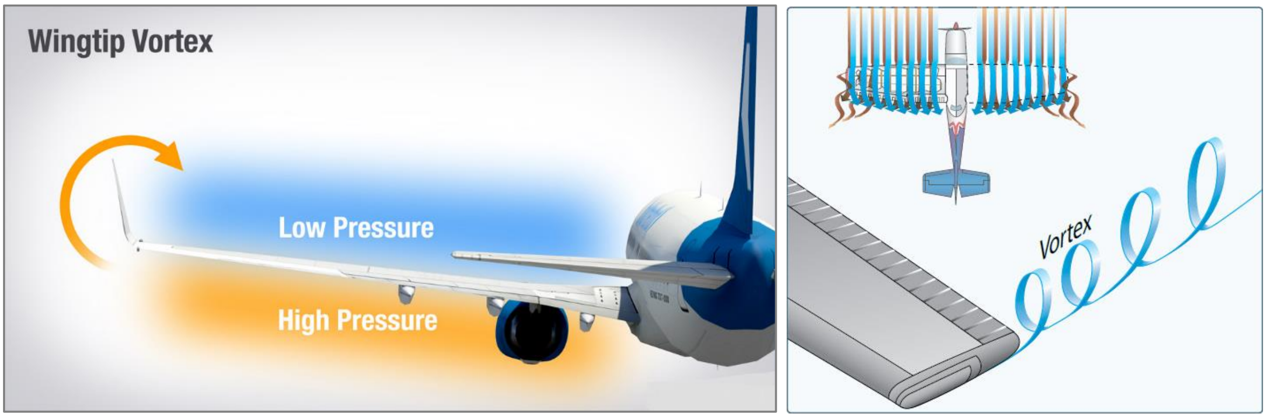

Figure 3.6: Visual representation of vortex generation due to a pressure differential and forward motion (Udris 2018) & (Flight Literacy 2015).

However, this study focuses on land vehicles, i.e. cars, and therefore this knowledge of how vortices can be formed or manipulated will be investigated to determine whether there are any benefits that be found that lead to an increase in aerodynamics efficiency. If vortex generators can be used to induce a flow that counteracts the drag created by the external shape, a potential reduction in the coefficient of drag could be found. This would essentially create a situation where by the vehicle becomes closer in design to a streamlined airfoil in raw C_D values.

3.6 Wind tunnel use for vehicle design

A conventional method used for aerodynamic design is via the use of a wind tunnel. This is a device for testing aircraft and automobiles in a controlled airstream under laboratory conditions. A majority of aeronautical advances have come from the use of wind tunnels to analyse flows, research new technologies and redesign existing. The development of new vehicles requires a vast amount of research and therefore the use of facilities that offer rapid, economical and accurate findings are preferable (Pope 1961).

In recent years the use of a wind tunnel in the designing stages of a vehicle has become ever more popular. The findings of these studies caused the rise in more curvaceous vehicle designs since the 1990’s. Various needs for understanding the phenomenon’s related to air flow has brought about the steep increase in the use of these facilities. Among the most important results that can be gained from wind tunnel experiments are aerodynamics forces and moments. As the confined laboratory conditions are repeatable it is perfect for obtaining measurements. The calculation of drag can be very important as it reflects the energy requirements and has a significant effect on a vehicles fuel economy and maximum speed. For racing car design the lift and side forces are just as important due to their focus on the controllability and high-speed stability. The lift forces are generally referred to as front and rear and used to isolate areas of interest (Barlow, Rae & Pope 1999).

Wind tunnel experimentation can also be used to investigate topics of interest such as:

- **Cooling flows:** engine, brakes, intercooler (turbo/supercharger setups).
- **Heating, ventilation and air conditioning (HVAC):** supply inlets/outlets and how they are influenced by the external pressure distribution, water or dirt ingestion into the air intake.
- **Noise, Vibration and Harshness (NVH)**: dictates comfort level, compliance with legislation, marketing, low NVH is perceived as a quality luxury vehicle.
- **Surface flows:** Wipers, washers, side mirrors and other features can change the airflow over the outer surface (Barlow, Rae & Pope 1999).

For the purpose of this research project the airflow over the roofline and rear section of the car is of interest.

3.7 Flow visualisation

It is very difficult to exaggerate the values of flow visualisation. Aerodynamic and hydrodynamic problems are much more readily understood when a mental image of the flow around a body is pictured. This is correct when the approach is theoretical, experimental, computational or a combination of any. However, if possible, the ability to see flow patterns on and around an object of interest helps to provide an insight into the problem. Flow visualisation is very beneficial as it provides a look into the flow regime in real-time. When associating this with the use of both wind tunnel experiments and CFD it can be used to validate both results and to ascertain whether the idealised flow patterns displayed on the monitor are in fact reality when seen in real life (Barlow, Rae & Pope 1999).

Classic flow visualisation for subsonic flows is done with the help of adding a visible agent into the flow at an upstream location and watching how it moves through the test section. Commonly a particle or dye tracer is used to convey the flow lines by way of smoke or oil (Barlow, Rae & Pope 1999). This method can provide a quick, qualitative assessment of the flow field; helping to guide initial concepts or the design of more detailed experiments. The use of a velocity probe can gain information at a certain location, but the use of flow visualisation provides a broad overview of the entire objects flow patterns (MIT 2002).

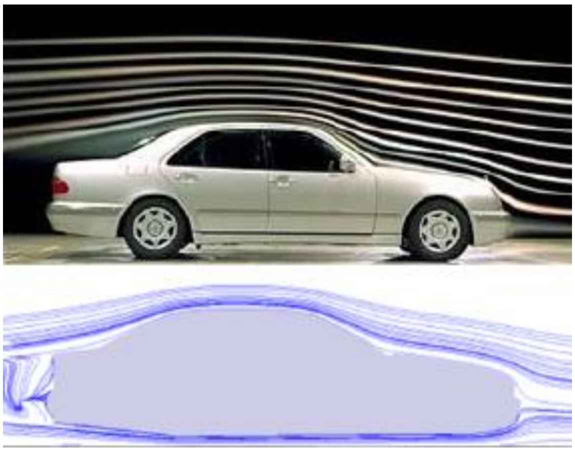

Figure 3.7: Experimental vs computational visualisations of streamlines (Evans 2012)

3.8 Boundary layers

The relative motion between an object and the fluid causes the molecules to form around the object and stick to the surface. In return, the velocity at the surface will be equal to zero. The molecules above the surface are slowed down due to the collision of the molecules below them. This phenomenon occurs in a comparably reduced nature above this layer and returns to normal flow velocity at a certain distance from the surface (NASA 2015). The distance at which the flow reaches 99 percent of the 'free-steam' velocity is defined as the boundary layer thickness (δ).

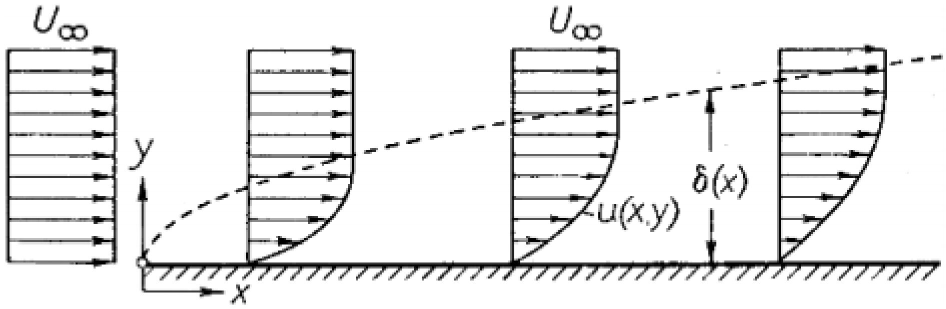

Figure 3.8: Boundary layer over a flat plate. Note the velocity gradient (Schlichting & Gersten 2017, p.30)

This boundary layer is dominated by viscous shearing forces and is therefore a region of relatively high velocity gradient. It is small in relation to the body dimensions and the flow transitions from the body's velocity to the free-stream velocity. These velocity gradients largely determine whether the drag on the body will be x or $10x$. The boundary layer has a multitude of properties that are very important for ascertaining the scaling effects. Critical aspects for consideration include:

- Location of where the boundary layer transitions from laminar to turbulent,
- Location of where the boundary layer separation occurs,
- The impact on boundary layer drag and thickness values brought about from an increasing Reynolds number; for example large Reynolds numbers indicate low viscosity and therefore a thinner boundary layer (Barlow, Rae & Pope 1999).

Schlichting and Gersten (2017) discovered in their earlier research that turbulent boundary layers have a much higher skin friction drag associated with them when in direct comparison with laminar boundary layers. This indicated that laminar flows require less energy to detach from the surface than turbulent layers. Other noteworthy boundary layer behaviour includes:

- Laminar boundary layers can be encouraged by a falling pressure gradient in the direction of flow,
- The maintenance of a boundary layer becomes more difficult with the increase in Reynolds number,
- If a favourable pressure gradient is designed over a large proportion of the body, then the extent of the laminar flow can be increased by utilising smooth surfaces and energising the boundary layer by surface blowing (Barlow, Rae & Pope 1999).

3.8.1 Wall shear stress

When a fluid flows over a body the layer in contact with the surface tries to drag the body along with friction, exerting a force on it. Similarly a faster moving layer than an adjacent one will have the same impact. The friction force per unit area is called shear stress and studies indicate that it is proportional to the velocity gradient (Cengel & Ghajar 2015). A practical approach results in an equation of:

$$\tau_w = C_f \frac{\rho V^2}{2} \tag{1.5}$$

Where C_f = dimensionless skin friction coefficient.

The frictional force over the entire surface can be determined from:

$$F_f = C_f A_s \frac{\rho V^2}{2} \tag{1.6}$$

Where A_s = surface area.

This will come into consideration when investigating the skin friction drag force on a vehicle whilst in motion. The higher the surface roughness, the greater the skin friction coefficient will be, along with overall drag.

3.8.2 Boundary layer separation

For small values of Reynolds number, it is possible for the flow to stay attached around the entire body. However, with higher flowrates the fluid may only be able to stay connected to the front side of the body and detach along the surface at a point dependant on the velocity and surface shape. When a fluid separates from a body, it forms a region between the body and the flow stream. Larger separation regions lead to increases in form drag. The effects of this flow separation are realised downstream with a reduction in airflow velocity; this region is known as the wake. Here, the pressure behind the body is much lower than the stagnation point at the front; creating recirculating and back flowing air. The separated region concludes when the two flow streams reattach (Cengel & Ghajar 2015).

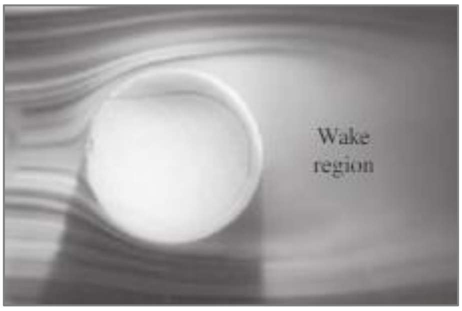

Figure 3.9: Visualisation of the boundary layer separation and wake region of a tennis ball (Cengel & Ghajar 2015).

Yadav, Rawal and Mishra (2018, p.131) discovered that around forty percent of the overall drag force is concentrated to the rear of a vehicle. They go on to state that flow separation is one of the key causes of aerodynamic drag. The height of a vehicle changes towards the rear and this increases the total flow area of the region. This in turn decreases the airflow velocity and creates a reverse flow, as seen in Figure 3.10. When airflow moves around the end of the roofline and down the rear window towards the boot it experiences this phenomenon. This reverse flow can be seen at point “C” and indicates a downstream pressure increase and thereby creating drag. On the contrary, at the upstream point “A” there is no opposing airflow because the boundary layer has adequate momentum to overcome the pressure gradient. For reference point “B” represents the balance between the momentum and pressure gradient of the boundary layer.

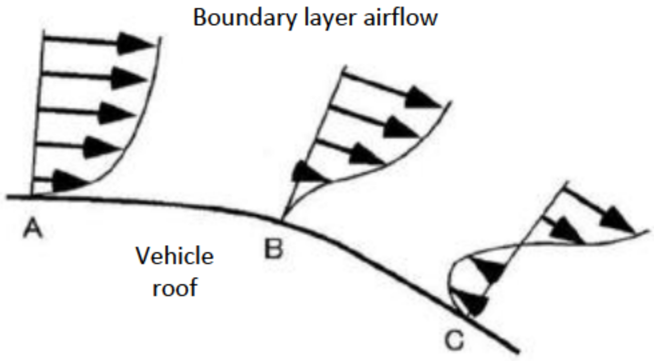

Figure 3.10: Theoretical velocity gradient at the rear section of a vehicle's roofline (Yadav, Rawal and Mishra 2018, p.132).

For laminar flows, the reduced boundary layer momentum results in the air not being able to adjust to the increase in pressure, leading to a separation from the body. Turbulent flow has increased momentum transfer due to the higher Reynolds number. This allows the boundary layer to overcome the adverse pressure gradient and stay attached to the body for a longer distance. Therefore delaying the separation and decreasing the wake behind the body (Bakkar, 2011, p.19). Travelling airflow has a greater tendency to detach at larger angles between points "A" and "C". As with both the STI and Evo this angle is greater than 25° due to the sedan body type. A coupe body type has less passenger headroom, allowing for a more sloping rear roofline. This reduces both the angle and the impact of boundary layer separation. The opposite is the case for a hatchback body type where there is a sharp drop-off before the rear windscreen.

Boundary layer airflow is unable to follow a sharp corner and continues its path, resulting in separation at the edge or some point down the slope based on its angle. Turbulent airflow now recirculates in a region behind the separation point (Bakkar, 2011, p.10). This knowledge can help engineers make important design cues by suggesting a reduction in the roofline to boot angle to delay the boundary layer separation.

3.8.3 Boundary layer control

There are several documented methods for controlling the development of the boundary layer. The majority focus can either supressing its separation, which in turn creates a reduction in pressure drag or keeping the flow laminar for as long as possible, which lowers the skin friction drag (Panaras 2012, p.67). Studies have shown that if the boundary layer formed on the wing of a flight vehicle is laminar and attached, then the skin friction and the form drag will be relatively small.

Gamiz (2013, p.4) details a study where vortex generators were installed on wind turbines to enhance the performance of the entire setup. It was found that the power generated, loading and life span of the turbines could be improved by using these devices. The efficiency of the turbines is heavily influenced by turbulent winds. It was found by adding vortex generators a delay of the boundary layer separation was achieved and the flow stabilised. In addition, the potential maximum values for lift and stall angles were increased with only a slight drag penalty. The inner blade of the turbine displayed a reduction in unstable airflow leading to longer rotor life. Another side effect of using vortex generators on a turbine blade is the positive reduction in stall induced noise emissions that could pose issues in built up environments.

Researchers have investigated the methods of flow control over a vehicle; these are classified as either passive or active methods. Examples of each are indicated as following:

- **Passive**: Addition of aerodynamic devices by way of introducing a rear wing, front splitter or vortex generators.
- **Active**: Modifying the shape of the structure or by using air jets, blowing or suction to modify the airflow.

Yadav, Rawal and Mishra (2018, p.131) describe how engineering aspects such as designing a vehicle to carry a specific number of people or include adequate luggage space makes it difficult to produce an aerodynamically ideal body shape. The use of vortex generators and rear wings was stated to help reduce drag on vehicles moving at a high velocity.

3.9 Vortex generators

A vortex generator is a passive aerodynamic device that is used to create spiralling airflow, i.e. a vortex, downstream of its position. A common example of where vortices are seen is at the wing tips of an aeroplane. This vortex occurs due to the pressure differential between the sides of the component's central fin. The airflow will move from the higher-pressure side to the lower-pressure side as per the laws of fluid dynamics and the relevant energy levels of each region. The positioning of the vortex generators can be normal to the oncoming airflow or at an angle to help develop vortices as seen in Figure 3.11. The majority of applications for vortex generators can be seen in the applied aerodynamics of aeroplane wings. However there are a range of additional uses in the aerospace and automotive sectors. Generally the engineering applications are in the form of flow separation control or mixing. The longitudinal vortices generated causes mixing of the high energy free-stream air with the slow-moving boundary layer air. The outcome increases the velocity of the boundary layer and delay its separation from the body

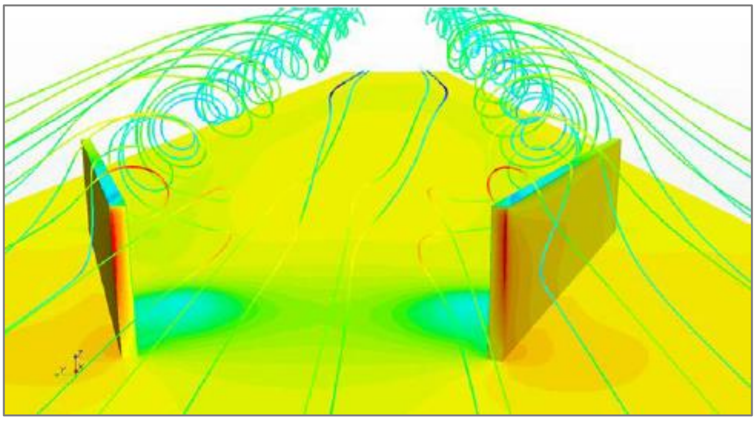

Figure 3.11: Airflow change from the use of vortex generators (Gamiz 2013)

The first mention of such device was by H.D. Taylor, of United Aircraft Corporation in 1947. It is unclear whether he was the inventor of the vortex generator or just the first person to conduct any experimental studies with the devices. The original vortex generators introduced by Taylor were vane or fin type devices with either a rectangular, delta or trapezoidal main shape and ran parallel to the airflow. Not only was one vortex generator used but several in series forming a row. The devices were projected normal to the surface and could be set at an angle of incidence to the oncoming airflow, creating a situation whereby the resulting flow becomes an array of trailing vortices. The original concept was designed to improve the efficiency of a tunnel diffuser. The premise was that it energised the boundary layer and therefore delayed its separation from the body the air was flowing over.

Currently, vortex generators are also used to enhance wing lift on aeroplanes and supress the extent of shock boundary layer interactions (Panaras 2012, p. 74). Figure 3.12 shows some easily available vortex generator designs, sourced online from eBay and manufactured in China. These examples are for use in the study and could help with determining the positive design elements of the most efficient vortex generator.

Figure 3.12: Vortex generator examples, sourced online

Gamiz (2013, p.4) found that an optimal layout of vortex generators can delay flow separation by creating vortices that add momentum to the boundary layer as the airflow in the free-stream has a higher velocity than the boundary layer and when combined the boundary layer sees higher energy airflow with increased velocity.

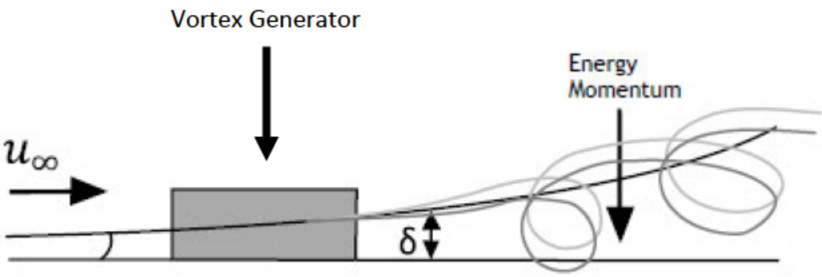

Figure 3.13: Downstream impact on airflow from use of a vortex generator (Gamiz 2013, p.8).

Most of the literature reviewed saw the use of vortex generators in place on aircraft or in aeronautical applications; however, the findings can still relate to land vehicles. Figure 3.14 visualises the use of vortex generators on an airfoil and the concept holds true for a rear section of a vehicle as well. It can be seen that the aerodynamic device alters the airflow and draws in the high energy free-stream flow into the slow-moving boundary layer, thereby holding the airflow to the object as long as possible before airflow separation occurs.

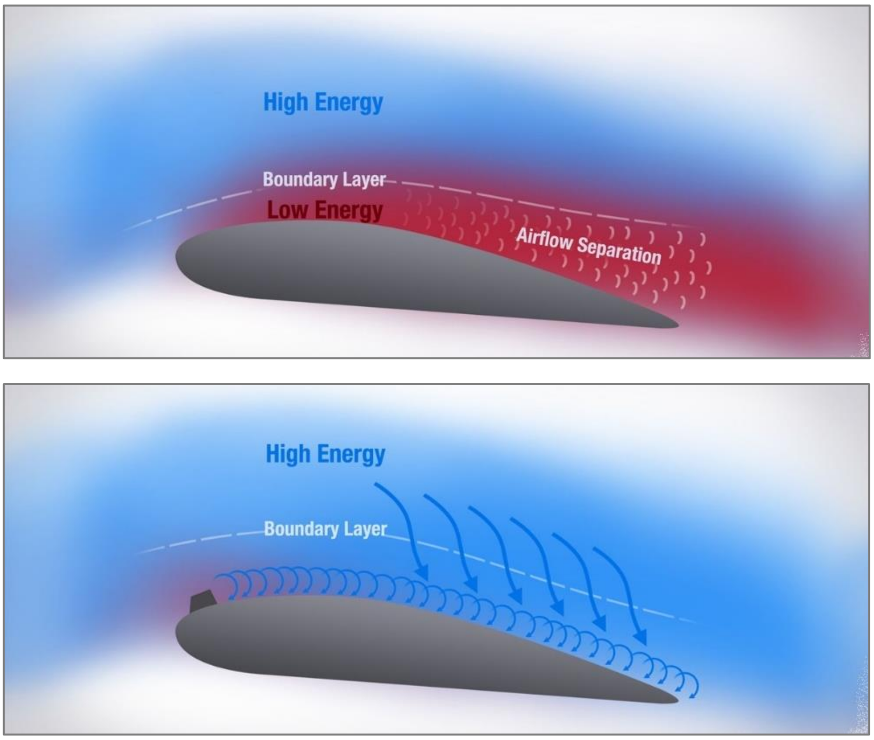

Figure 3.14: Visual representation of a wing without vortex generators (above) and with vortex generators (below) (Udris 2018)

One of the first studies involving vortex generators was by Lina and Reed (1950), which was a classified research memorandum of the National Advisory Committee for Aeronautics (NACA). Many arrangements installed on an airfoil were tested at varying speeds and it was determined that for all the cases vortex generators were effective in reducing or eliminating separation of boundary layers on wings and diffusers at subsonic speeds. Transonic speeds were also investigated, and it was seen that separation due to compressibility shock could as well be reduced.

3.9.1 Vortex generator design

Vortex generators themselves create a drag force due to the energy required to create the turbulent downstream airflow. This force was discovered to be minimal at most and a negligible amount when compared to the form drag created from the vehicles blunt shape. The overall effect of the vortex generators can be calculated by totalling both the positive and negative impacts. From research it was found that the delay in the flow separation and the amount of drag created by the vortex generators themselves was directly proportional to the size of the devices. This indicates as the relative size increases so does the enhancement to delaying the boundary layer separation but at the same time increases the drag component due to the structures size (Yadav, Rawal and Mishra 2018, p.132). Therefore there must be an optimum height of the device in order to increase its effectiveness. According to many researchers, including Yadav et. al. and Gopal et. al. the most efficient height of a vortex generator is nearly equal to the boundary layer thickness (δ).

Further studies by Lin (2002, p.391) investigated the use of low-profile vortex generators, which have a height of ten to fifty percent of the boundary layer thickness ($0.1 \leq h/\delta \leq 0.5$). It was found that the passive aerodynamic devices were still effective in separation control. The induced streamwise vortices helped to delay boundary layer separation from the body but the downstream coverage was decreased due to the height of the vortex generators.

The 2017 Honda Civic Type R (CTR) utilises vortex generators in its design. However the height of the devices is much smaller than the design used on the Evo 8 MR. The press release stated the vortex generators and the rear wing helped to minimise drag and increase downforce, leading to an improvement in high speed stability. There was no technical data included and therefore the effectiveness cannot be quantified. The CTR is a hatchback body type but includes an aerodynamic design with its roofline to boot angle of < 20°. Whereas on a more traditional hatchback design where the roofline angle is much greater the use of vortex generators may not be enough to stop the flow from separating. Yadav, Rawal and Mishra (2018, p.136) discovered via testing that the impact of using these devices was minimal as the drag reduction was slight when used on a hatchback vehicle.

Raykowski (1999) tested whether differing the incident angle of the vortex generator produced additional benefits over positioning the devices normal to the oncoming free-stream airflow. This study included angles from 10° - 30° and investigated aspects such as spanwise row density, heights and using multiple rows of vortex generators. The findings indicated that there was a minor drag reduction when the height of the devices was above the boundary layer thickness. However, it was noted that these devices can also produce drag penalties due to the angle of incidence. The author stated that the optimal incident angle was 25° but noted additional testing with more parameters is required to conclude the findings. This paper also commented on the possibility that what was found for this particular airfoil application may not be as relevant for another aircraft as design changes could alter the effectiveness of the devices. Therefore this indicates there is not a “one size fits all” optimal setup for all systems but the likelihood each situation would have to be analysed individually to determine the parameters leading to the greatest reduction in drag, thereby the optimal design. Aspects such as vortex generator height relative to boundary layer thickness, the positioning relative to each other and the quantity used are to be studied.

3.10 Wind tunnel conditions

The conditions for a model tested in a wind tunnel are not the same as for those tested in free air; the adjacent solid walls obstruct the natural airflow and the varying Reynolds number impacts the flow patterns around the model along with laminar and turbulent regions of the flow and any separations.

It should be noted there is no difference between having the model stationary and the air travelling around it instead of vice versa. The wind tunnel used for the experiments was an open-return design which limits the corrections required to achieve accurate results. For use of a closed-return wind tunnel setup would require further analysis to quantify the measured variables. For example the variation in the static pressure gradient along the test section walls produces a thicker boundary layer and drag force known as the horizontal buoyancy. This acts in the same direction as the drag and is only negligible in an open-return setup. Any tests undertaken in a closed-return setup would generate small forces that need to be accounted for and removed from results (Pope 1961).

Barlow, Rae & Pope (1999) assert that when automobiles are used in the wind tunnel that the length must be sufficiently long so that separated flow regions close above and below the scale model before the end of the test section and entering the diffuser. If not, the pressure in the separated region will not read accurate results and a significant increase in drag will be found.

3.10.1 Blockage effects

Willemsen (1997, p.439) states that when a scale model is placed in the test section of a wind tunnel, the free lateral motion of the air flow around the model is obstructed by the adjacent solid walls. These lateral boundaries provide many different types of lateral constraints, but for the purpose of this study the following is most relevant:

- **Solid blocking:** The model restricts the area through which the air must flow and by continuity and Bernoulli's equations an increase in dynamic pressure and therefore velocity as the air flows around the model. An open test section would have negligible impacts as the air can expand after travelling past the model.
- **Wake blocking:** The flow pattern is altered due to the presence of the model. The velocity outside of this wake region must be more than inside it due to the law of continuity to keep a constant volumetric flow rate. The pressure differential that arises from this influences the boundary layer and increases the velocity at the model. This also impacts the size of the wake, leading to an increase in drag. Usually for an open test section the effect is negligible but can still be a factor in a traditional small-scale wind tunnel (Pope 1961).

A commonly used method of determining whether the model is at a correct scale for use within a specified wind tunnel is to calculate the blockage ratio. This is defined as the ratio of the frontal area of the body to the cross-sectional area of the wind tunnel's test section. For a vehicle, the projected frontal area is commonly used to more accurately represent the overall design. It is recommended in the international best practice guidelines to limit the blockage ratio to less than 5 percent for wind tunnel experiments and less than 3 percent for CFD research (Janssen, Blocken, & van Wijhe 2017, p.111).

Larger ratios increase the chance for issues relating to the boundary corrections and creates more complex analysis to gain accurate results. By reducing the blockage ratio the impacts of the wind tunnel walls can be minimised. For the tests undertaken as part of this study the calculations below were required:

Projected frontal area of scale model = $\text{Width} * \text{Height} = 72\text{ mm} * 54\text{ mm} = 3888\, mm^2$

Wind tunnel test section: cross-sectional area = $305 * 305 = 93025\, mm^2$

$$\therefore \text{Blockage ratio} = \frac{3888\, mm^2}{93025\, mm^2} = 4.18\ \%$$

This is under the recommended 5% limit for wind tunnel analysis. There needs to be considerations that the projected frontal area is overestimated as in reality this value would be less due to the area surrounding the vehicle as seen in Figure 3.15. It is suggested to use eighty five percent of the calculated area. For this example this would lower the blockage ratio to 3.55%.

Figure 3.15: The front view of the scale model indicating the projected frontal area

3.10.2 Boundary layer conditions

Flow conditions in a wind tunnel are not completely similar to unbounded airstreams in "free air" when concerned with ground vehicles. The distance of some or all stream boundaries from the object tested are generally less than the corresponding distances in actual real-world situations. It is possible that the air flow stream may not have the same distribution and properties in space and time. The operational variations, however small, can have significant effects on the surface stress distribution and associated total forces. The existence of lateral boundaries on the solid walls and the boundary layers is an example that would not be present in actual scenarios (Barlow, Rae & Pope 1999).

The boundary layer thickness (δ) must be calculated for this study to analyse whether it will impact on the wind tunnel tests. The Reynolds number must first be calculated.

Assumptions:

1. Air is an ideal gas and at a steady operational temperature of 20°C and 1 atmosphere
2. The characteristic length is set as the width of the wind tunnels square test section
3. The parameters of the airflow are taken at the assumed temperature and pressure

Data for air at 20°C and 1 atm:

- Density (ρ) = 1.204 kg/m^3
- Dynamic viscosity (μ) = 1.8205 *10^{-5} m^2/s

Data assumptions based on experiments:

- Velocity (V) = 30 m/s (less than the maximum of the wind tunnel)
- Characteristic length (Lc) = 305 mm (width of wind tunnel test section)

$$Re = \frac{\rho * Lc * V}{\mu} = \frac{1.204 * 0.305 * 30}{1.8205e^{-5}} = 605\ 141 = 6.05 * 10^5$$

As this Reynolds number is above the critical value of $5 * 10^5$ it is classified as turbulent. If the airflow velocity is below 25 m/s it would be under this critical value and therefore be laminar, or more technically some form of transitional flow. The variation in Reynolds number with the change in airflow velocity at $Lc = 305\ mm$ is plotted in Figure 3.16. The laminar and turbulent regions are displayed along with the critical Reynolds number. N.B. The transitional range is not shown.

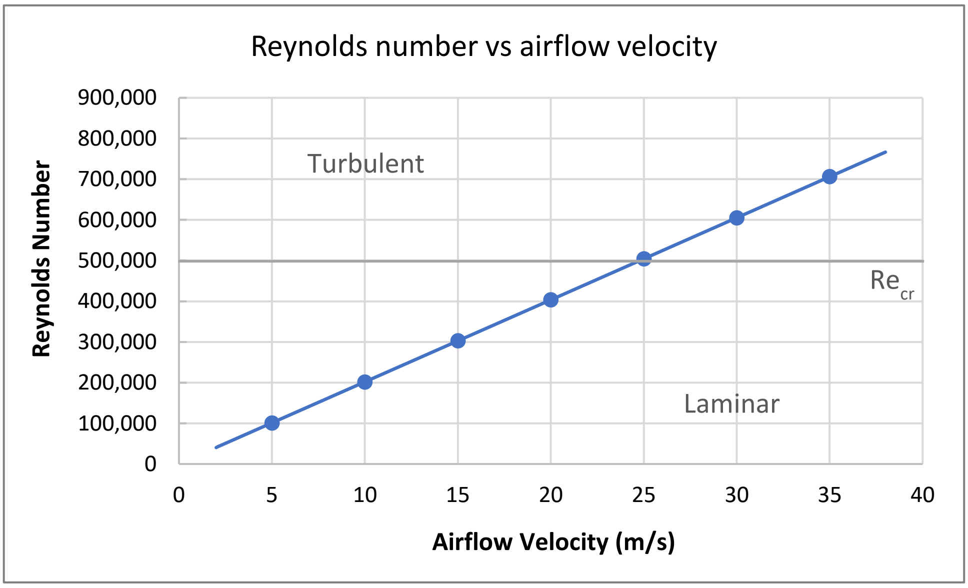

Figure 3.16: Plot of varying Reynolds number with airflow velocity at Lc = 305 mm

The boundary layer thickness can be calculated via the following equation, where x is the distance from the leading edge of the floor. In this instance this will be taken as 0.6 m.

$$\delta = \frac{4.91x}{\sqrt{Re}} = \frac{4.91 * 0.6}{\sqrt{6.05 * 10^5}} = 0.00379\ m = 3.79\ mm \qquad (1.7)$$

The equation indicates that the boundary layer thickness increases as the airflow velocity decreases. It can also be seen that the distance along the horizontal axis of the test section from the leading edge plays a significant role in determining the thickness of the boundary layer. More data points were calculated in a Microsoft Excel spreadsheet and plotted in Figure 3.17 to ascertain the boundary layer thickness over the velocities created by the wind tunnel. The distances from the leading edge of the test section were split into 0.1 m points.

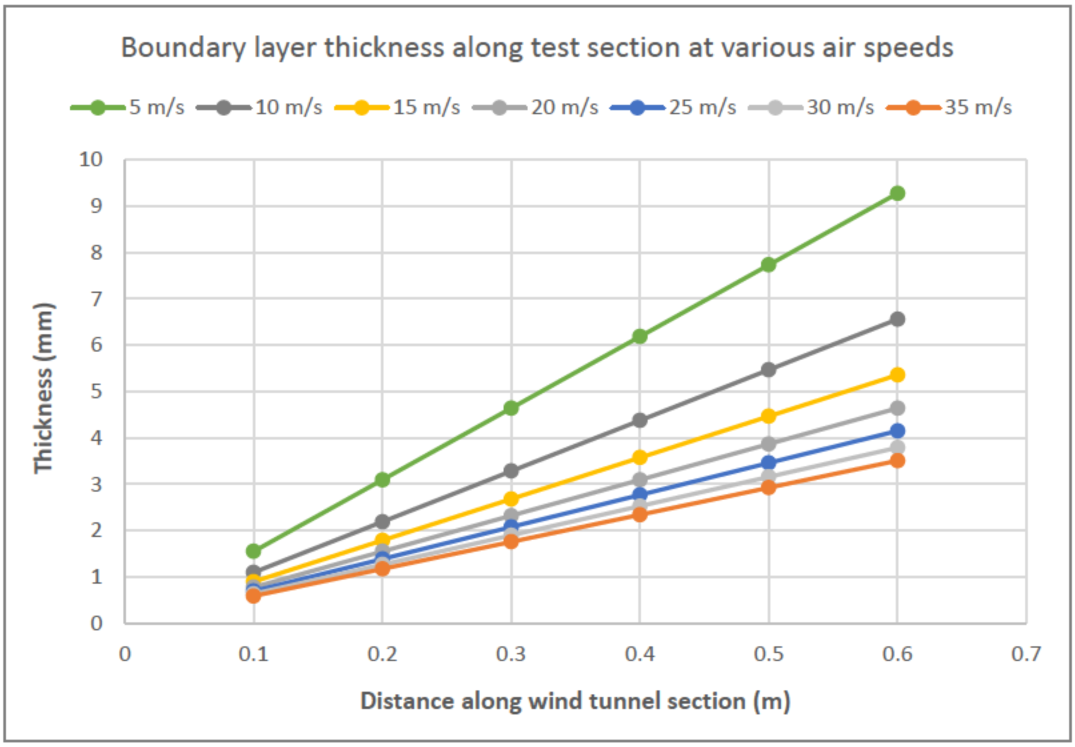

Figure 3.17: Plot of varying boundary layer thickness with airflow velocity

3.10.3 Scale factor of aerodynamics/similarity

Engineers use scale models including vehicles, in wind tunnels to test, re-design and improve air flow characteristics. It is more practical than a full-scale design and can provide accurate results due to the laws of scaling (Aero Performance Engineering 2010).

The two wind tunnels available are located at USQ block Z113 and P7. The maximum air flow generated by each machine is 36 m/s and 15 m/s respectively. This corresponds to a relative rating of 130 km/h and 54 km/h each. As this study focuses on performance cars, higher air flow velocities are preferred. This allows for an extended look into the performance of vortex generators and their impact on the reduction of lift or downforce generation. It is possible the efficiency of these aerodynamic devices alters with air flow velocity. Preferably speeds of interest would be > 100 km/h or 27.8 m/s as performance cars used on the track, such as the Evo 8 MR can exceed this speed on the straight away and in the corners. The use of a scaled model also brings with it issues relating to the practicality of the experiments as the airflow has to be upscaled 24 times the full-scale airflow due to the relative size differences. Therefore the velocities achieved in the wind tunnel do not correspond to the same velocities on a full sized vehicle.

One of the main considerations when testing scale objects is whether or not it will correlate with its full-sized counterpart Reynolds number. In order to have the same value for a scaled experiment the velocity needs to be inversely proportional to the reduction in size. For example, a 1/3 scale object would require a 3/1 increase in the numerator in order to return the same Reynolds number. This can be seen in the equation below, where the constants of density and dynamic viscosity cannot be altered leaving only the velocity to be changed, as detailed below:

$$Re = \frac{\rho * Lc * V}{\mu} \rightarrow If\ L_c\ is\ reduced\ then\ V\ must\ be\ increased$$

3.11 CFD of vehicles

The dynamics of a vehicle can be analysed via numerical simulation, i.e. CFD. This easily allows for complex experimental tests to be performed in an efficient manner without the use of a physical setup. Revisions can be undertaken with ease and results can be visualised in real time. CFD can be used for validation of the wind tunnel tests. By performing the tests in a narrow computational domain it can resemble the cross-sectional area of the wind tunnel. The blockage effects caused by the domain boundaries are found by comparing the differences in the results when these conditions are removed (Janssen, Blocken, & van Wijhe 2017, p.106).

Barbut and Negrus (2011, p.21) state that CFD can be used to successfully analyse the airflow patterns under the car. This is an area that can be difficult to evaluate in real world situations along with wind tunnel as many vehicles have low clearances with the road. They found that the post-processing of the CFD data allowed to gain an understanding of the efficiency of undercarriage airflow and enabled a strategy where designs could be revised to visually represent the improvements. They found that CFD was essentially the only efficient tool for detailed flow analysis and has the potential to introduce worthwhile changes to the aerodynamics of a vehicle.

A study by Perzon (2001) indicated that validation studies can include uncertainties between both CFD and practical experiments due to the boundary condition differences. When an experiment in a wind tunnel is undertaken, it is common for CFD studies to follow. To maintain a level of accuracy some researchers add a wind tunnel model/boundary condition for more accurate representation of the overall situation. The study found that where the blockage ratios were not similar between wind tunnel and CFD experiments the pressure distribution around the transitional airflow areas between the windscreen and the roof were poorly predicted. CFD used for new vehicle aerodynamic testing helped to better simulate the correct road conditions. 2D and 3D tests were undertaken to see whether adding slotted walls to the wind tunnel model used for CFD could lower the blockage ratio and further accommodate a real-world situation. It was found that by doing so the entire wake structure changed when compared to on road conditions. The author mentions that if the blockage ratio is large then the results leading to drag reduction may have to be validated via other forms of testing.

The modern automotive vehicle designer is continuously encountering engineering constraints that help to deliver what is seen on the road tomorrow. The increase in simulation software has made great leaps towards solutions for all types of performance and cost targets. Duncan et.al (2010) researched the effects of a rotating wheel in CFD, something that is not commonly studied. This allowed for a greater representation of on road conditions, along with a moving road; which differs from conventional fixed-floor wind tunnel experiments. It was found that the digital process of predicting the drag effect of a specific design could be confidently ascertained and that an understanding of how aerodynamic changes affect the drag results. This provides enough knowledge to revise designs if necessary and leads to quicker solutions than traditional experiments.

3.12 Other passive aerodynamic devices

3.12.1 Gurney flap

During preseason vehicle testing in 1971, Dan Gurney, an ex-Formula One driver and team owner conceived an idea that incorporated a small additional spoiler to be attached to the trailing edge of the rear wing. This is a classic case of necessity being the mother of invention as the original piece was fabricated and installed within the hour to allow for further vehicle testing. At first the track lap times were not improved, but after further analysis it was discovered that the large increase in downforce at the rear of the car created a situation where the front of the car was experiencing more lift and thereby understeering. Once the aerodynamic balance was restored by increasing frontal downforce the effects of the gurney flap were fully visible (Formula One Technical Dictionary 2018).

A gurney flap is a small extension to the wing that is at an increased angle of attack that dramatically sharpens the exit angle of airflow over the wing. It helps to generate more downforce as it is essentially increasing the chord length of the wing without the drag penalty that a larger and steeper angle wing would produce (McLaren Racing). Since the invention, many studies have been undertaken and today the applications spread further than motorsport as we are seeing benefits from gurney flaps in the subsonic and supersonic airfoil design; such as delta wings. Due to the simplicity of the structure it has many engineering applications. Wang, Li & Choi (2008) studied the effects of using a gurney flap on an airfoil and found that there was a significant improvement to aerodynamic performance when in operation. When experimented with use on a helicopter rotor it was seen to provide an additional 10% lift. The subsonic airfoil experienced increases in upper surface suction and lower surface pressure, which facilitated a greater lift force.

This design can also be utilised on an inverted airfoil shape, i.e. a rear wing on a vehicle. Gurney flaps have become mainstream to the extent that some are available for certain performance vehicles. Figure 3.18 shows how the design is adapted for use on a Honda Integra Type R, note the gurney flap wraps around the trailing edge of the wing. This version is made from dry carbon fibre and is therefore expensive. Typically a gurney flap on a street car is considered an aesthetic upgrade as much, if not more, than a functional one.

Figure 3.18: Gurney Flap on an Integra Type R (Password:JDM 2014)

Chapter 4: Research Methodology

4.1 Overview

The data collection phase of this research project will include two distinct elements, these are:

- Experimental:
    - Full-scale testing
    - Small-scale wind tunnel testing
- Computational:
    - CFD analysis

It was beneficial to include full-scale testing to help add extra depth to the findings. The CFD analysis alone would provide the data required to form a conclusion, it would however not have any practical aspects and a pure desktop study is not what was of interest. An overview of each aspect is provided below:

Full-scale testing: Provides background to the topic with hopes to visualise the airflow characteristics over the rear windscreen of a vehicle. The ideal results will indicate a reduction in turbulent airflow when the vortex generators are positioned above the rear windscreen. Video footage will allow for analysis to indicate the relative performance of the passive aerodynamic devices. The results are not calculable beyond simple freeze frame angle measurements leading to the understanding of how vortices in the boundary layer create a delay in separation.

Small-scale wind tunnel testing: Will involve using the wind tunnel located at USQ's Z Block to obtain drag and lift forces on a scale vehicle with and without vortex generators used. Preliminary testing can include full-sized vortex generators to validate changes in downstream airflow characteristics. The 1:24 scale vehicle will be used with 3D printed scale vortex generators attached to the roofline in various designs and positionings. Load cells will be used to calculate the forces exerted by the model. The addition of the vortex generators will aim to produce more negative lift (downforce) on the rear section of the car. This will add weight to the press release statement from Mitsubishi that claimed the devices made the rear wing more useful, thereby generating more downforce.

CFD analysis: The results will provide quantifiable data to help ascertain the effectiveness of vortex generators used on vehicles. The 3D scanned 1:24 scaled car model will be imported into CAD software where 1:24 scale vortex generators will be added to the model. It will then be imported into CFD software where it will undergo various situations based on the wind tunnel testing. It can however enable quick revisions and additional tests that cannot be performed in the latter. The data retrieved from such experiments will be included in the report and comprehensively detailed. The majority of the meaningful information will be extracted from the CFD studies. Flow visualisation screenshots from pressure contour plots, streamlines and velocity vector plots will add to the extensive investigation. However, due to the scale model being 24 times smaller, the results cannot be directly extended to the full sized vehicle beyond an indication.

4.1.1 Timeframe

The combined courses of ENG4111 and 4112 run for the entire academic year of Semester 1 and 2. Starting in late February and continuing to the finalisation of results and documentation in mid-October leaves seven months to fulfil the requirements of the courses. The whole timeframe for this research project in Gantt chart form is included in Appendix D of this report. To keep track of the progress several phases where used.

Phase 1: Initiation – This indicates the start of the research project. Background information was researched, the project overview and resources were identified. Also this included the completion of the project specification (Appendix A), project plan and resource analysis documentation that was due 20th March 2019.

Phase 2: Literature review – The long process of reviewing and collating useful information that related to my area of investigation was included in this phase. Originally thought to be completed by the end of semester one, but after communication with the project supervisor it was extended to take the whole allotted time as it was possible new data will emerge after further tests and possible revisions could occur. This phase also included where vortex generators have been used previously, both on aircraft and land vehicles.

Phase 3: Design and manufacture – The vortex generators were 3D scanned and scaled in CAD software. They were to be used with the imported 3D scanned model of the Subaru WRX STI. An assembly was created and exported into CFD format. Also scale vortex generators were 3D printed to be used with the small-scale wind tunnel tests.

Phase 4: Experiments – Included the three main tests: wind tunnel, full-scale and CFD testing. Each had to be understood with a detailed procedure before any tests were undertaken or results were gained. A risk assessment was completed prior to testing along with gaining the necessary resources.

Phase 5: Analysis of data – The collection and storage of data from the experiments was done during testing and the results section was constantly updated to reflect the findings. The discussion of the results formed a large basis of the report, including any correlations with findings from previously reviewed literature.

Phase 6: Dissertation documentation – The dissertation was continuously updated throughout both semesters, with each of the aforementioned headings creating the majority of the set out for the document. The residential school conference seminar was created based on this document and the findings were adapted for a presentation. The last phase of this research project was to finalise the document and ensure it was submitted by the due date.

4.1.2 Resources

This research project is not only theoretical but has experimental aspects. It will include a literature review and several practical tests; to be carried out at university. The resources that will be required can be broken down into the following headings:

Need to purchase:

- Various vortex generator designs sourced online,
- 1:24 scaled model cars for use in wind tunnel tests,
- Load cells to measure the drag and lift forces,
- Various twine lengths to be used in the full-scale tests as visual indication of air flow.

Need access to:

- University wind tunnel. Either Z Block (Z113) or P Block (P11 or P7),
- CAD software packages (CREO Parametric),
- CFD software packages (ANSYS Fluent, DesignModeler, SpaceClaim, CFD-Post),
- 3D scanning and printing capabilities,
- Smoke generator for use with the wind tunnel tests,
- GoPro camera for full-scale tests,
- High speed camera for wind tunnel tests (if available),
- High powered computing equipment for data analysis (if necessary).

4.2 Experimental – Full-scale methodology

The tests involved using full-sized vortex generators attached to the trailing edge of my car's roofline. Small pieces of natural jute twine were attached to the rear windscreen via tape and positioned at three distinct areas covering the majority of the windscreen's area. The notion was that the pieces of twine will flutter/rotate when no vortex generators are located upstream and noticeably less when they are. From research the position of the visual indicators, i.e. twine was important as boundary layer separation can occur at different positions along the rear windscreen based on the angle from the roof to the boot. Therefore it may be that the top level of twine moves less than the bottom level as by the time the air flow reaches the latter it has separated from the vehicle.

This test provides background to the topic and helps to visually identify the airflow characteristics over the rear windscreen of a vehicle. The ideal results will indicate a reduction in turbulent airflow when the vortex generators are positioned before the windscreen. Slow motion video capture will allow for analysis that can indicate the relative performance of the passive aerodynamic devices. The results are not calculable beyond simple freeze frame video measurements leading to the understanding of how vortices in the boundary layer create a delay in separation. This is a practical addition and adds a depth that a desktop study alone cannot.

4.2.1 Setup

The video capture was courtesy of a GoPro action camera (2014 model) and used in conjunction with the suction cup mount shown in Figure 4.1. The footage was taken at a resolution of 1280x720 @ 50 frames per second (FPS). This was chosen over the 1920x1080 Full High-Definition (FHD) video format available as 25 FPS was the limit for this camera version. A higher frame rate was chosen over a higher pixel density to allow for smoother slow-motion capture and ease of analysis brought about by the additional FPS.

Figure 4.1: GoPro camera (left) and
associated suction mount (right)

The camera was positioned on the vehicles wing which provided a good field of view for the entire rear windscreen and the roofline when the vortex generators were in position. The GoPro suction mount is rated up to 250 km/h so it was a viable solution.

Natural jute twine (shown in Figure 4.2) was used to visually indicate the relative motion of the airflow over the rear windscreen. A 6 mm high-quality variant was sourced from a craft store. It is a vegetable fibre and commonly used in textile industries to create hessian; therefore it was up to the task and this ensured it could withstand the fast airflow velocities without fraying excessively. Various materials and thicknesses were researched before using this twine. It may seem like a trivial undertaking in order to determine which twine should be used but any thinner string or yarn may well have been too light. This reduction in mass could have increased its susceptibility of being influenced too easily from the airflow and would not have been able to show any discernible differences in the before vs after situation. Similar to how dental floss moves easier and more irrational in a slight breeze compared to the same length rope cord if hung to freely rotate below a fixed point.

Figure 4.2: Original jute twine 6 mm (left) and secondary jute twine 3 mm (right) used as the visual indicators

4.2.2 Test procedure

There were several parameters that needed to be considered to create the most repeatable experiments. All tests were carried out on 3rd August 2019 between the hours of 9:00 am and 12:00 pm along Handley Street (located behind USQ McGregor College); Figure 4.3 shows the locality of the tests. Toowoomba Regional Council (TRC) state this road borders on the land use zones of Community Facilities, Higher Education (HE), Low-Medium Density Residential, Urban Residential (U) and Rural Residential (RR1). This road is relatively flat and straight for 1 km which facilitated the necessary distance for acceleration. The effect of cross winds would be reduced as there was only small steering corrections required to maintain the path. The smooth asphalt surface limited sporadic twine motion that could be found on a rough surface. There is some foliage on both sides of the road but not enough to mitigate against excessive winds from affecting the results.

Figure 4.3: Location of the test road. Note the TRC land zone uses.

There was to be three speeds tested on the road, 60 km/h, 80 km/h and 100 km/h. Any higher speeds were not possible as to adhere to public roads speed limits. Use of an airport runway would have allowed for these higher speeds and more motion of the twine. However, this notion was declined as communication with both Wellcamp Regional Airport and Toowoomba City Aerodrome could not facilitate my research due to either a high volume of commercial aviation traffic or relative Council policies that do not allow for land vehicle operations on the runway.

The rear windscreen wiper was removed for the tests as to not impact on the airflow. The lengths of twine were positioned in five distinct rows to make up a total of twenty-seven pieces of twine covering the rear windscreen.

4.3 Experimental – Small-scale wind tunnel methodology

The premise of the experiment was to use scale model cars in the wind tunnel on campus to visualise the airflow over the body and obtain the drag and lift forces before and after the installation of the vortex generators. To make the task efficient it was beneficial to use two scale models, one that was used as the control with no vortex generators installed and another with the scale vortex generators attached to the trailing edge of the roofline. The wind tunnel required a horizontal support rig in order to allow the model to be positioned in the centre of the test section where boundary layer conditions would not impact the results. The following sub-sections provide the necessary information regarding the testing setup and procedure.

4.3.1 Wind tunnel information

USQ has several wind tunnels on campus. One located at Z113 with a maximum airflow velocity of 36 m/s and is explained in detail below. The other two are located in P11 and P7 with maximum rated airflow of 40 m/s and 15 m/s respectively. Access to the wind tunnel site was organised beforehand with the technicians and a suitable time frame of testing was scheduled.

All tests were carried out in the TecQuipment AF1300 subsonic wind tunnel available at USQ Z113. This machine is a compact, open-circuit suction design primarily used to study aerodynamics. The fan assemblies are located down-stream of the test section and the air is drawn through this area with a suction force. The cone shape of the left section (refer to Figure 4.4) accelerates the air linearly as it passes through the test section. From here the air passes through a grill (to limit debris), then a diffuser, followed by the variable-speed axial fan. Once the air has moved through the system it is silenced and pushed back out into the atmosphere. The test section has dimensions of 600 mm (length) x 305 mm (width) x 305 mm (height).

Figure 4.4: TecQuipment AF1300 Subsonic Wind Tunnel
(TecQuipment 2018)

The setup features electrical sensors on the optional instrumentation and can export the data in real time to monitor, calculate and chart relevant parameters on a computer display. The test section of the wind tunnel had clear sides for ease of viewing and were removable to position the model in the area required. The area available for use was 305 mm by 305 mm and 600 mm long. The range of air velocities that can be attained are between 0 m/s and 36 m/s (TecQuipment, 2018).

4.3.2 Smoke machine

The wind tunnel tests provide an opportunity for qualitative results along with quantitative ones. Sometimes, it is beneficial to see the flow around an object just as much as calculating the drag or lift forces. A smoke machine helped to aid with the flow visualisation during the tests. USQ had an Aerolab smoke generator available for use as shown in Figure 4.5. The machine uses propylene glycol and this oil is vaporised by an electric heating element. This in turn creates a thick white smoke that is useful for wind tunnel tests, as a large volume of air travelling through a test section requires a large quantity of smoke to visualise the airflow. The safety data sheet (SDS) for the oil can be found in Appendix C.

Figure 4.5: Aerolab smoke machine with
propylene glycol oil (Aerolab 2016)

This machine is of the highest quality and is very expensive. The principle design engineer of the Aerolab smoke generator is also the author of the technical book "Low-speed wind tunnel testing" which is referenced several times in this study.

4.3.3 3D printed vortex generators

Scale vortex generators were used to accompany the scale vehicle in the wind tunnel. Due to the large scaling factor of 1:24 of the vehicle, the same scale could not be achieved by the vortex generators as the resolution of the 3D printer required was too fine. Table 4.1 indicates the relative dimensions of the various scaling factors.

Table 4.1: Vortex generator dimensions based on scaling factor

Variant	Dimension (mm)	Scaling Factor			
		1	1:6	1:12	1:24
1	Length	80	13.3	6.7	3.3
	Width	31	5.2	2.6	1.3
	Height	27	4.5	2.3	1.1
2	Length	53	8.8	4.4	2.2
	Width	24	4	2	1
	Height	24	4	2	1

The first batch 3D printed vortex generators were at 1:6 scale of the full-sized object. It can be seen in Figure 4.6 that the resolution of the printer was unable to create a smooth product at these sizes. Ruling out the possibility of printing 1:24 scale, which would have matched the vehicle.

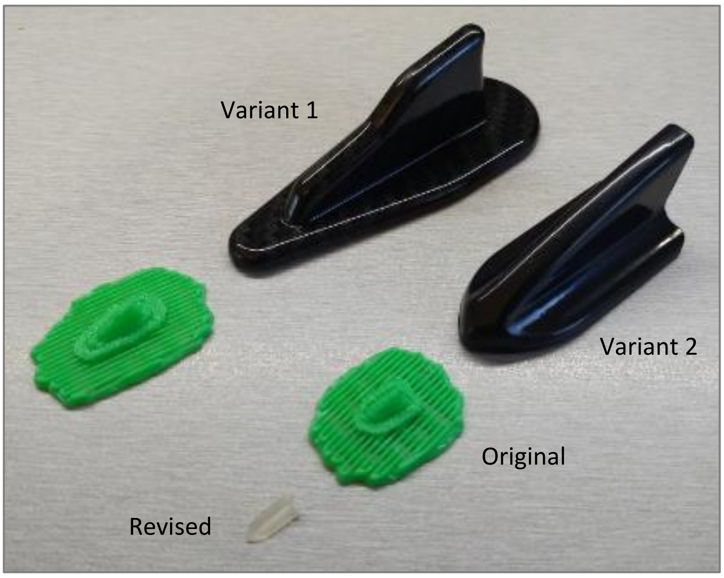

Figure 4.6: Original and revised 3D printed 1:6 scale vortex generators.
Note the printed support base still intact.

The revised 3D printing was completed on a more technically advanced setup at USQ. This allowed for a 1:12 scale design to be used, it is not shown in the above figure as it is too small to define the shape. The higher the resolution, the greater the cost. The original printings were \$0.01 per gram whereas the revised printings were \$1 per gram, this is equivalent to 100 times the cost. For this study the charge was waived by the university. The secondary 3D printer used was the ProJet HD 3500Plus from 3D Systems. This was a UV cured acrylic plastic variant and each layer printed has a thickness of between 32 and 16 micrometres (μm), which is classified as high or ultra-high definition respectively. Usually 3D printers use a filament to create the project, but this machine used a liquid polymer to render the final piece over a six-hour time frame. There was a wax support base for the vortex generators and this had to be melted off in an oven for a couple hours to ensure the piece was to the original dimensions provided in the .STL format.

4.3.4 Scale model vehicle setup

The vehicle needed to be held above the floor in the wind tunnel for the experiments. Otherwise the boundary layer and ground effect properties would have reduced the accuracy of the results. The wind tunnel used a side mount setup that included a 12 mm rod extended through the test section and into a clamp. This allowed for removal of the existing airfoil in place and design of a new rod to be used with my vehicle model. The staff at the USQ Workshop were contacted and helped with the fabrication of the setup. The model was drilled and glued to ensure it would be kept static whilst positioned in the wind tunnel. Otherwise if a non-interference fit was achieved in the process the model would have rotated about the rod and the measurement of the lift and drag forces would have been inaccurate. Figure 4.7 shows the vortex generators and mounting rod attached to the scale vehicle for the experimental tests. Note how the rod sits flush with the edge of the vehicle to minimise airflow disturbances. For additional photos of the control vehicle with no vortex generators attached, the overall length of the rod setup and the AutoCAD drawing for the design, refer to Appendix F.

Figure 4.7: Scale vehicle with vortex generators
attached and wind tunnel mounting rod.

The 3D printed vortex generators were at 1:12 scale, which were the smallest possible to allow the pieces to be glued onto the model due to the extremely small size and the printer's resolution. Therefore it was not feasible to achieve the 1:24 scale in order to match the vehicle. This indicates the vortex generators were twice the size they would be in real life and the results needed to be analysed with this consideration. It can be seen above that no front windows were included in the scale model. To limit the turbulence this would have created, mock windows were made from cardboard and sticky-taped to the model to maintain the streamlined side profile (refer to Figure 5.11)

4.3.5 Testing procedure

The wind tunnel tests followed a set procedure that is outlined within the following section. This allowed for efficient testing and ensured all data recorded is comparable. The wind tunnel system includes equipment that can measure the drag and lift components of the model by way of load cells. The force displayed by the equipment was in Newtons.

The air speed is controlled via a manual input knob located on the control system. It is however not completely accurate, as was found during the Mechanical Practice 4 course. Therefore it was beneficial to use the existing pitot tubes installed to measure a pressure differential within the test section. A pitot tube is a flow measurement device commonly used on aircraft as airspeed indicators. These devices work on Bernoulli’s principle whereby a difference in static and total pressure indicates a relative velocity. The following equations summarise this notion:

$$\text{Bernoulli's principle:}\quad \text{static pressure} + \text{dynamic pressure} = \text{total pressure}$$

$$P_{static} + P_{dynamic} = P_{total} \rightarrow P_{static} + \frac{1}{2}\rho v^2 = P_{total} \qquad (1.8)$$

$$\therefore v = \sqrt{\frac{2(P_{total} - P_{static})}{\rho}}$$

In this case static pressure is the ambient pressure measured from within the test section of the wind tunnel, this will be close to 101.3 kPa. The density of air at this pressure and 20°C is 1.204 kg/m^3.

The following section outlines the procedure for operating the wind tunnel and obtaining the data required for the calculations.

1. Ensure all equipment is in good working order prior to starting tests.
    a. Refer to the created risk management plan (RMP) for ideal safety procedures.
2. Switch on the computer attached to the wind tunnel that has the software used to measure the pressure differences.
3. Open the test section via the side hatch and remove the existing aerofoil and pitot tubes that are used for the Mechanical Practice 4 course.
    a. Install the scale model rig with no vortex generators, to be used as a control.
    b. Ensure the model is level, this will reduce the likelihood of inconsistent drag and lift forces.

4. Zero all the pressure sensors and move the pitot tube into the centre of the wind tunnel.
    a. Calibrate the wind speed by using the measurements at this position
5. Record the air density and static pressure at no airflow.
6. Switch on the fan control system and turn the wind speed control knob until the desired air speed is attained (displayed on the computer screen).
7. Record the various parameters at this air speed (shown in Table 4.2).
8. Increase the air speed for each additional step and record required data.
9. After the data is collected for the highest air speed, lower to 20 m/s.
10. Initialise the smoke machine and use a GoPro to video the flow visualisation.
11. Switch off the wind tunnel fan and wait until it is safe to open the side hatch.
    a. Remove the model and install the second one which has vortex generators attached.
12. Repeat steps 4 to 10, recording all data and using the smoke machine to visualise the flow around the model.
13. Switch off the fan and wait until it is safe to open the side hatch.
    a. Remove the model, clean any residue left from the smoke machine oil and reinstall the aerofoil with pitot tubes to the exact same scenario before starting the tests.
14. Exit the computer software and power down the machine.

Throughout testing, ensure all data is written in the collection tables created.

Table 4.2 specifies the order of testing and what parameters are recorded at each air speed to accommodate the calculations. After the first test, the model (control) is to be removed from the wind tunnel and replaced with another which had the vortex generators installed. The data collection procedure was the same for this test.

Table 4.2: Wind tunnel testing procedure and data to be collected

Task No.	Airspeed (m/s)	Data to be collected
1	0	Static pressure, air density
2	5, 10, 15, 20, 25, 30	Dynamic pressure, static pressure, drag force, lift force
3	20	Flow visualisation using smoke machine

4.4 Computational – CFD methodology

This desktop study was undertaken to analyse the airflow patterns over the vehicle with and without vortex generators installed. The benefit of using a computational method was the ability to obtain quantitative data from the software that indicated the relative lift and drag forces of the vehicle, at varying speeds. In order to make the study as similar as possible to the wind tunnel the model was 3D scanned and used for the analysis. This maintained a level of correlatability between both tests and acted as a verification of what was seen in the wind tunnel tests. The following sub-sections discuss the events that led up to the testing.

4.4.1 3D Scanning

3D scanning uses a high-quality 1.3-megapixel camera, with depth sensing technology to analyse and store data based on three dimensional geometries of real-world objects. The benefit of having a 3D scanner available was the ability to scan the 1:24 scale car model and directly import it into CAD software. The machine was located at USQ's Maker Space and was a Shining 3D brand, version Einscan-SE. This reproduces CAD models by scanning the object and then grouping all the images together into a water-tight model that can be exported to CAD programs in various formats such as .STL, .PLY, .OBJ and .3MF. The setup is shown in Figure 4.8.

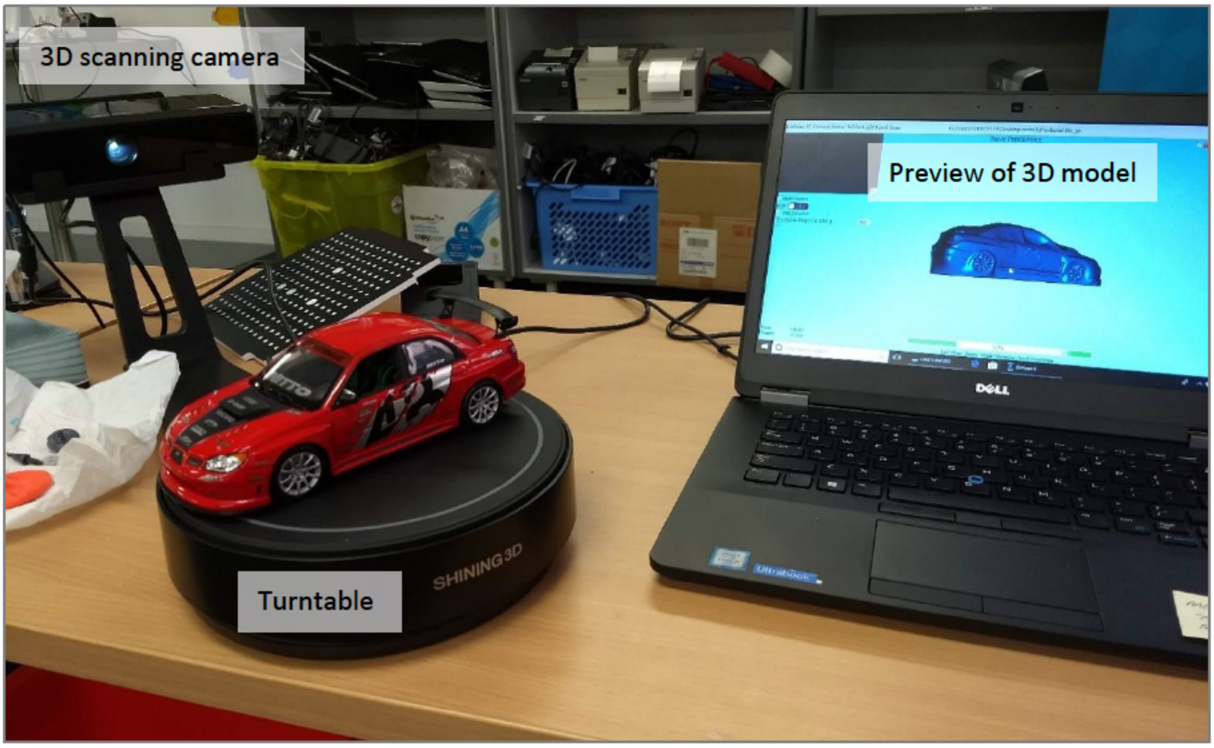

Figure 4.8: USQ 3D Scanning Equipment

There were a few small issues with scanning of the scale model. The clear and reflective nature of the plastic windows along with the glossy paint work and decals made the 3D scanner miss a fair amount of the detail on the model, including the entire rear wing. After this initial scan painter's tape was used to cover the model in an attempt to stop the reflections. This resulted in the scanner picking up adequate detail, but the tape overlap lines were large enough to impact the accuracy of the model.

After advice it was found that by using white acrylic paint on the model the glossy nature could be transformed into a more matte finish. Even though it didn't seem like a significant alteration on the surface, this allowed the scanner to be able to identify the missing detail of previous attempts. A 3D scan of both the model with and without the rear wing was taken in order to allow for various stages of CFD studies. The car was also scanned on its side to allow for an accurate representation of the roof and undercarriage to be detected. The resulting 3D model generated was more than sufficient to be analysed. For additional photos of the revisions on the scale model, see the photos in Appendix G.

4.4.2 CFD setup

The computational testing involved using a 3D scanning of the scale vehicle used in the experimental wind tunnel tests. The software used for the testing was ANSYS, which is a program that includes many simulation software suites. The ones of importance for this study were Workbench, Meshing and Fluent, as detailed below:

- Workbench: Combined all the installed ANSYS applications into a neat overview structure that allows for access to each and monitors product workflow.
- Meshing: An automated mesh generation tool that produced the most appropriate mesh for accurate solutions. It can also be refined by the user's inputs. For example if one specific area is of investigation then a finer mesh would allow for greater precision of results but will take longer to compute.
- Fluent: Contained the broad physical modelling and technical capabilities required to model fluid flow, turbulence, heat transfer or research and development applications. These range from airflow over an airplane wing, to internal combustion within an engine (ANSYS 2019).

There were three stages in the CFD simulation; pre-processing, execution and post-processing. A correct setup will ensure accurate results of a quantifiable nature. The three stages are described below:

- Pre-processing: Requires that the flow domain be setup along with the geometry for testing. Revisions to the mesh might be required to simplify the model in order to exclude features that do not have effects on the flow field. There is as fine balance between ascertaining the optimum mesh size to maintain accuracy whilst not consuming unnecessary computational resources.
- Execution: Involves the solving and number crunching of the test. The user can choose which solver setting is to be used and the appropriate numerical method. Other constants such as material properties, initial and boundary conditions are to be defined.
- Post-processing: The results are displayed from the tests. Visualisation of the flow fields and the desired flow properties are exported. Validation of the simulation can be run, and documentation of the findings can take place (Korff 2018).

It should be noted there were a variety of problems relating to the 3D model. The scanned object in .STL format was incompatible with the CFD software and conversion to .STEP or .IGES had to be completed. This created a multitude of geometry errors relating to self-intersecting faces and non-manifold bodies. These errors created significant work as part of the analysis and took over forty additional hours to fix and obtain results; of which would have been able to be gained within a quarter of this time.

Chapter 5: Results and Analysis

5.1 Experimental – Full-scale

5.1.1 Preliminary testing

Before the bulk of the tests were undertaken a preliminary run was used to identify any faults in the setup and to ascertain the ideal testing procedure. The location of the GoPro camera was positioned in the centre of the rear wing. This gave it a location of 130 mm above the rear wing and the lens was aimed at a downwards angle to ensure the field of view was adequate.

The trial run used three different lengths of twine to determine the most appropriate length. The idea was that a too short piece may not move enough with the airflow and a too long piece may move excessively. The weight of the twine will affect the motion as well. The dimensions for the twine, as indicated in Figure 5.1, were 5 mm, 10 mm and 15 mm.

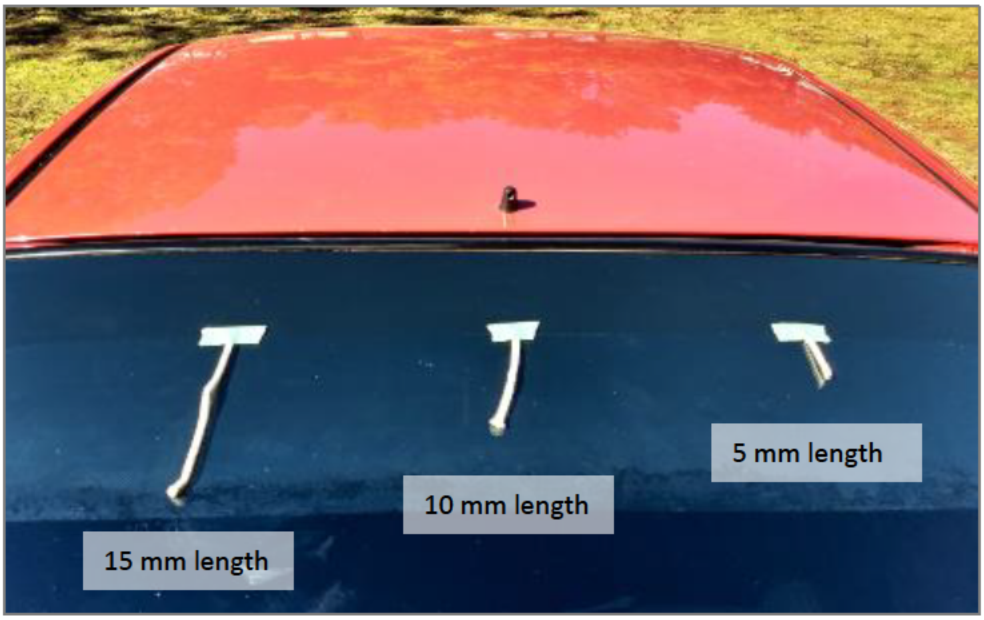

Figure 5.1: Preliminary setup indicating the different lengths of the twine

Three different speeds were chosen to assess the motion of the twine; 50 km/h, 70 km/h and 90 km/h. The results were compiled from analysis of the video recordings. Table 5.1 summarises the findings:

Table 5.1: Preliminary findings with twine at top of windscreen

Speed (km/h)	Twine Length		
	5 mm	10 mm	15 mm
50	No discernible motion	No discernible motion	No discernible motion
70	Little to no motion	Little to no motion	Little to no motion
90	Little to no motion	Little to no motion	Slight motion

These results indicate that the vehicle aerodynamics are of a high level and the boundary layer is still attached were the twine was located. A secondary test was run with the twine moved down towards the bottom of the windscreen as in theory there would be a greater chance that the boundary layer has separated over the increased distance. The findings of this test showed that there was more motion of the twine and this was even greater at higher speeds. The 15 mm twine became quite responsive to airflow changes but never rotated greater than 10°. This movement is still relatively slight and less than expected; in order to create greater motion and therefore be able to see the impact of vortex generators there either must be an alteration in the vehicles speed or the use of a lighter material.

It was at this point the secondary jute twine was purchased from Bunnings. As it was half the thickness, at 3 mm, it was much lighter and featured less weaving per unit length. Another test was undertaken, and it returned more positive results as the airflow induced greater twine movement.

These results indicated that the longer the length of twine, the more it would be impacted by the airflow. There was however, a limit to this length for practical reasons as there needs to be a multitude of pieces attached to the rear windscreen. For the actual tests the most appropriate length of twine to used going forward was the 15 mm.

5.1.2 Test results

The weather conditions were sunny, calm, with temperatures of 14.7°C, humidity of 55% and wind of 13-17 km/h E. It was chosen to undertake the tests on a day where the wind speed was low to mitigate against unwanted cross winds that would have affected the results. A control test whereby no vortex generators were installed was completed first to allow for a before and after situation. This helped to identify any improvements to the airflow. After the control tests the vortex generators were positioned along the trailing edge of the roofline, at the same distance apart and in line with the rear wiper fluid spray nozzle. Figure 5.2 shows the final positioning of the twine and vortex generators for the tests. Please note the green painters tape was used to protect my vehicles paint from the double-sided tape. For additional photos including the control test see Appendix E.

Figure 5.2: Vortex generator test setup.
N.B. the rear windscreen wiper arm was removed

Table 5.2 details the findings of both the control and vortex generator tests. Please note the findings are based on video playback analysis that involved investigating the amount of rotation of the twine and relative motion before and after the installation of the vortex generators. The angle of rotation was roughly estimated by observing a common piece of twine for all tests.

Table 5.2: Findings of the full-scale tests

Speed (km/h)	Findings		Max Rotation (°)	
	Control	Vortex Generator	Control	VG
60	Little to no motion of the twine	Little to no motion of the twine	6	5
80	Slight motion of the twine	Slight motion of the twine	8	7
100	Slight motion of the twine	Slight motion of the twine	10	9

From a previous study by Raykowski (1999) it was seen there was the greatest reduction in drag when the incident angle of the vortex generator to oncoming airflow was at 25°. With this knowledge in mind an additional test was undertaken to determine whether this could be replicated. This angle was tested at the fastest velocity (100 km/h) to ascertain whether or not this would improve upon what was already found. Unfortunately what was discovered was unimpressive. There was no discernible difference from the original 100 km/h test, and it did not reveal any additional information that could be discussed. Extra photos are provided in Appendix E where the angle of incidence is displayed.

Both the control and vortex generator tests were filmed to help indicate the relative findings of the practical experiment. At each velocity the footage was combined into a single clip to make comparison easier. These videos can be found at their corresponding YouTube links below:

Testing vortex generators at 100km/h: https://www.youtube.com/watch?v=rOtDiuWdAEA&t=10s

Testing vortex generators at 80km/h: https://www.youtube.com/watch?v=wi9bHr8FYZc

Testing vortex generators at 60km/h: https://www.youtube.com/watch?v=fcg0uFFIG9Q&t=25s

A screenshot of the video footage is provided in Figure 5.3. It was seen that twine consistently had greater movement on the outside when compared to the pieces in the middle of the windscreen. An explanation would include the curving design of the windscreen that allows air to rush up over the rear quarter panels onto the windscreen which mixes with the flow from the roof, creating slight turbulence. Importantly enough this turbulent region was confined to the outskirts and didn't impact with airflow in the middle of the windscreen.

Figure 5.3: Experimental tests in motion.
N.B. The lack of rotation due to high aerodynamic efficiency

5.1.3 Analysis

Overall, the tests displayed a relative lack of motion from the twine pieces. These underwhelming results indicate that the boundary layer has not separated from the body over the rear windscreen. This was carried over both studies, with the control and vortex generator tests only showing slight increase in motion at the highest speed.

There was an explanation for this, and it lay in the design characteristics of the test vehicle. As a Honda Integra Type R has a coupe body type the roofline to boot angle is much less than a sedan, thereby producing a more streamlined shape. In fact, the angle is 17° compared to the STI with 26° and Evo 8 with 27°. A reduced angle allows the boundary layer to stay attached for longer and potentially not detach at all. As the angle increases so does the likelihood the boundary layer will separate from the body.

Even though the results are inconclusive and not what was expected, there is a positive to come from the tests. The findings indicated that there would be a greater likelihood that the STI vehicle tested in the wind tunnel and via CFD will create a situation where the boundary layer has separated from the body, due to the larger roof to boot angle. This should encourage a discovery of whether the use of vortex generators is beneficial.

These full-scale tests were not conceived to gain quantitative data in such a way to produce conclusive results. It was seen as a way to visualise the boundary layers delayed separation from the body. The ideal results would have seen a remarkable amount of movement of the twine pieces for the control tests and discernibility less motion when the vortex generators were installed. However, the tests showed that there were minimal differences between the before and after situations and this could not help to provide a definite conclusion that vortex generators work.

This motion of twine was found by analysing the video footage of each test and using a protractor on the monitor to estimate the angle of rotation of the twine piece. To ensure consistency between the tests a common piece of twine was of investigation. This method was basic, but the only way to record the motion. If there was software that had this capability it would have produced more accurate scientific results.

5.2 Experimental – Small-scale wind tunnel

The following images were taken to display how the scale model was positioned within the test section of the wind tunnel.

Figure 5.4: Position of the model in wind tunnel

Figure 5.5: Position of the model in wind tunnel (close-up)

5.2.1 Test results

All the data identified in the methodology that was required for the calculations was recorded throughout the testing and displayed in the following Tables. The pressure was recorded in the wind tunnel by way of a pitot tube positioned before the model and at a height in line. This helped to calculate a more accurate airspeed value than what was displayed on the computer screen.

Table 5.3: Recorded data and calculations for the control test

Test 1: Scale Model w/o vortex generators (control)								
Displayed Airspeed (m/s)	Air Density (kg/m3)	ΔPressure before the model (Pa)	Pressure after the model (Pa)	Calculated Airspeed (m/s)	Drag force (N)	Lift force (N)	Coefficient of Drag	Coefficient of Lift
0	1.23	0	0	0	0	0		
5		15	17	5.26	0.02	0.02	0.30	0.30
10		62	62	10.04	0.19	0.06	0.79	0.25
15		136	138	14.87	0.45	0.13	0.85	0.25
20		248	250	20.08	0.86	0.23	0.89	0.24
25		383	380	24.96	1.29	0.37	0.87	0.25
30		553	553	29.99	1.91	0.58	0.89	0.27

Table 5.4: Recorded data and calculations for the vortex generator test

Test 2: Scale Model with vortex generators								
Displayed Airspeed (m/s)	Air Density (kg/m3)	Pressure before the model (Pa)	Pressure after the model (Pa)	Calculated Airspeed (m/s)	Drag force (N)	Lift force (N)	Coefficient of Drag	Coefficient of Lift
0	1.23	0	0	0	0	0		
5		15	18	4.94	0.04	0.01	0.69	0.17
10		60	64	9.88	0.19	0.04	0.81	0.17
15		136	141	14.87	0.47	0.10	0.89	0.19
20		246	250	20.00	0.86	0.22	0.90	0.23
25		385	391	25.02	1.37	0.35	0.92	0.23
30		553	572	29.99	2.02	0.55	0.94	0.26

N.B. The calculated airspeed was based on the pressure upstream of the scale model and using the following equation:

$$v = \sqrt{\frac{2 * P_{upstream\_differential}}{\rho}} \tag{1.9}$$

The pressure measured before the model was at a height of 150 mm off the floor, which correlates with the middle of the test section. As the wind tunnel inlet is compact the velocity of air differs throughout the 1D cross-section; meaning the airspeed displayed on the computer will not be completely accurate for positions other than where the pitot tube is positioned. From previous wind tunnel experiments this discrepancy between the floor and middle are significant due to boundary layer flows.

The drag and lift forces were plotted in Figure 5.6 and 5.7 to indicate the relative changes between the control test without the vortex generators and the following test when they are installed.

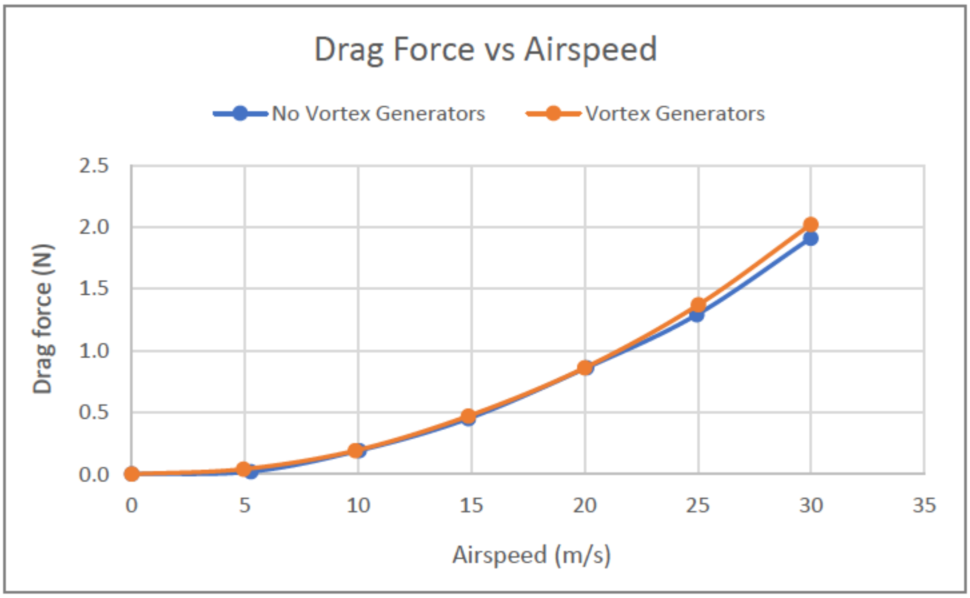

Figure 5.6: Drag force vs airspeed for both tests

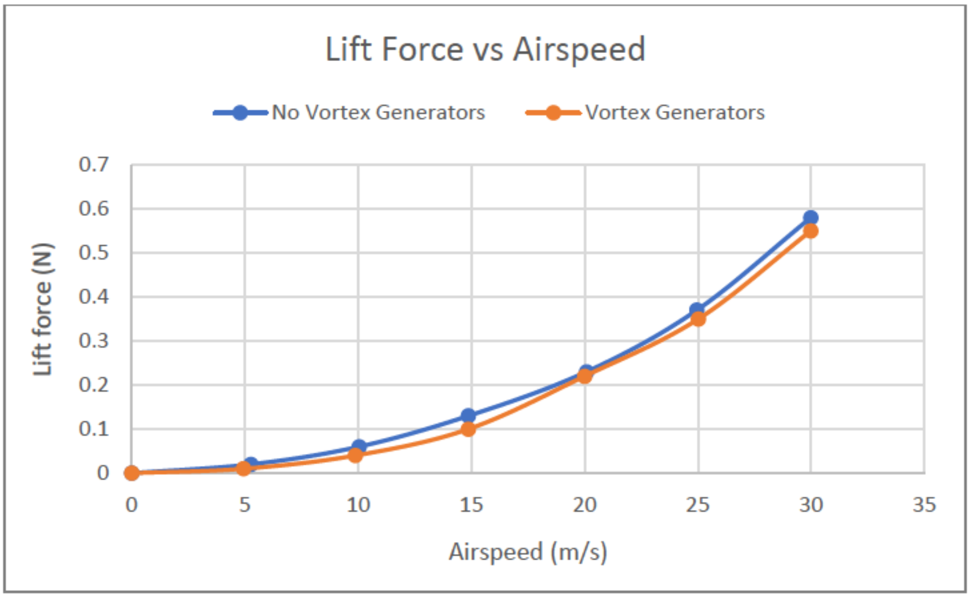

Figure 5.7: Lift force vs airspeed for both tests

The values for C_D and C_L were calculated at each data point and plotted in Figures 5.8 and 5.9 respectively. It is interesting to see that the values change with airflow velocity. Both tests are included in the same chart for correlation.

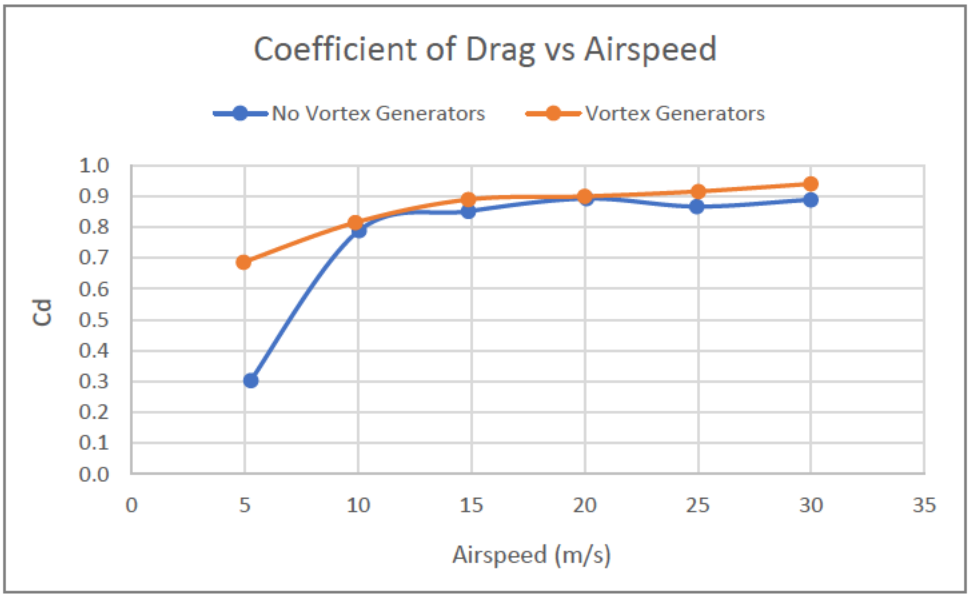

Figure 5.8: Coefficient of drag vs airspeed for both tests

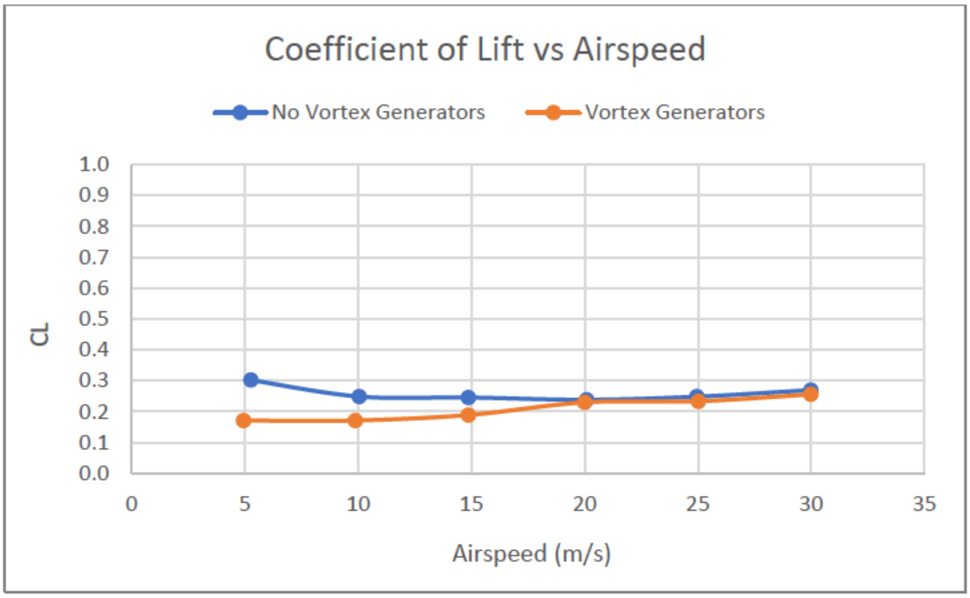

Figure 5.9: Coefficient of lift vs airspeed for both tests

A smoke machine was used to help visualise the flow around the vehicle. The most indicative findings are shown in Figures 5.10 and 5.11. The test setup was not ideal which made it difficult to see the flow over the surface of the vehicle.

Figure 5.10: Smoke streamlines flowing over the control vehicle

Figure 5.11: Smoke streamlines flowing over the vortex generator vehicle

Video footage was captured during both smoke visualisation tests and edited into a short clip. The YouTube link is included below:

https://www.youtube.com/watch?v=qJIIZxGVXjU

5.2.2 Analysis

The experiments in the wind tunnel provided a clear understanding of how the drag and lift forces both increase exponentially with greater airflow velocity. By measuring the pressure upstream of the scale model it was beneficial to include the calculated airspeed through the wind tunnel test section. This allowed for a more accurate curve to be plotted; even though the discrepancy between the displayed airspeed and calculated airspeed was in the order of less than 5% at low velocities and 1% at higher velocities.

The drag force of the secondary model with the vortex generators showed an increase when compared to the control. For example, at the highest airspeed (30 m/s) tested the drag exerted on the load cell was 2.02 N compared to 1.91 N. These forces are relatively small however when directly compared they differ by 5.4% and the curve indicates this would only become larger upon faster velocities. At first glance this seems to be contrary to the hypothesis but upon further investigation reasoning behind the results can be discovered. In the literature review several studies identified that there was an optimal height of the vortex generator to optimise its effectiveness. It was also seen that if the passive aerodynamic device was greater than a specific height, relating to the boundary layer thickness not only does the usefulness of the device diminish but a negative impact on drag would be ascertained. This is what was found in the small-scale wind tunnel tests as the vehicle was at a 1:24 scale whereas the vortex generators were at a 1:12 scale. This essentially brought about a situation whereby they were double the size they were designed for and lead to creation of substantial form drag (refer to Section 3.2). Unfortunately, this was the setup that was most achievable. The use of a larger scale model would not have been possible due to the test section size requirements and the potential for boundary layer effects to impact the data collected. Also the vortex generators could not be 3D printed at a smaller scale (i.e. 1:24) due to their dimensions becoming too small for the resolution of the printer, where anything less than 1 mm in width at the shallowest section was impossible to replicate.

Engineers of performance cars tend to influence design aspects that lead to a reduction in the overall lift of a vehicle. Amongst other things this increases the traction of the tyres to the road, which provides greater handling characteristics. The addition of a rear wing can help to create negative lift (downforce) and ensure the net lift force is acting downwards. From the data retrieved from the testing it was seen that throughout all airspeeds the lift force exerted by the vehicle decreased slightly when the vortex generators were installed. At the maximum velocity tested of 30 m/s there was a 0.03 N reduction in lift when compared to the control test. Even though this value is small a trend occurs throughout the entire range of tests, indicating there is a correlation between the use of vortex generators and a reduction in lift forces. For reference the largest difference (negating outliers) was recorded at 15 m/s where the lift was 30% less. However, it should be noted at such small values slight differences are magnified. This can be seen for the data collected at 5 m/s where the difference was 100% but the actual forces recorded were 0.01 N and 0.02 N respectively, which can be misleading if not studied in detail. The original press release from Mitsubishi stated that the vortex generators helped direct airflow over the rear wing to increase its efficiency. This would mean it creates more downforce and in doing so the lift would be reduced. This is what could possibly be occurring in the small-scale wind tunnel tests.

The smoke machine was to visualise the flow around the vehicle and provide an indication of the flow over the roofline at various speeds. Unfortunately, it was discovered that it would not be possible to attain this information due to a number of factors. The relatively short wind tunnel inlet with small radius of curvature had the potential to influence the velocity distribution profile and mix the airflow, reducing the effectiveness of the smoke visualisation. Also, the small scale of the vehicle reduced the frontal surface area, this resulted in a wide stream of smoke that encapsulated the model instead of hitting a fine point on the model and traveling over. It could be possible that smoke visualisation is common for larger scale and even full-scale vehicles but are not ideal for use on smaller objects due to the limitations of the device. It was therefore not possible to visualise the additional turbulence that the boundary layer separation causes and to ascertain whether the addition of vortex generators could produce a visible reduction in the turbulent rear wake behind the vehicle.

There were a number of undesirable factors that were involved with the testing. For the scale model to be held in position at the centre of the test section a 12 mm metal rod needed to be drilled and glued into the side of the vehicle. This rod extended out of the test section and would have impacted the aerodynamics of the overall shape. However, as both models had the same setup a direct comparison between before and after the vortex generators were installed would still provide indicative results; just not the accurate data of a true representation of a vehicle with them installed. It was also noticed that the scale model with the vortex generators installed was not positioned perpendicular to the metal positioning rod. Due to the gluing of the rod to the door of the model there was an angle of less than 5° that could have varied the results. The test section where the model was positioned normally housed an aerofoil which extended out both sides of this perspex section. This meant there was a 40 mm diameter hole in one side that would normally be covered with the aerofoil setup. In order to ensure the pressures recorded were accurate it was required to cover this gap with some tape. This was not an ideal solution but the only fix that could have been applied. The effectiveness of this method was adequate but still discussed.

5.3 Computational - CFD

5.3.1 3D vehicle model used for computational analysis

The 3D vehicle model was opened in CREO Parametric software for pre-study viewing and analysis. Figure 5.12 indicates the accuracy of the model. The 3D scanning process, while accurate, resulted in a less than perfect representation when imported into CAD software. The lack of front windows on the actual scale model created a slight depression in the side profile when creating a water tight model in the scanning software. This has the potential to cause slight alterations in the airflow around the model in the CFD software.

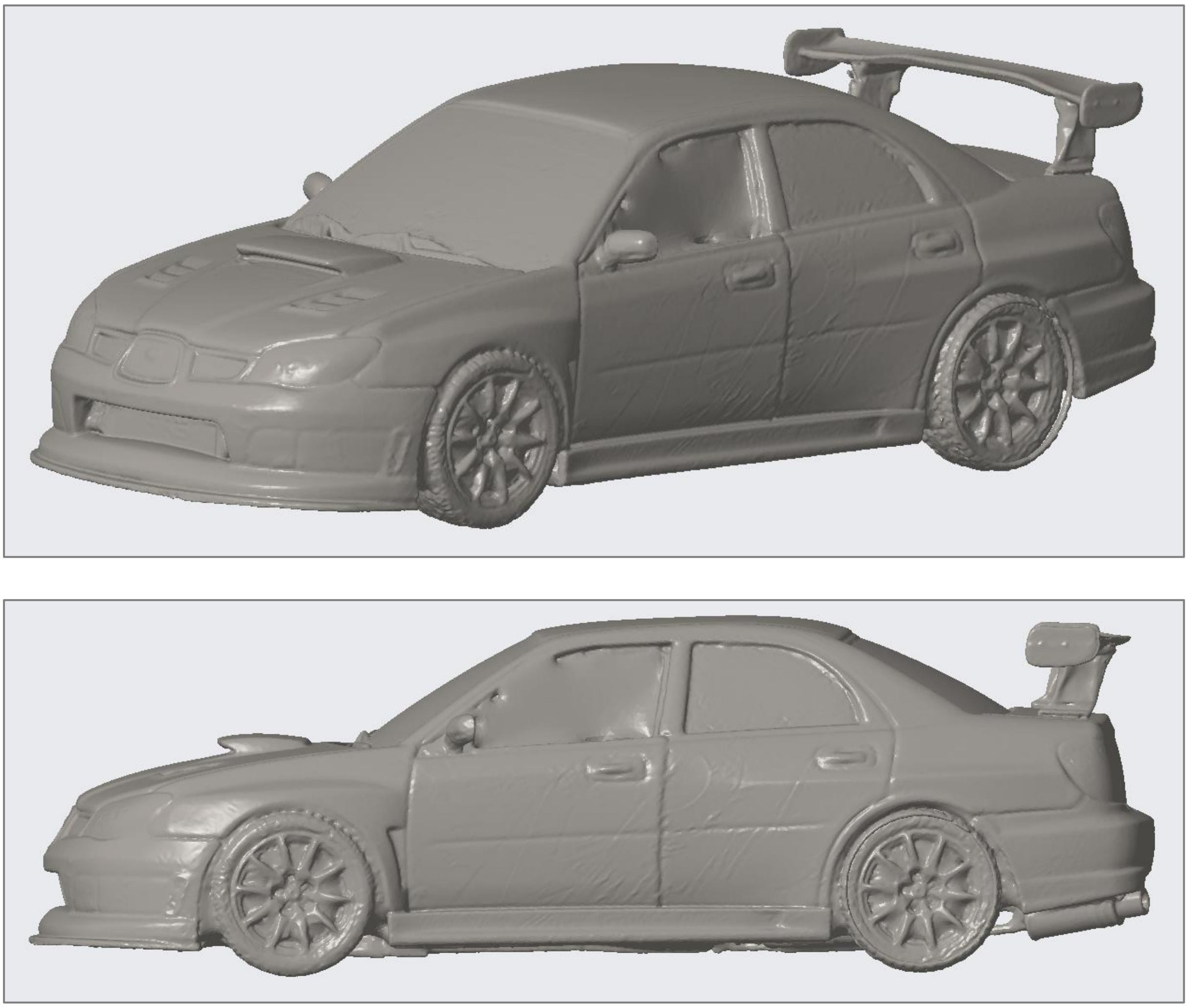

Figure 5.12: 3D model with wing, angled view (top) and side view (bottom)

The scale model was scanned both with and without the wing installed. This allowed for additional CFD analysis if time permitted. For additional photos of the CAD model without the wing refer to Appendix H. Overall the 3D models created from the scanning process was of adequate quality and accuracy to allow for CFD modelling. It should however be mentioned the presence of the hood scoop is not included in the design of the Lancer Evo 8 MR and may change the airflow over the front section of the vehicle if the boundary layer separates before the roof it might be beneficial to remove the hood scoop in CAD before the final CFD results are taken.

5.3.2 3D scanned vortex generators

Four variants the vortex generators were 3D scanned and their 3D models are displayed below to indicate the relative design changes of each. Variant 3 was chosen for the CFD analysis as it closely represented the design used on the Mitsubishi Lancer Evolution 8. A scale of 1:24 was achieved for the CFD testing.

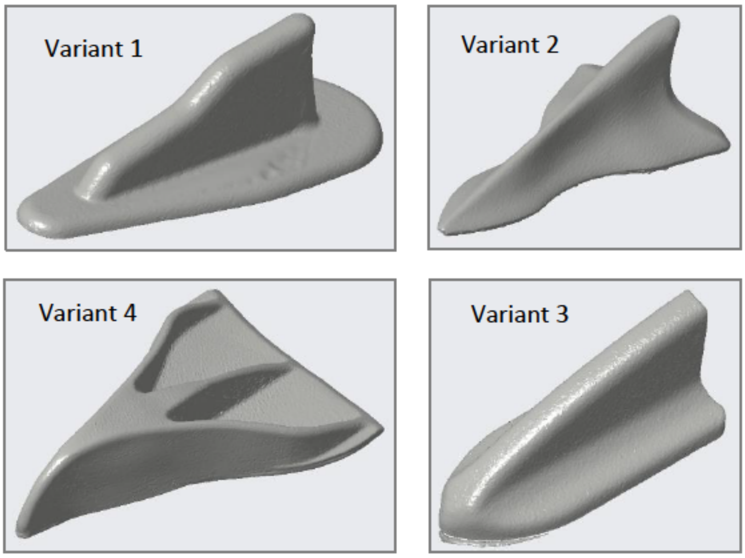

Figure 5.13: 3D scanned CAD models of various vortex generator designs

5.3.3 Revision of 3D scanned objects

Due to the high resolution of the 3D scanning equipment the file size for both the model car and vortex generators was excessive. For example, a simple scan involving 20 snapshots (over the 360° range) and medium detail for a vortex generator returned a .STL file size of 84.2 megabytes (MB). This size was increased for the model car as it was very detailed and required a more thorough scan. Large file sizes made analysis difficult and the computational times too long. It was therefore decided to reduce the file size via third-party software to reduce the strain put on the Z Block computers.

The reason as to why the file size was large is due to the scanned object's polygon mesh. This encompasses a collection of vertices and faces that add together to create the final mesh. It was discovered that by simplifying this mesh it reduced the file size significantly, but adequate detail remained for CFD testing. A program called MeshLab was used to re-mesh the model into a simpler form. Table 5.5 indicates the relative compression achieved by using the quadratic edge collapse decimation technique.

Table 5.5: Technical comparison before and after refining the polygon mesh

Re-mesh computation	Vertices	Faces	File size (MB)	Compression (%)
Before	862 341	1 724 678	84.2	97
After	26 951	53 896	2.6	

The reduction in file size produced a noticeably smoother surface finish but maintained an adequate level of surface detail. The original surface roughness of the 3D scanned objects came from the applied white acrylic paint on the objects which was a requirement to ensure the camera could pick up all the detail.

However, it should be noted that this compression in file size did have significant negative impacts that were only discovered once CFD studies were underway. This relative reduction in quality caused a slew of geometry errors to be encountered when the object was imported into ANSYS and where enclosures and Booleans were required in order to start testing. This did not just occur with the 3D scanned vehicle but also when the vortex generators were positioned on the roof as this added detail created more errors that put a halt on testing until they could be fixed.

From research it was found that the main cause of all the errors was the fact the 3D scanned objects are saved as a mesh (.STL) and the compatibility of this format with CAD and CFD software is minimal as these platforms prefer to analyse a solid object. It was possible to use the ANSYS SpaceClaim software to merge the faces of the mesh into a solid object and then export as a solid model (.STEP). This however still posed problems whereby the vortex generators were deleted from the file for reasons out of my control. The only solution was to use the mesh file and save into solid form once already created the ANSYS Workbench save file. That way no additional exporting then importing was required, this seemed to fix the issue.

Countless methods were used to try and patch the object in order to be able to run the tests. The use of various third-party software and even SpaceClaim and DesignModeler's in-built repair functions were attempted to create a model with no geometry errors. This was additional work that was not expected and took dozens of hours in order to find a method that would work based on a trial-and-error approach.

Due to the aforementioned geometry errors the 3D model needed to be revised in order to allow for a CFD study. Without these alterations the analysis would not compile, and no results could be obtained. The ANSYS SpaceClaim software included a function whereby the model could be shrink-wrapped. This feature removed high definition faces and vertices and made the object more streamline. By doing so some detail was lost but it essentially removed all the geometry errors that came from the 3D scanning and file conversion process. This reduction in model quality was a necessary step in moving forward with the computational study. In Figure 5.14 this revision is shown, the shrinkwrap is set to a gap of 3 mm. Any smaller would increase the resolution of the model but took exponentially longer to process and substantial increases in file size. After many attempts and crashed software this size was determined to be the most acceptable for the tests.

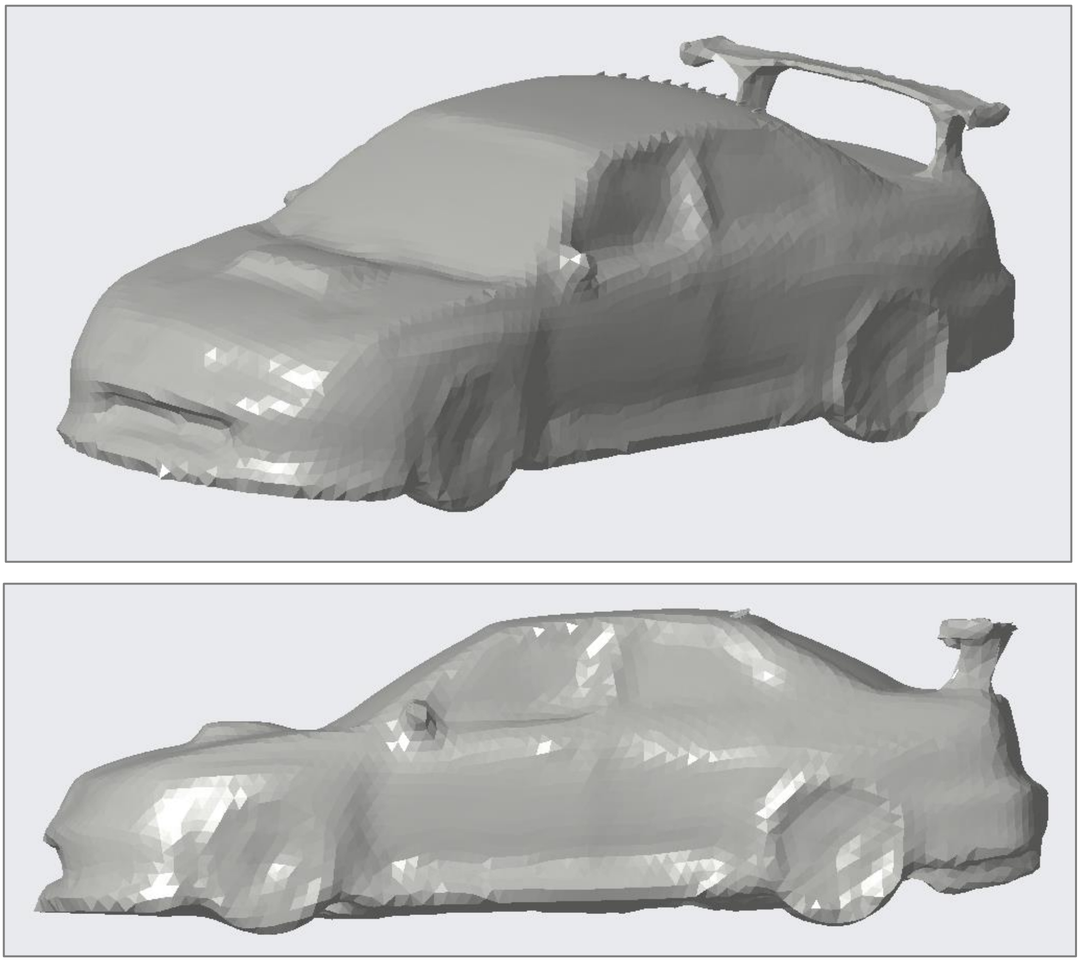

Figure 5.14: Revised 3D model used for CFD analysis.
N.B. the shrinkwrap and vortex generators

5.3.4 Singular vortex generator testing

To help visualise the flow patterns downstream of a vortex generator it was beneficial to perform a study on a singular device. By using the third variant it lined up with the testing performed on the full vehicle and provided a look into how this device performed by itself.

The ANSYS setup was the same as the full vehicle test, including the mesh sizing and calculation used. The only real difference was the enclosure was edited to fit the device. For this test the enclosure didn't need to simulate the wind tunnel test section but how the device is used in real life, where it is installed on the roof of a vehicle (i.e. no flow under the device). This was attempted to be replicated in ANSYS, but an enclosure requires a gap between the object and its boundary (cannot sit flush). Therefore a gap of 1 mm in the negative y-axis was the best achievable outcome, and it did not influence the results.

Once run, the computation achieved a convergence of $1 * 10^{-4}$ for the tests. Airflow velocities from 5 m/s to 30 m/s where studied and it was found that the effect of the vortex generator on the downstream airflow could be easily identified. Figure 5.15 displays how the device creates turbulence in its wake and mixes the high velocity free-stream airflow (orange/yellow) with the slower moving airflow (green/blue). It is noticeable that the region of fast-moving air does not continue its horizontal path after the vortex generator but deflects downwards into the turbulent wake. This is the very concept that was detailed in the literature review.

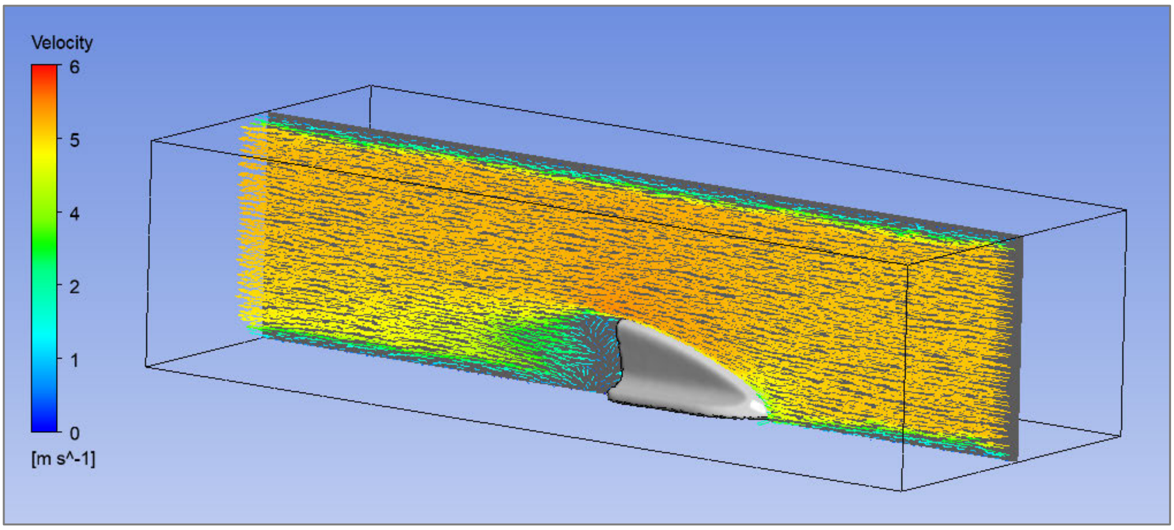

Figure 5.15: Vector plot of 5 m/s airflow over a vortex generator

Note the boundary layer of slow-moving air along the bottom surface. This is due to the no-slip boundary conditions created in ANSYS. The top surface can be neglected as it is merely the extent of the enclosure. The streamlines were created by way of a vector plot, a trial-and-error approach was used to find a suitable scale for the lines and the quantity that displayed the information well. When more vectors are added it was easier to distinguish the downward motion of the free-stream airflow as shown in Figure 5.16. Due to the turbulence of the rear wake this device is seen to also create its own form drag which negatively affects the theoretical benefit of the device and this is why its relative sizing for each application is of great importance.

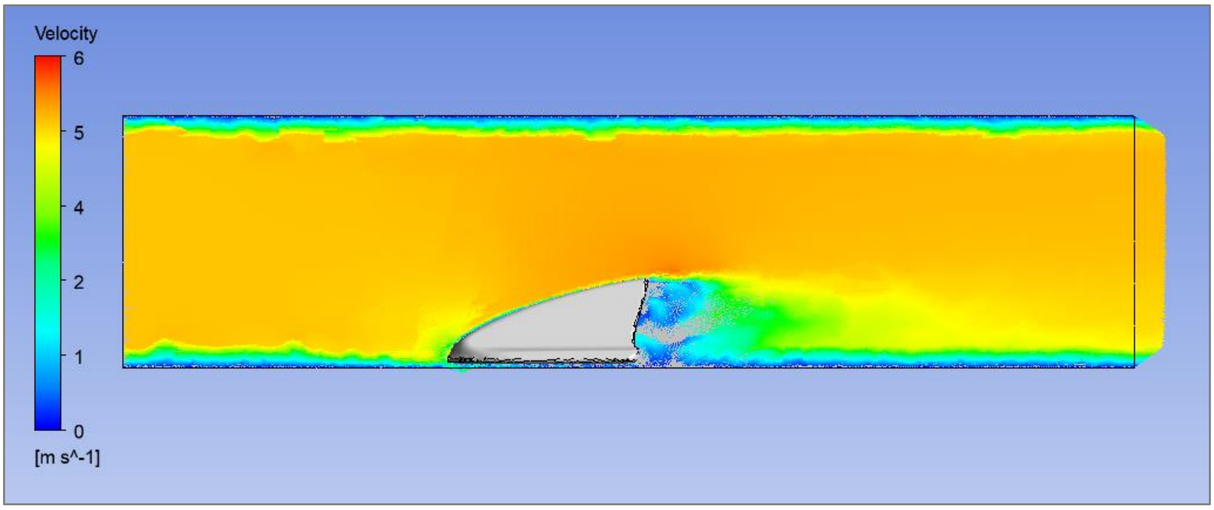

Figure 5.16: Side view featuring more vectors

5.3.5 ANSYS setup

For the pre-processing stage the wind tunnel was modelled in ANSYS DesignModeler to encompass the scale vehicle with the same dimensions as its real-world counterpart. This would allow for correlation between the experimental and computational tests. A Boolean was created to subtract the vehicle from the surrounding enclosure to allow for an external flow analysis. Figure 5.17 identifies the boundaries of the wind tunnel, set up as a flow domain and are labelled as shown. These surfaces along with the vehicle were meshed using ANSYS Meshing, the additional details of the mesh are shown in Appendix I.

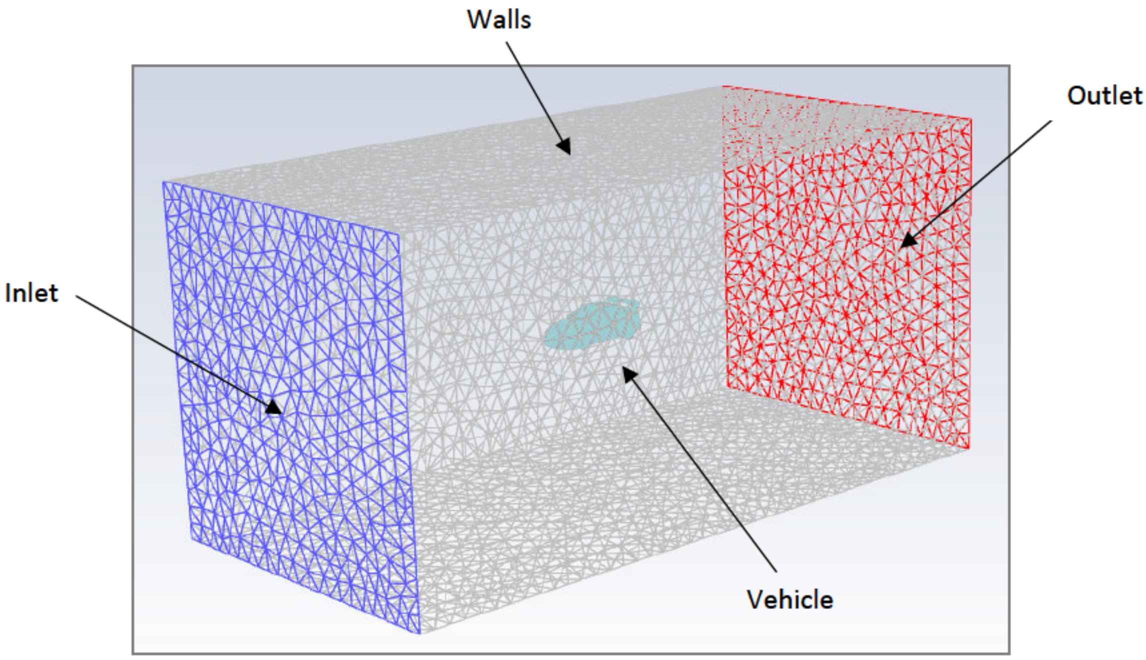

Figure 5.17: Mesh setup used on the computational experiments.
N.B. inlet and outlet positions

Once the mesh was created then Fluent was used to run the simulations. The program was run for a 3D test, with double-precision enabled and use of parallel processing power. Once in Fluent there was a few basic steps to ensure the study would run well. This included:

- Setting up the viscous model as laminar flow (k-epsilon, k-omega and Reynolds stress were also tested but not used for the final results),
- Ensuring the fluid and solid materials were correct, i.e. air density @ 15° C,
- Boundary conditions were set up for the inlet, walls and outlet,
    - Inlet: absolute velocity magnitude, in the negative z component direction, with varying airspeed from 5 to 50 m/s.
    - Walls: stationary with no slip shear condition and negligible roughness,
    - Outlet: gauge pressure set to zero,
- Hybrid initialisation to help estimate the relative convergence of the solution $(1 * 10^{-7}$ was reached),
- Mesh was checked, improved and repaired as necessary.

The calculations were setup to have 500 iterations at a reporting interval of 1 second.

There were two parallel tests undertaken for this study with the only difference being one vehicle had the vortex generators installed whereas the other one (control) did not. This was to have a baseline result for a traditional vehicle and allow for a direct comparison with what was found after installing the aerodynamic devices.

5.3.6 Test results

The following sub-sections provide detailed plots of both tests, i.e. with and without vortex generators. Airspeeds from 5 m/s to 50 m/s were investigated and the plots are a result of the 20 m/s calculation. ANSYS CFD-Post was used to view and export the results instead of Fluent as it was more user friendly.

There were two ANSYS Workbench files for each test. One had an enclosure that replicated the full size of the wind tunnel in order to obtain the lift and drag values that can correlate with the small scale tests. However when the test section was very large the streamlines were not easily distinguishable around the vehicle and it was decided to use another enclosure size that was more suited to this visualisation. Therefore a smaller second enclosure was used for some plots.

Vectors

After trial-and-error a total of 5000 equally spaced points with a symbol size of 0.7 was used to display the velocity profile over the vehicle. Figure 5.18 is plotted along the YZ plane's centreline (which corresponds with the centre of the vehicle) whereas Figure 5.19 was offset by 0.02 m as to show how the rear wing influences the flow.

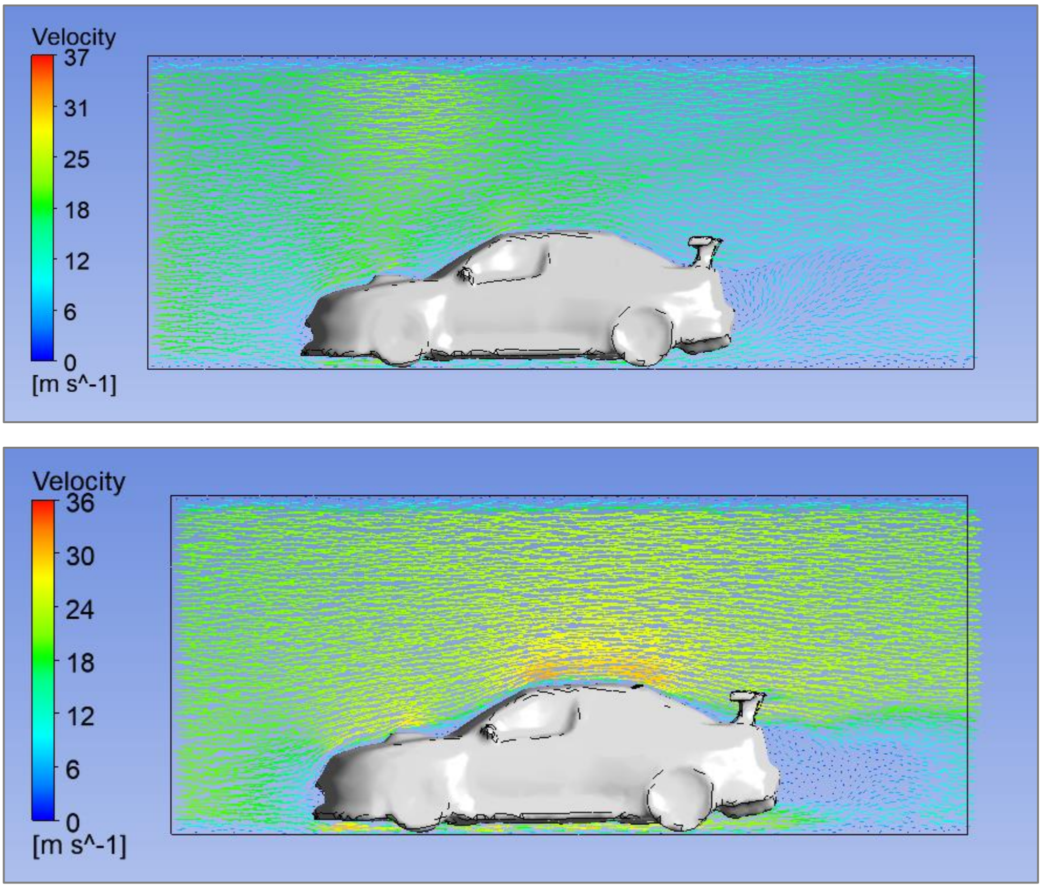

Figure 5.18: Vector plots of the control (top) and vortex generator test (bottom) from a side view along the YZ plane's centreline

The increase in velocity above the vehicle at first seemed to be due to the enclosure size. However, upon modelling it within a very tall enclosure the vectors continued to behave as shown and even got less accurate, so it was decided to use the smaller enclosure to produce the best visuals.

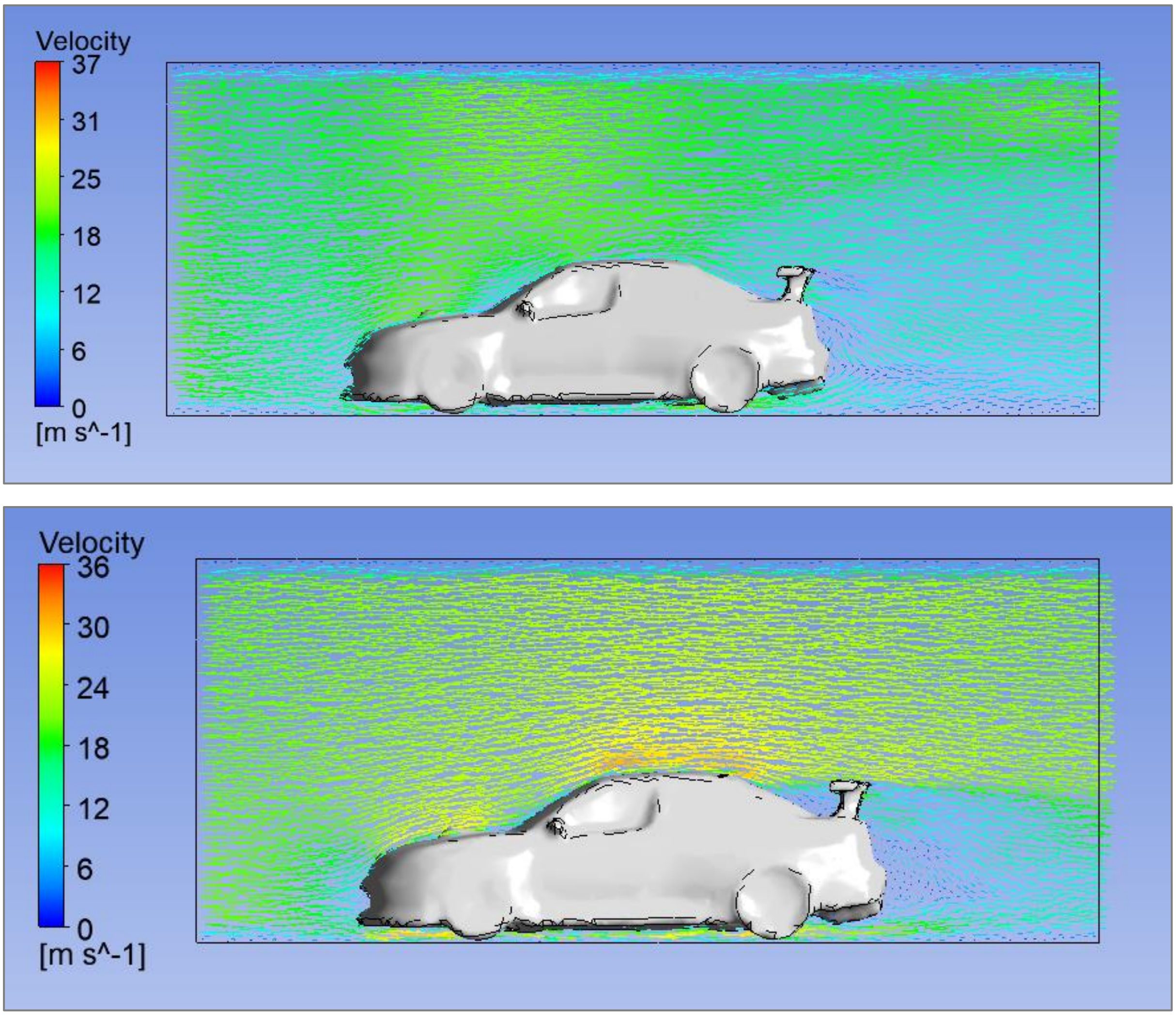

Figure 5.19: Vector plots along an offset of the YZ Plane

Contours

The pressure distribution around the vehicle was displayed by using a contour plot. A large range of contours were experimented with, between 14 and 100, and after analysis it was found that when 50 contours were used it was more than adequate for displaying the regions of high and low pressure. Figure 5.20 identifies the area such as the stagnation point the front of the vehicle, the impact from the hood scoop and the turbulent wake region behind the vehicle.

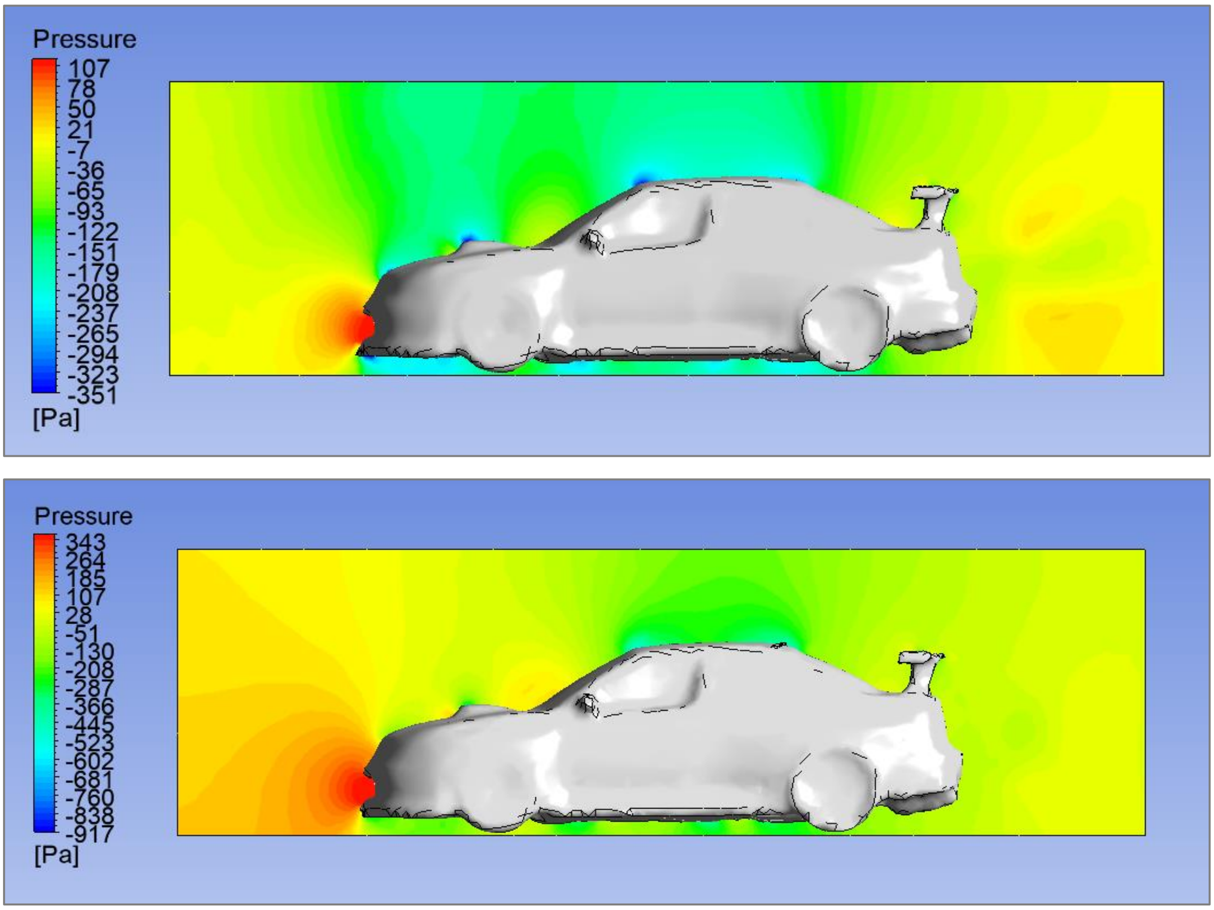

Figure 5.20: Contour plots of the control (top) and vortex generator test (bottom)

N.B. The legend for the contour plot was not customisable and was based on the number of contours used in the plot. As more than a dozen contours were used the legend was not ideal with a multitude of value ticks. The only way to reduce the number was to reduce the contours, which produced an image that was not ideal. It was therefore chosen to keep the large number of contours.

An additional test was undertaken with a taller enclosure in an attempt to remove the large regions of low pressure above the vehicle, but the results were the same.

Streamlines

In addition to the vector plots, streamlines plots were included. The benefit of streamlines is that it visualises flow that is impacted by sharp edges such as the hood scoop or the rear wing. For this study 60 equally spaced streamlines were placed on the YZ plane for Figure 5.21.

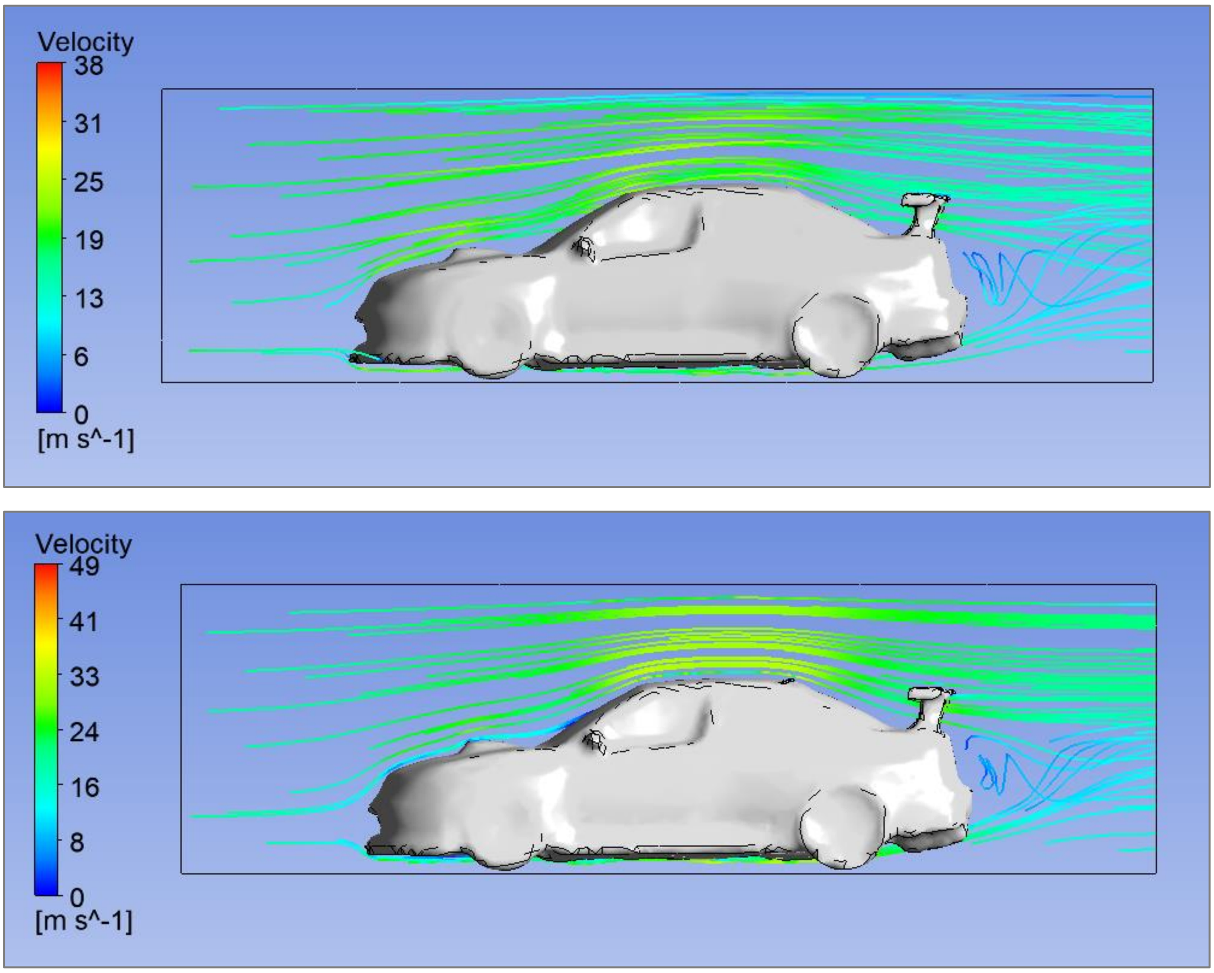

Figure 5.21: Streamline plots of the control (top) and vortex generator test (bottom)

The streamlines shown below in Figure 5.22 were positioned at an offset of 0.02 m to show how the side of the rear wing impacts the airflow. Once again 60 equally spaced streamlines were input into the calculation. It can be seen that the flow from under the vehicle attributes to the overall turbulent wake region behind.

N.B. The higher velocity streamlines over the roof of the vehicle are not due to the small enclosure. The same test parameters were repeated on a taller enclosure with the same results.

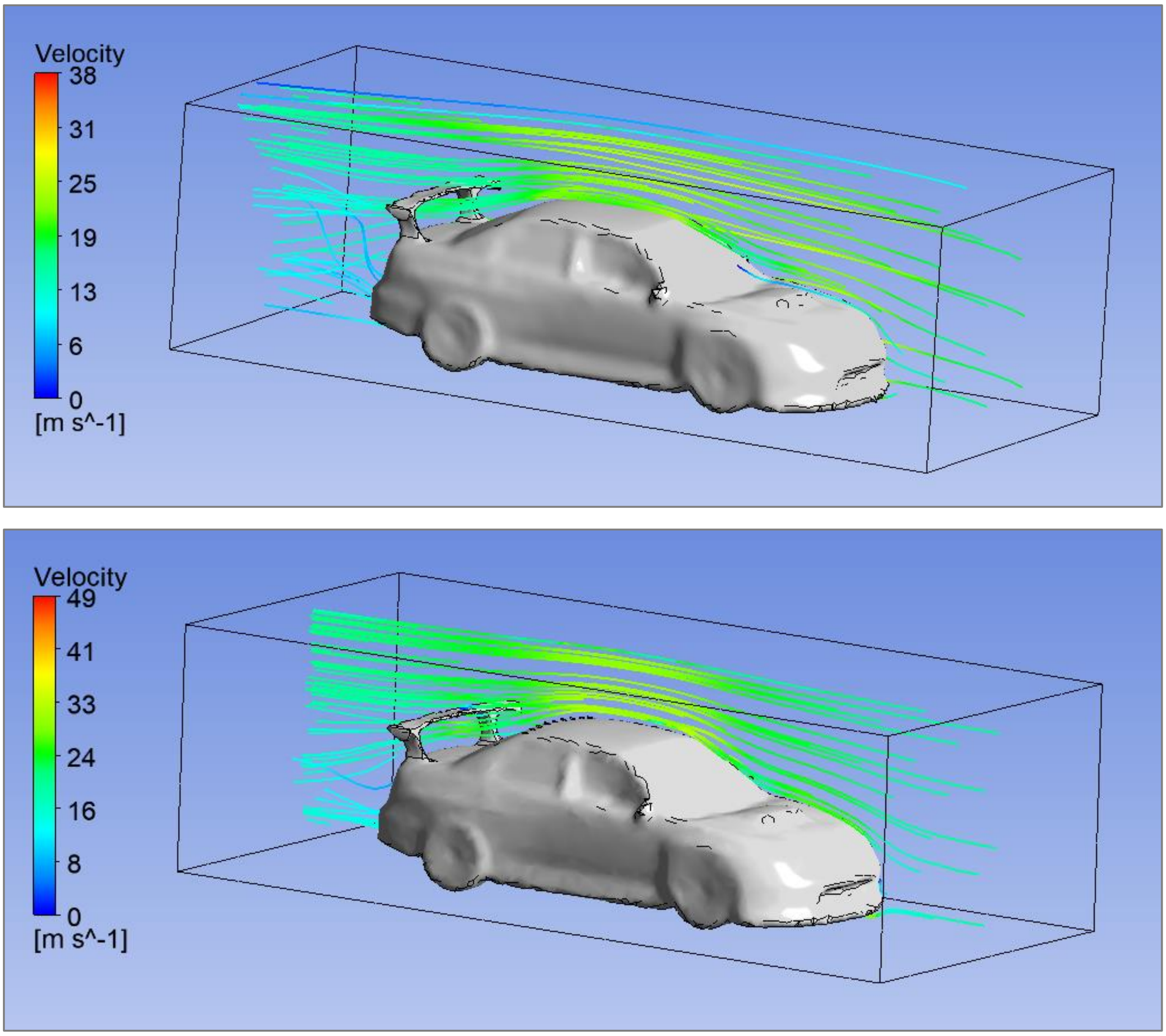

Figure 5.22: Streamline plots from another angle.
N.B. the flow under the wing

Drag and lift forces

The ANSYS Workbench file that replicated the full size wind tunnel as an enclosure was used to calculate the drag and lift forces at various airspeeds. This was undertaken to determine the effectiveness of the vortex generators and see if there was any quantifiable data that could predict how they impact the drag of a vehicle. The lift force and drag coefficient were also recorded.

ANSYS Fluent was run with 500 iterations at double-precision and using 2 CPU threads to calculate the following data from the solver built into the software. The scaled residuals convergence was consistently achieving $1 * 10^{-5}$ for the models tested. The finest mesh resolution was implemented that kept the specific number of cells under the 512 000 limit imposed by the educational version of ANSYS. Any further revisions to the mesh or by using the improve mesh feature in Fluent returned the same results, indicating the setup was accurate. An example of the scaled residuals convergence plot and the drag force plot are shown in Figures 5.23 and 5.24 respectively. It can be seen that 500 iterations may have been excessive with the drag force calculations being mostly constant approaching the 150 iteration mark.

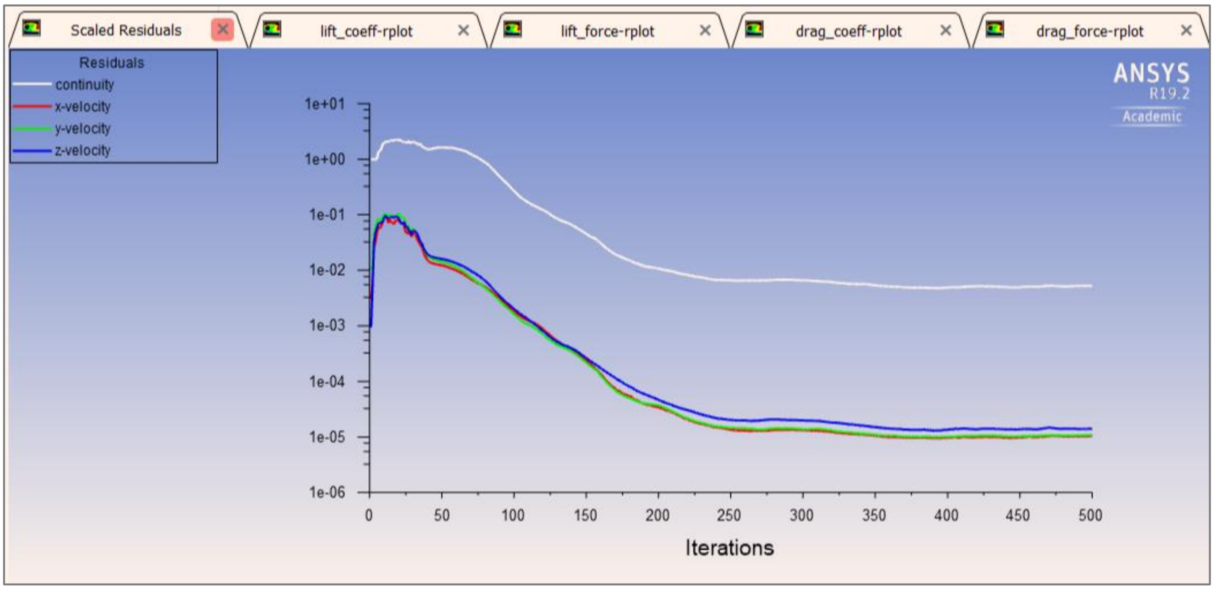

Figure 5.23: Scaled residuals convergence plot over 500 iterations

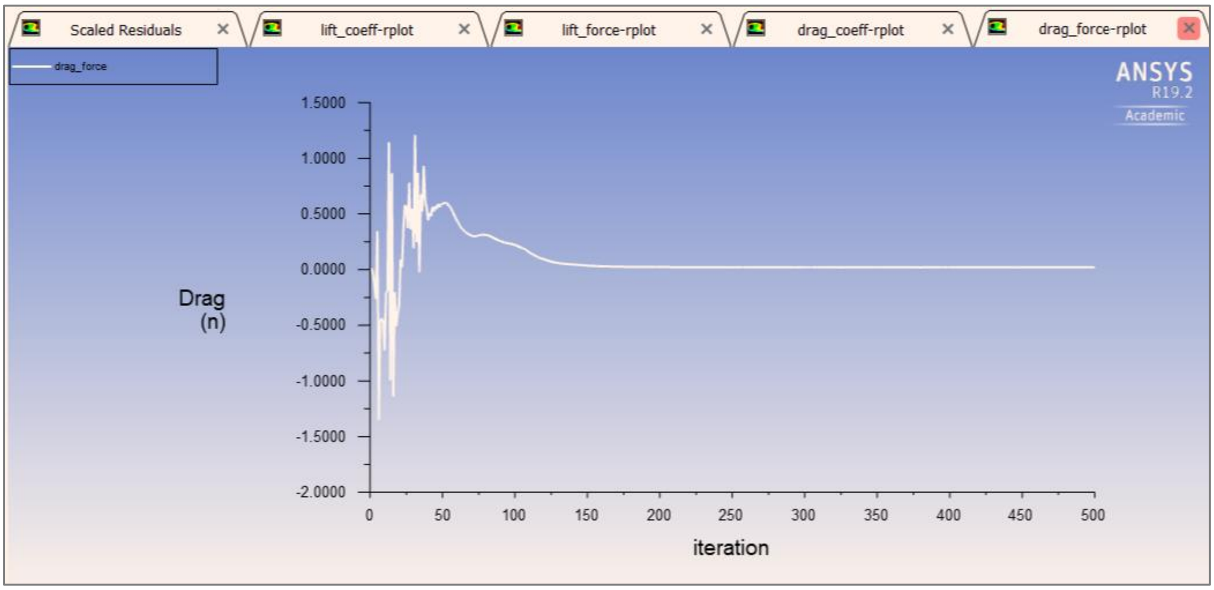

Figure 5.24: Drag force plot over 500 iterations

The data calculated by the Fluent solver for the drag and lift forces, along with the coefficients are compiled into Table 5.6.

Table 5.6: CFD test results

Airflow Velocity (m/s)	Test 1: Scale Model w/o vortex generators (control)				Test 2: Scale Model with vortex generators		
	Drag Force (N)	Lift Force (N)	Coefficient of Drag		Drag Force (N)	Lift Force (N)	Coefficient of Drag
5	0.0235	-0.0108	0.04		0.0209	-0.0058	0.03
10	0.0902	-0.0439	0.15		0.0796	-0.0239	0.13
15	0.1985	-0.0902	0.32		0.1737	-0.0650	0.28
20	0.3552	-0.1724	0.58		0.3095	-0.1136	0.51
25	0.5514	-0.3055	0.90		0.4747	-0.1534	0.78
30	0.7955	-0.3685	1.30		0.6883	-0.2374	1.12
35	1.0752	-0.5270	1.76		0.9169	-0.3320	1.50
40	1.3986	-0.7149	2.28		1.2145	-0.3471	1.98
45	1.7673	-0.8354	2.89		1.5192	-0.5208	2.48
50	2.1856	-0.9614	3.57		1.8492	-0.6962	3.02

Figures 5.25 and 5.26 display how the variables of drag and lift are affected by the increasing airspeed.

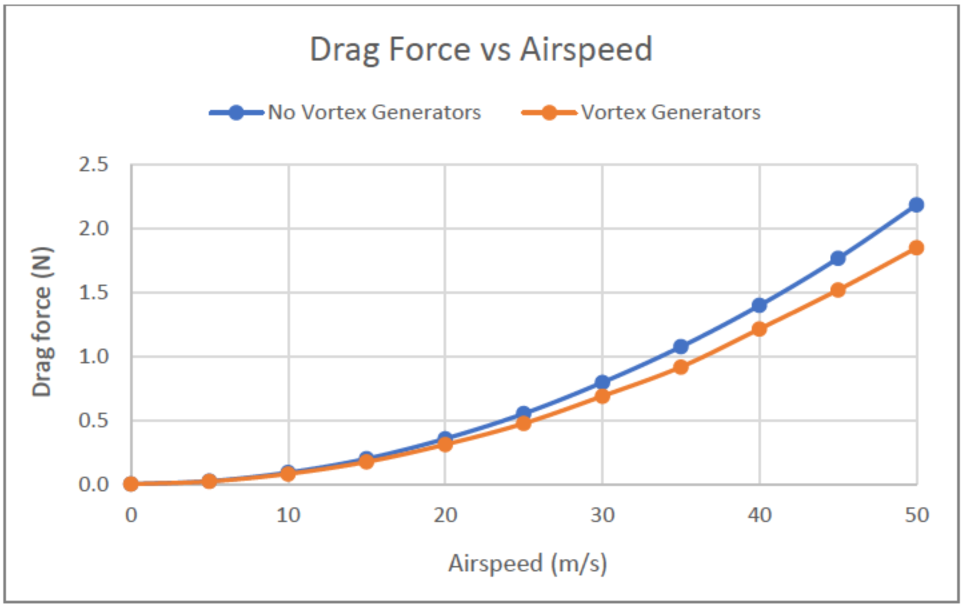

Figure 5.25: Drag force vs Airspeed for both tests

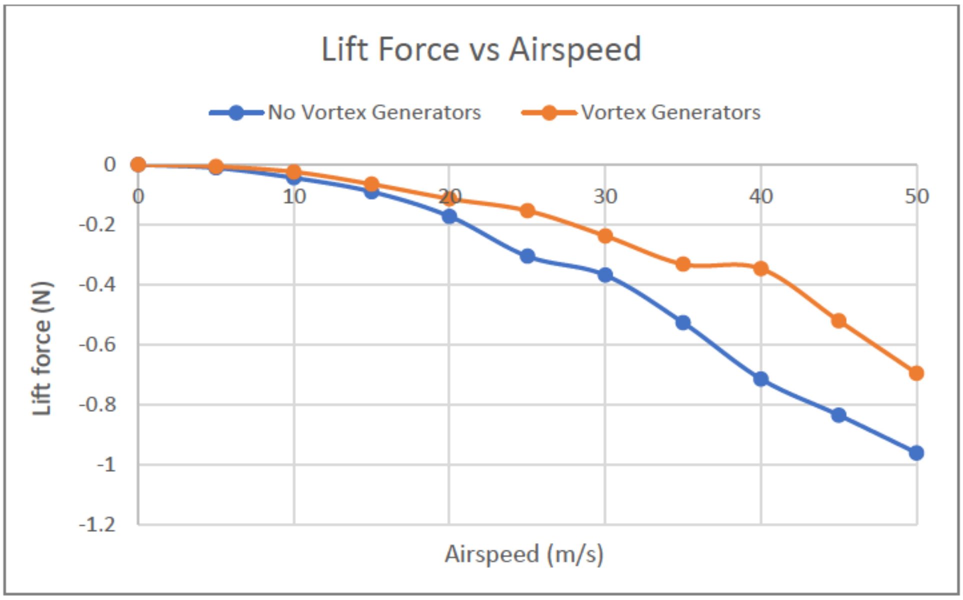

Figure 5.26: Lift Force vs Airspeed for both tests

5.3.7 Analysis

The use of computational analysis allowed for visualisation of the theoretical information researched in the literature review. The singular vortex generator test displayed how the oncoming laminar airflow is pushed around the device and a vortex is formed. This turbulent air downstream pulls the free-stream airflow towards the boundary layer. Visually this is identified where the "orange" airflow of fast velocity is seen to spread downwards soon after the passing the device. These results indicate that the aerodynamic device does impact the downstream airflow and therefore upon further testing may produce results that impact the drag or lift forces acting on the entire vehicle.

Later, CFD tests involved looking at the complete vehicle and analysed the flow over the shape. The vector plots show the change in velocity of the airflow over the vehicle and helped identify areas of faster moving air which correspond to lower pressure at that point. These plots indicate the boundary layer has separated by the base of the rear windscreen as the thickness has increased to nearly one eighth the height of the rear wing. The large updraft from the flow travelling underneath the vehicle adds to the turbulent wake region significantly, inducing a large proportion of the drag. The 0.02 m offset vector plot conclusively shows the impact the wing has on the airflow. As the oncoming air hits this aerodynamic device it is deflected downwards, this decreases the lift force on the rear of the vehicle. It can also be said that there is a drag penalty from the wing as shown in the slow moving vectors behind it.

When vortex generators were installed the vector plots indicate that there is an increase in airspeed at a point directly after the devices (refer to Figure 5.19). This would lead to the understanding they are mixing the airflow. The wake region at the rear of the vehicle looks to be more focused downwards compared to the controls more upward wake. A larger quantity of airflow is seen to be travelling over the rear wing. However this did not correlate with the lift forces obtained from the test data.

Pressure differentials plotted via contours help to determine the regions of high and low pressure around the vehicle. The model tested followed general convention where there is an area of high pressure at the front of the vehicle, known as the stagnation point. It is at this point where the air either flows up over the hood or down under the vehicle. From research it was found that a larger frontal area increases drag; therefore many vehicles are designed to reduce this area. The plot showed that there is a large stagnation point on the STI where the air dam is used to help direct airflow into the engine bay, potentially to lower operating temperatures. There is however a trade-off, and more drag is created. Along the roofline the pressure is relatively constant but at the trailing edge it becomes of higher pressure, indicating the reduction in velocity of the airflow and potentially a situation where the boundary layer is beginning to separate. The wake of the vehicle is clearly seen in the contour plot where there is turbulence in the pressure distribution. This created a recirculation of air behind the vehicle that leads to form drag.

The inclusion of vortex generators does not visually impact the pressure regions over the vehicle. Even though the reported values are different they are not relatively accurate and were mostly neglected as the coloured contours allow for identification of pressure areas. Ideally there would have been a region downstream of the vortex generators that had lower pressure leading to an indication that the airflow was undergoing more mixing than the control test and faster moving air.

Streamlines are used to show how the airflow travels over the vehicle and can identify areas of recirculating air. The recorded screenshots show that the hood scoop impacts airflow significantly. The sharp angle rams the oncoming air into the turbo intercooler but at the same time this performance part also produces a drag penalty. It can be seen in the plot that the air is pushed up off the scoop and this causes boundary layer separation and the airflow to detach from the body. This can also be seen on the contour plot where there is an area of high pressure at the stagnation point of the scoop (at the base) and an area of low pressure at the top of the scoop. The airflow continues downstream where it impacts the rear of the front windscreen, likely causing more drag. From here the airflow stays attached up onto the roof where it experiences a region of low pressure. As the flow reattached before where the vortex generators were positioned it was not required to delete the hood scoop feature in CAD software before the flow analysis.

The addition of vortex generators to the test do not add significant weight to the study. Both before and after screenshots are very similar with a specific amount of air traveling down the rear windscreen, showing possible detachment and then a large volume of air being pushed downwards by the rear spoiler. It should be noted that the screenshot for the control test has some rough streamlines traveling down the side of the vehicle that obstruct the view of purely the roofline to boot airflow. Many revisions were done but the image provided was the most appropriate. For both situations there is a significant volume of air travelling under the rear wing likely indicating its usefulness at producing downforce.

The drag and lift forces recorded at each step between 5 m/s and 50 m/s were plotted to visualise how faster moving air impacted these parameters. The results indicated quite conclusively that the inclusion of vortex generators on this specific design reduced the overall aerodynamic drag that the vehicle created. This was ideal and helped address the deficiencies found by the other experimental tests. It was seen that as airspeed increased so did the difference between both sets of test data in terms of the raw forces. Table 5.7 summarises this difference between each test at a specific airspeed. N.B. positive and negative symbols are used to identify how the vortex generator test faired in comparison. For reference if the vortex generator test produced the same results as the control there would be a 0% difference displayed in the table.

Table 5.7 Comparison of the forces recorded in both tests

Airflow Velocity (m/s)	Difference between control test and vortex generator test (%)	
	Drag Force	Lift Force
5	-11.10	+45.67
10	-11.78	+45.53
15	-12.48	+27.95
20	-12.87	+34.11
25	-13.91	+49.79
30	-13.48	+35.58
35	-14.72	+37.00
40	-13.16	+51.45
45	-14.04	+37.66
50	-15.39	+27.58

From these tests it is clear that drag continues to reduce as airspeed increases whereas the lift force fluctuates more. As these values recorded are minute they may not be accurate enough to use on a technical basis.

Chapter 6: Discussion

6.1 Discussion of results

The full-scale experiments featured testing of only one variant of the four vortex generator purchased. Unfortunately, as stated in the preceding sections the tests did not produce conclusive results. Therefore it was not warranted to perform any further testing with the other designs as this was decided to be unbeneficial and an inefficient use of time. If the control test (without the vortex generators) produced unpredictable motion of the twine pieces then further study could have been undertaken. If this was the case all variants could have been tested and the results may have indicated the effectiveness of the aerodynamic devices and whether there was an optimal design for the test vehicle. If a less streamline vehicle by design, notably a sedan was used as the test vehicle the likelihood of obtaining results that visualised how vortex generators impact airflow would have been increased. Ideally the tests should have been run on an Evo 7, 8 or 9 (as they share the same design architecture) to match the vehicle of investigation in the hypothesis. Unfortunately, due to the rarity and overall cost of the vehicle, obtaining one was out of the question.

If use of an airplane runway was allowed, the greater speeds reached would have likely created boundary layer separation on the highly aerodynamic test vehicle. Various local airstrips were contacted but due to the volume of flights and TRC rules and regulations no street vehicles were allowed on their runway. In essence, as this experiment was intended to help visualise the impact of the downstream airflow past vortex generators and not produce scientific data the inconclusive results do not make or break the investigation. It actually leaves room for someone else to re-test on another vehicle, hopefully one with a larger roof to boot angle that will provide the opportunity to view what these devices can do when used on a vehicle with low aerodynamic efficiency, such as a traditional sedan or notchback design.

Originally it was thought that the small-scale experiments could have been undertaken in water as the higher density of the fluid allows for greater flow visualisation when compared to using a smoke machine. Hydrogen bubbles or coloured dye would have shown the motion of the flow around and over the vehicle, clearly identifying the areas of pressure differences and the rear wake volume. If used it may have been able to show the difference in size of this region after vortex generators were installed, as any reduction in drag would have decreased the wake volume. However, these resources were not available on campus and the next best resource to use was the wind tunnel, which is of more use when retrieving drag and lift forces due to having a load cell that can measure the values that the model exerts in both the x and y directions.

The results obtained in the wind tunnel were indicative of what was expected based on the literature reviewed. Unfortunately this meant the drag force increased for the vortex generator test due to the relative sizing difference between the vehicle (1:24) and the devices (1:12). It was stated in the analysis section that 3D printing and handling limitations due to the small size of the device meant that this was the only possibility. Also any larger scale model would not have been able to fit in the test section of the wind tunnel before being influenced by the boundary layer conditions. The results showed that the lift force was less on the scale vehicle with the vortex generators in use. This slight reduction indicated that the rear wing was producing downforce, lowering the net lift.

It seems quite unreasonable but if there was access to a full sized wind tunnel, the likelihood of the smoke visualisation producing conclusive results would have been increased. The machine itself used in the study was of high quality and produced a large quantity of smoke but the relative lack of size of the model made displaying the airflow over specific areas difficult.

The CFD study did not correlate with the data collected from the wind tunnel as accurately as expected. This may have been due to the shrink-wrapped appearance of the 3D model, which was required to remove a multitude of geometry errors picked up from the 3D scanning process and conversion from a mesh to a solid object. This reduction in external quality made the vehicle overall more streamlined, lowering the drag created by the body. This was reflected in the results where there was a noticeable drop in drag force throughout all airspeeds compared to the wind tunnel tests. However, as both models had the same quality a correlation between CFD results was possible.

It is almost certain that another variant of the vortex generator, if tested, may have produced different results. Not only for the singular device CFD but also for a row positioned on the roofline. Due to testing only one variant this is purely speculation, but the concept is reinforced by the literature reviewed. The CFD tests conclusively showed the impact that the rear wing has on airflow. If additional tests were performed without the wing it could have produced data to show how effective it is at reducing lift. This could have also calculated the drag penalties from the additional form drag. This was the initial idea as the scale model without the wing was 3D scanned and a CAD model was created but due to the ever increasing quantities of geometry errors encountered throughout this study it was put on standby in case there was additional time at the end to include.

The drag and lift forces obtained from the CFD analysis followed the same convention as what was found in the small-scale wind tunnel tests. As the simulation used an enclosure of the same dimensions it was to be expected to return similar results. The drag created by the body increased along with the airspeed, but at an accelerating rate. These results are constant with what was expected. What was not expected however was the lift force to become negative even at low speeds.

It continued its downward trend as the airspeed increased. This is either a computational solving error or an indication that the vehicle is producing considerable downforce even from a slow speed. The notion of a rear wing is to create downforce and the variant on the vehicle tested may have produced real noticeable downforce. It should be noted the design is based on an APR performance wing which has a 3D aerofoil design to increase its effectiveness when compared to more standard designs. The initial R&D of this product includes CFD from the manufacturer, so there is no doubt it works well.

The validity of the results can be determined by the scaled residuals plot. For the tests completed there was a consistency in the convergence, typically around $1 * 10^{-5}$, which occurred well before 500 iterations. Also the mesh was as fine as the educational version of ANSYS allowed. This in return provided a consistency to the recorded data that is more than likely accurate to a level that is warranted in an engineering technical report.

There were additional concepts that were beyond the scope of this project but could have been investigated if time was available. From the ANSYS screenshots taken and literature reviewed a significant amount of the overall aerodynamic drag of a vehicle comes from the underbody flow. A study into positioning vortex generators underneath the vehicle instead of the roof would have been of interest. The majority of vehicles are designed to have a large sweeping design of the rear bumper in order to reduce sharp angles as this induces a larger rear wake and therefore drag force. This design cue may reduce any benefit from using vortex generators but without any investigation the answer is unknown. Also when considering mainstream applications the effect on aesthetic appeal would need to be considered. Not every consumer would appreciate a row of what could be referred to as “shark fin” shaped objects along the trailing edge of the roofline. So implementation under the vehicle would not damage the overall design flow. It should be mentioned that many modern vehicles have done away with the traditional antenna design and are adopting these shark fin looking variants, first seen on BMW’s in the mid to late 2000’s. This could be good news for the vortex generator design as if they closely match the existing antenna then they would not look out of place. It was noticed whilst undertaking this study that even the Domino’s pizza delivery vehicles have a large rooftop advertising sign that is shaped like a shark fin vortex generators. Surely with this and the trend towards the new antenna design it can be concluded that the shape is streamline in such a manner that it does not produce unwarranted form drag.

The end results from the CFD studies were positive, with an indication towards the reduction in drag of the model that used the vortex generators. This however is a small scale undergraduate study that could be expanded upon to provide greater depth of information and conclusive results that can be related back to a full scale vehicle. The worst case scenario of this study would not have provided any data worth analysing or else indicated the opposite of the hypothesis, where drag increased significantly from using vortex generators. If so, then further testing would not be recommended. However, as this was not the case, additional work can follow from this investigation to gain an extensive look into optimising these devices and discovering whether there is a design that is more effective. Once this is completed then the device could be sized accordingly and pitched to the manufacturer for implementation on a vehicle of interest.

It would have been beneficial to have been able to discuss this topic with Mitsubishi themselves. However the Australian Headquarters were of no help with my investigation as they directed me to contact the Japanese offices. This was impossible for myself as the website was in the local Japanese language and in order to send an email through via google translate it still required input of a Japanese home address of which I obviously did not have. The following questions and comments are purely speculation but are considered of importance.

- When Mitsubishi included vortex generators into the design of the Evo 8 MR did they perform testing to back up their claims?
- If so, was there any benefit or were they just a marketing gimmick or “go fast” accessory?
- Assuming the devices did work as reported was the final design the most effective or was it purely chosen to follow design cues or abide by local government regulations, i.e. no sharp edges?

In the end, from my point of view, it would be highly likely that a company with pedigree and racing heritage (who named the vehicle after respect to their racing division; MR stands for Mitsubishi Racing) would have ensured the vortex generators were a performance piece that actually provided a benefit instead of just producing a part for looks. If it was another company without experience in the field of performance cars then it would be questionable.

6.2 Comparison with original plan

The original notion of this research project was to investigate whether or not the aerodynamic devices entitled vortex generators actually produce noticeable benefits when used on a vehicle. The goal was to undertake both experimental and computational testing to provide a broader range than what a desktop study could provide. Overall, the data collected and the results calculated helped to understand the original hypothesis, even though some of the tests produced inconclusive results they were still important to the body of knowledge.

When planning this research project there were additional ideas to be studied that involved looking into the vortex generator design in general. However, testing of only one device was used in the CFD studies. Although this was more than adequate to answer the original hypothesis, additional studies could have provided a detailed look into how the shape of the device influences flow. From this, an optimisation of the design characteristics could have been performed to make the most effective device. However, this topic would have easily snow-balled into a large undertaking and is potentially another whole dissertation. With this in mind and by using efficient management of time it was decided to not continue with this investigation as the current project scale was enough.

Finally, as there was quantitative data retrieved from the CFD testing this is a clear indication that the study was worthwhile. Additionally it was a benefit to see that the inclusion of the vortex generators at the trailing edge of a small-scale vehicle does in fact reduce the drag force when compared to the same vehicle without them. The original aim was achieved throughout this study and by having experimental and computational aspects it provided the greatest chance of succeeding. If the investigation relied on one method only, that is the full-scale or small-scale testing, it would not have provided the conclusive information required to answer the hypothesis.

6.3 Reflection

This investigation proved to be a much larger undertaking that first anticipated. I chose a topic of interest that I did not have substantial prior knowledge of in order to challenge myself and wrap up all that I have learnt throughout my time studying mechanical engineering. This capstone course has compiled many aspects of what was taught throughout this program and allowed the opportunity to work on a self-motivated assignment where it was in your best interest to make the most of university connections to ensure the quality of the work was the highest possible.

Before this research project I have not used ANSYS except for one Professional Practice 1 CPD activity. The benefit of using such a tool was seen during this event and it was decided that my research would include CFD aspects. It was very important to be able to gain quantitative results that indicated one way or the other if vortex generators performed as they were sold by the automotive companies. This was made possible by using ANSYS.

This investigation would have been able to be expanded upon with testing of additional vortex generators via computational analysis if there was not as many errors encountered in ANSYS. The time spent to understand how ANSYS operated and finding error after error that halted my progress was completely unbelievable. Dozens of hours were spent understanding the errors thrown and reworking the 3D models to a state where no geometry errors were encountered. This often meant reducing the quality of the models via third-party software (that I had to learn how to use) which created a situation where they would not be able to correlate as accurately to the real world counterpart due to the variation in surface detail. In addition the sheer amount of time for ANSYS simulations to run including the pre-requisite meshing and Boolean creation was unprecedented and led to a longer time-frame for testing.

6.4 How can these results be used by the industry?

Originally this study was to have a focus on the performance car aspects but during the course of the year it was discovered there may be more opportunities with mainstream cars. Firstly when considering the performance car aspect, a reduction in drag of a vehicle leads to a higher top speed and better handling characteristics if more of the free-stream airflow is directed over the rear wing. This in turn promotes more downforce that increases traction to the wheels under hard cornering situations.

The findings from this report can be used as a stepping-stone for future research projects involving vortex generators. The foundations have been set with the literature reviewed and the experiments performed for this project. Engineers in the automotive industry design vehicles to become more efficient, both in terms of fuel consumption and drag reduction. In the future when electric vehicles are more common on the road than their petrol variant the aerodynamics will still need to be refined to make the most efficient use of power. The drag of a vehicle increases the power required to accelerate to a speed or maintain it and this drains fuel or in the case of an electric vehicle, charge. If vortex generators are adopted by automobile manufacturers the results may help to reduce reliance on fossil fuels in the form of petrol consumption or the production of electricity (if non-renewable based). The impact might be slight at best but with the quantity of vehicles on the road it might combine into a worthwhile effort.

Chapter 7: Conclusion

The effectiveness of a vortex generator when used on a vehicle was the focus for this research project. The literature review and subsequent experimental and computational aspects of this study assisted in in gaining a thorough understanding of the topic. It was found that these aerodynamic devices influence the passing airflow by creating small vortices (that is turbulence) downstream of their positioning which aids in mixing the free-stream airflow with the slow moving boundary layer.

From research it was discovered that the overall effectiveness of a vortex generator relates to the height of the device compared to the boundary layer thickness and this needs to be taken into consideration when in the designing stage. If the device is too small it won’t produce any benefits and if it is too large any benefits will be outweighed by the form drag the body itself creates. This indicated that there is not one size that suits all applications and there needs to be additional R&D based upon the vehicle of investigation.

The full-scale tests were originally intended to visualise the boundary layer separation from the body. Unfortunately as the test vehicle had high aerodynamic efficiency, and a small roof to boot angle, the control test indicated that the boundary layer was still attached to the surface. This made viewing any benefits of the vortex generators difficult as their intended job of delaying the boundary layer separation was not required. Additional tests on a vehicle with a larger roof to boot angle is recommended.

Further experiments involving small-scale vehicle in a wind tunnel was undertaken to gain drag and lift force data over a range of airspeeds from 5 m/s to 30 m/s. The results indicated that when vortex generators were installed the drag force rose and lift force decreased. Upon further analysis this relative increase in drag was due to the differing scales of the vehicle and vortex generators. Due to limitations a matching scale was not practicable.

Quantifiable data was retrieved from the CFD testing. The correct scale of 1:24 for the vehicle and vortex generators was achieved and airspeeds up to 50 m/s were tested. From the first measurement at slow velocity the results indicated a reduction in drag force on the vehicle with the vortex generators installed and this trend continued up to the maximum velocity tested where the reduction reached 15%.

The vector, contour and streamline plots added to the study in terms of raw data but were not conclusive in the findings displayed. The overall accuracy of the tests was justified by the scaled residuals convergence, meaning the setup was adequate including the mesh size. Due to the testing being undertaken on a scaled vehicle the results can only be an indication of what could potentially be found on the full-sized counterpart and not conclusive in the findings.

It would be ideal to have further testing undertaken at an undergraduate or postgraduate level that investigated vortex generator designs. This could identify whether there is an optimum shape of the device that produces the best mixing of airflow downstream of the device. Additional studies would help identify for a specific application how sizing the device correctly provides the greatest benefit of the device. There is definite potential for this study to become a technical journal publication or even mainstream adoption if all the right boxes were ticked and conclusive results showing significant benefits were obtained.

Chapter 8: List of References

Aero Performance Engineering, 2010, *Wind Tunnel Testing*, internet article, viewed 19th March, http://www.aero-performance-engineering.co.uk/wind-tunnel-testing

Aerolab, 2016, *Smoke Generator*, internet article, viewed 23rd August 2019, https://www.aerolab.com/products/smoke-generator/

ANSYS, n.d. *Fluent*, internet article, viewed 26th July 2019

APR Performance, 2014, *Racing Applications – GTC-300 Adjustable Wing*, internet article, viewed 5th May 2019,

http://aprperformance.com/racing-product/gtc-300-adjustable-wings/

Bakkar, A, 2011, *Applied Computational Fluid Dynamics – Lecture 11: Boundary Layers and Separation*, university lecture, viewed 10th August 2019,

http://www.bakker.org/dartmouth06/engs150/11-bl.pdf

Barbut, D, Negrus, E, 2011, *CFD Analysis for Road Vehicles - Case study*, National Institute for Aerospace Research Bulletin, Vol 3, Issue 3, pp. 15-22, viewed 15th June 2019,

https://www.researchgate.net/publication/265893323_CFD_analysis_for_road_vehicles_-_Case_study

Barlow, J, Rae, W, Pope, A, 1999, *Low-Speed Wind Tunnel Testing*, New York, USA, John Wiley & Sons, Inc, viewed 21st March

Bar-Meir, G, 2013, *Basics of Fluid Mechanics*, Open Textbook Library, viewed 16th March 2019 https://open.umn.edu/opentextbooks/textbooks/basics-of-fluid-mechanics

Cengel, Y, Ghajar, A, 2015, *Heat and Mass Transfer – Fundamentals & Applications*, McGraw-Hill Education, New York viewed 3rd April 2019.

CT Auto Parts, 2018, *Mitsubishi Performance Parts*, internet article, viewed 8th March 2019, https://www.ctautoparts.com.au/lancer-evo-7-8-9-abs-carbon-vortex-generator-roof-fin-spoiler.html

Drela, M, 2006, Course Code 16.01, *Unified Engineering – Fluid Mechanics – study guide,* Massachusetts Institute of Technology (MIT), Cambridge, pp. 1-4, viewed 16th March 2019,

https://ocw.mit.edu/courses/aeronautics-and-astronautics/16-01-unified-engineering-i-ii-iii-iv-fall-2005-spring-2006/fluid-mechanics/f11_sp.pdf

Dumas, L, 2008, *CFD-based Optimisation for Automotive Aerodynamics*, Optimization and Computational Fluid Dynamics. Springer, Berlin, Heidelberg, pp. 191-215, viewed 3rd April 2019,

https://link.springer.com/chapter/10.1007/978-3-540-72153-6_7

Encyclopædia Britannica, 1998, *Aerodynamics*, Encyclopædia Britannica, Inc, internet article, viewed 6th March 2019,

https://www.britannica.com/science/aerodynamics

Evans, M, 2012, PHYS207, *Fluid Mechanics* - study guide, University of New England (UNE), Armidale.

Flight Literacy, 2015, *Aerodynamics of Flight - Wingtip Vortices*, internet article, viewed 11th April 2019,

https://www.flightliteracy.com/wingtip-vortices/

Gamiz, U, 2013, *Fluid Dynamic Characterization of Vortex Generators and Two-dimensional Turbulent Wake*s, Polytechnic University of Catalonia - School of Industrial Engineering of Barcelona, pp. 1-88, viewed 4th May 2019,

https://www.tesisenred.net/bitstream/handle/10803/134597/TUFG1de1.pdf?sequence=1&isAllowed=y

Gopal, P, Senthilkumar, T, 2012, *Aerodynamic drag reduction in passenger vehicle using vortex generator with varying yaw angles*, Journal of Engineering and Applied Sciences, vol. 7, no. 9, pp. 1180-1186,

http://www.arpnjournals.com/jeas/research_papers/rp_2012/jeas_0912_777.pdf

Grand Canyon University, n.d, *Ethical Concerns*, Center for Innovation in Research and Teaching, internet article, viewed 31st March 2019,

https://cirt.gcu.edu/research/developmentresources/tutorials/ethics

Gurney Flap, 2018, internet article, Formula One Technical Dictionary, viewed 23rd July 2019,

http://www.formula1-dictionary.net/gurney_flap.html

Janssen, WD, Blocken, B & van Wijhe, HJ 2017, CFD simulations of wind loads on a container ship: Validation and impact of geometrical simplifications, vol. 166, pp. 106-116, viewed 13th June 2019,

https://www.researchgate.net/publication/316593520_CFD_simulations_of_wind_loads_on_a_container_ship_Validation_and_impact_of_geometrical_simplifications

Jonuskaite, A, 2017, *Flow Simulation with SolidWorks*, Arcadia University of Applied Sciences, Research Paper, pp.1-47, viewed 19th March 2019,

https://www.theseus.fi/bitstream/handle/10024/133447/Jonuskaite_Akvile.pdf?sequence=1&isAllowed=y

Katz, J 2006, *Aerodynamics of Race* Cars, Annual Review of Fluid Mechanics, vol. 38, no. 1, pp. 27-63, viewed 4th May 2019,

https://www.annualreviews.org/doi/pdf/10.1146/annurev.fluid.38.050304.092016

Klingelhoefer, S, 2011, *Super Street feature - 1997 Acura Integra Type-R*, internet article, viewed 3rd April 2019,

http://www.superstreetonline.com/features/sstp-1111-1997-acura-integra-type-r

Korff, A, 2018, *What Every Design Engineer Needs to Know about Computational Fluid Dynamics*, PTC CREO, internet article, viewed 27th July 2019,

https://www.ptc.com/en/cad-software-blog/what-every-design-engineer-should-know-about-cfd

Lewington, N, 2016, *Aerodynamics Fundamentals for Automotive*, Society of Automotive Engineers - Australasia Aerodynamics Seminar, pp. 1-85, Ford Motor Company, viewed 4th April 2019

http://www.saea.com.au/resources/Documents/aero101-SAE-A-Seminar.pdf

Lin, J 2002, *Review of research on low-profile vortex generators to control boundary-layer separation,* Progress in Aerospace Sciences, vol. 38, no. 4, pp. 389-420, viewed 28th July 2018,

https://www.sciencedirect.com/science/article/pii/S0376042102000106

Lina, L, Reed, W, 1950, *A Preliminary Flight Investigation of the Effects of Vortex Generators on Separation Due to Shock,* National Advisory Committee for Aeronautics (NACA), Research Paper, pp. 1-30, viewed 9th March 2019,

https://ntrs.nasa.gov/archive/nasa/casi.ntrs.nasa.gov/19930086465.pdf

McLaren Formula One Racing Team, n.d. *Gurney Flap*, internet article, F1 Glossary, viewed 23rd July 2019,

https://www.mclaren.com/racing/f1-playbook/gurney-flap/

Marchesin, FP, Barbosa, RS, Gadola, M & Chindamo, D 2018, *High downforce race car vertical dynamics: aerodynamic index,* Vehicle System Dynamics, vol. 56, no. 8, pp. 1269-88.

https://www.tandfonline.com/doi/pdf/10.1080/00423114.2017.1413196?needAccess=true

Massachusetts Institute of Technology (MIT), 2002, *Fluid Mechanics Module – Introduction to Flow Visualisation*, internet article, viewed 22nd March 2019,

http://web.mit.edu/fluids-modules/www/exper_techniques/1.Flow_Visualization.Intro.pdf

Mitsubishi Motors, 2004, *Mitsubishi Motors Launches Lancer Evolution VIII MR Hi-Performance 4WD Sports Sedan*, press release, internet article, viewed 8th March 2019,

https://www.mitsubishi-motors.com/en/corporate/pressrelease/products/detail992.html

Motor Trend, 2004, *Subaru Impreza WRX STI and Mitsubishi Evolution 8 Comparison*, internet article, viewed 10th March 2019,

https://www.motortrend.com/cars/mitsubishi/lancer-evolution/2005/rally-sedan-comparison/

National Aeronautics and Space Administration (NASA), 2015, *Aerodynamics, What is Drag?,* internet article, viewed 16th March 2019,

https://www.grc.nasa.gov/www/k-12/airplane/drag1.html

Panaras, AG 2012, *Vortices in Aerodynamics*, in Aerodynamic Principles of Flight Vehicles, American Institute of Aeronautics and Astronautics, pp. 29-128, viewed 9th March 2019,

https://arc.aiaa.org/doi/abs/10.2514/4.869174

Password: JDM 2014, *JDM DC 94-01 Integra - Dry Carbon Fiber Gurney Flap*, internet product listing, viewed 23rd July 2019,

http://www.passwordjdm.com/PasswordJDM-Dry-Carbon-Fiber-Gurney-Flap-94-01-Integra-Type-R-2DR-P10562.aspx

Perzon, S, 2001, *On Blockage Effects in Wind Tunnels – A CFD Study*, SAE Technical Paper, Volvo Car Corporation, viewed 15th June 2019,

https://saemobilus.sae.org/content/2001-01-0705

Pope, A, 1961, *Wind-Tunnel Testing*, New York, USA, John Wiley & Sons Inc, pp. 1-500, viewed 21st March 2019

Raykowski, K, 1999, *Optimization of a Vortex Generator Configuration for a 1/4-Scale Piper Cherokee Wing*, university dissertation, Embry-Riddle Aeronautical University, viewed 10th August 2019, https://pdfs.semanticscholar.org/6d13/9ee16cd25d0945016a074be10d56c95b8e44.pdf

Safe Work Australia, 2018, *Identify, assess and control hazards*, internet article, viewed 9th March 2019,

https://www.safeworkaustralia.gov.au/risk

Schlichting, H, Gersten, K, 2017, *Boundary-Layer Theory*, Springer-Verlag, Berlin, pp.1-707, viewed 2nd April,

https://link.springer.com/content/pdf/10.1007/978-3-662-52919-5.pdf

Solmaz, S, 2018, *Aerodynamics of Road Vehicles in the Computational Domain: A Summary*, SimScale Blog, viewed 19th March,

https://www.simscale.com/blog/2018/02/aerodynamics-road-vehicles/

TecQuipment, 2018, *AF1300 Subsonic Wind Tunnel*, internet article, viewed 10th March 2019,

https://www.tecquipment.com/subsonic-wind-tunnel-300mm-only

Udris, A, 2018, *This Is How Winglets Work*, internet article, viewed 11th April 2019,

https://www.boldmethod.com/learn-to-fly/aerodynamics/how-winglets-work-and-how-wingtip-vortices-form/

United States Department of Energy, 2018, *Official US Government Fuel Economy Information*, internet article, viewed 1st April 2019,

https://www.fueleconomy.gov/feg/Find.do?action=sbs&id=5632&id=40609

United States Department of Transportation (DOT), 2012, *Helicopter Flying Handbook – Chapter 2: Aerodynamics of Flight*, Federal Aviation Administration, pp. 1-27, viewed 3rd April 2019,

https://www.faa.gov/regulations_policies/handbooks_manuals/aviation/helicopter_flying_handbook/

Wang, J, Li, Y & Choi, K 2008, *Gurney flap—Lift enhancement, mechanisms and applications*, Progress in Aerospace Sciences, vol. 44, no. 1, pp. 22-47, viewed 23rd July 2019, https://www.sciencedirect.com/science/article/pii/S0376042107000784

Willemsen, E 1997, *High Reynolds number wind tunnel experiments on trains*, Journal of Wind Engineering and Industrial Aerodynamics, vol. 69-71, pp. 437-47, viewed 13th June 2019, https://www.sciencedirect.com/science/article/pii/S016761059700175X

Yadav, A, Rawal, P & Mishra, R, 2018, *Modelling and simulation of aerodynamic performance of Vortex generators for hatch back type cars*, Journal of Vibroengineering, pp. 131-135, viewed 21st May 2019, https://www.jvejournals.com/article/20399

Zikanov, O, 2010, *'Essential Computational Fluid Dynamics'*, New Jersey, USA, John Wiley & Sons Inc, pp. 1-320, viewed 31st March 2019.

Chapter 9: Appendices

9.1 Appendix A – Project specification

For:	Luke Greenbank
Title:	Determining the effectiveness of vortex generators with regards to automotive applications.
Major:	Mechanical
Supervisor:	Ahmad Sharifian-Barforoush
Confidentiality:	N/A
Enrolment:	ENG4111 – ONC S1, 2019
	ENG4112 – ONC S2, 2019
Project Aim:	To investigate the effectiveness of vortex generators, how they alter air flow characteristics, ascertain the most efficient design that impacts performance and obtain quantifiable data to indicate a reduction in drag or lift coefficients.
Programme:	**Version 1, 20th March 2019**

1. Research background information relating to fluid flow, subsonic aerodynamics, vortices, boundary layer separation and control.
2. Review literature that relates to the use of vortex generators on vehicles.
3. Specify experiments of the study, including wind tunnel, CFD and real-world.
4. Design and manufacture various scale vortex generators based on already available examples, OEM specifications or my own ideas.
5. Perform preliminary testing to ascertain whether these components change air flow characteristics.
6. Perform tests in wind tunnel and on my own vehicle. Use CFD to obtain quantifiable data.
7. Determine the most appropriate design of a vortex generator, taking into consideration various aspects in order to maximise airflow performance.
8. Use the information researched and tests performed to analyse the data and provide an answer to the hypothesis. This quantifiable data should indicate whether there is a reduction in drag or the coefficient of lift.

If time and resources permit:

9. Design and manufacture a full-sized vortex generator that is the most effective at its given task of reducing the boundary layer separation.
10. Make recommendations as to whether these vortex generators could be included in new designs of vehicles.
11. Indicate where this research can be taken and expanded upon in future studies.

9.2 Appendix B – Risk assessment

This research project has phases for design, manufacture and testing; each with their own hazards. A risk is defined as the potential of losing something of value. In the context of this research project this refers to the possibility of personal injury. Whilst undertaking this research I need to ensure any risks associated with the design, manufacture and experimentation of the vortex generators will be mitigated.

Safe Work Australia states effective management of risks improves worker health and safety as well as productivity. There are five steps in the risk assessment process:

- Step 1: Identify hazards (work environment, equipment, materials, substances),
- Step 2: Analyse consequences (potential injury, property damage),
- Step 3: Assess risk (probability, severity of injury or loss),
- Step 4: Determine action and implement controls (redesign, removal, new methods, audit),
- Step 5: Review control measures (Safe Work Australia 2018).

As with any university activity, safety is of great concern, especially when the use a laboratory is required. This section outlines the potential risks of the experimental testing phase and how I can lessen potential hazards. Using the USQ Safety Risk Assessment template, effective management of these risks could be obtained. Figure B.1 shows the risk assessment matrix that determines the risk of a hazard when correlating the probability of it occurring with the consequences if it does. This forms the basis of what control measures are required for each hazard in order to mitigate against any damages from occurring.

Eg 1. Enter Consequence

Eg 2. Enter Probability

Eg 3. Find Action

	Consequence				
Probability	**Insignificant** No Injury 0-$5K	**Minor** First Aid $5K-$50K	**Moderate** Med Treatment $50K-$100K	**Major** Serious Injuries $100K-$250K	**Catastrophic** Death More than $250K
Almost Certain 1 in 2	M	H	E	E	E
Likely 1 in 100	M	H	H	E	E
Possible 1 in 1000	L	M	H	H	H
Unlikely 1 in 10 000	L	L	M	M	M
Rare 1 in 1 000 000	L	L	L	L	L
Recommended Action Guide					
E=Extreme Risk – Task ***MUST NOT*** proceed					
H=High Risk – Special Procedures Required (See USQSafe)					
M=Moderate Risk – Risk Management Plan/Work Method Statement Required					
L=Low Risk – Use Routine Procedures					

Figure B.1: Risk Matrix (USQ 2018)

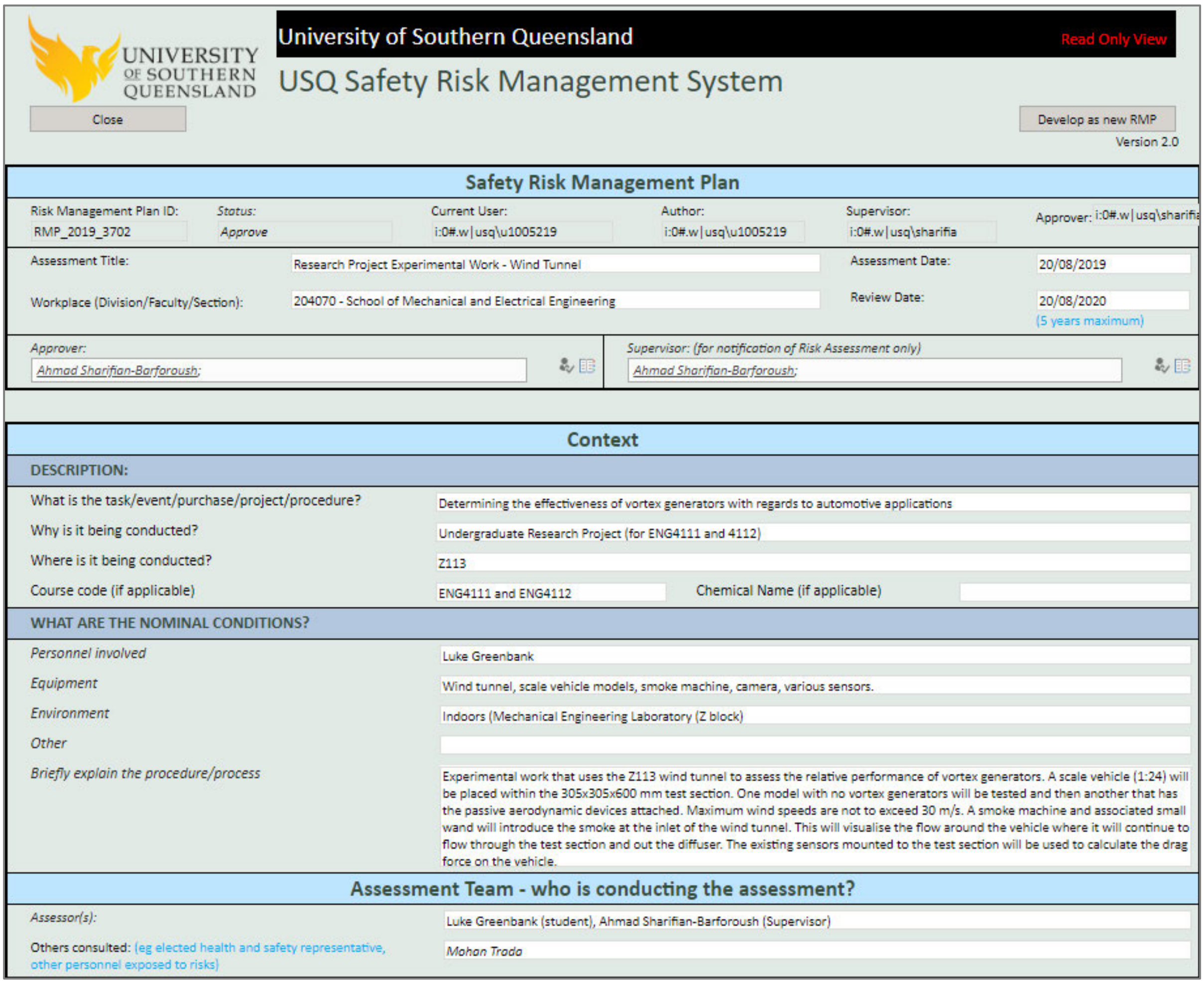

UNIVERSITY OF SOUTHERN QUEENSLAND

University of Southern Queensland — Read Only View

USQ Safety Risk Management System

Close | Develop as new RMP | Version 2.0

Safety Risk Management Plan

Risk Management Plan ID:	Status:	Current User:	Author:	Supervisor:	Approver:
RMP_2019_3702	Approve	i:0#.w|usq\u1005219	i:0#.w|usq\u1005219	i:0#.w|usq\sharifia	i:0#.w|usq\sharifia

Assessment Title:	Research Project Experimental Work - Wind Tunnel	Assessment Date:	20/08/2019
Workplace (Division/Faculty/Section):	204070 - School of Mechanical and Electrical Engineering	Review Date:	20/08/2020 (5 years maximum)

Approver: Ahmad Sharifian-Barforoush;

Supervisor: (for notification of Risk Assessment only) Ahmad Sharifian-Barforoush;

Context

DESCRIPTION:

What is the task/event/purchase/project/procedure?	Determining the effectiveness of vortex generators with regards to automotive applications
Why is it being conducted?	Undergraduate Research Project (for ENG4111 and 4112)
Where is it being conducted?	Z113
Course code (if applicable)	ENG4111 and ENG4112 — Chemical Name (if applicable)

WHAT ARE THE NOMINAL CONDITIONS?

Personnel involved	Luke Greenbank
Equipment	Wind tunnel, scale vehicle models, smoke machine, camera, various sensors.
Environment	Indoors (Mechanical Engineering Laboratory (Z block)
Other	
Briefly explain the procedure/process	Experimental work that uses the Z113 wind tunnel to assess the relative performance of vortex generators. A scale vehicle (1:24) will be placed within the 305x305x600 mm test section. One model with no vortex generators will be tested and then another that has the passive aerodynamic devices attached. Maximum wind speeds are not to exceed 30 m/s. A smoke machine and associated small wand will introduce the smoke at the inlet of the wind tunnel. This will visualise the flow around the vehicle where it will continue to flow through the test section and out the diffuser. The existing sensors mounted to the test section will be used to calculate the drag force on the vehicle.

Assessment Team - who is conducting the assessment?

Assessor(s):	Luke Greenbank (student), Ahmad Sharifian-Barforoush (Supervisor)
Others consulted: (eg elected health and safety representative, other personnel exposed to risks)	*Mohan Trada*

Figure B.2: USQ Risk Assessment Cover Sheet (USQ 2018)

Figure B.1 visualises the consequence vs probability matrix that is used for risk determination and classification. Due to the nature of the research project there are several hazards that can take place in each of the stages; design, manufacture and experimentation. The risk level and adequate safety controls are listed below along with existing safety controls and proposed solutions.

Table B.3: Risk assessment for experimental

Hazard	Risks associated with hazard	Risk level (consequence, probability)	Existing safety controls	Risk Assessment	
				Probability	Risk Level
Access to Z113 lab for other users	Physical injuries	Minor	Ensure all people in close vicinity are notified about the operation of the wind tunnel. Signs may need to be erected to indicate the relative hazards such as high noise and airflow.	Unlikely	Low
Use of the laboratory	Physical injuries	Minor	Wear appropriate clothing such as long pants and closed in shoes, at all times.	Rare	Low
Trips, slips and falls. Hazards from hoses or equipment	Range of injuries	Minor	Safety procedures that involve ensuring all equipment used is within a designated area, Have a clear walkway around the equipment. Any warning signs required must be displayed.	Rare	Low
Placing the scale vehicle in the wind tunnel	Trips, slips and falls	Insignificant	Ensure scale model dimensions will fit within the machine prior to installing in wind tunnel.	Rare	Low
Wind tunnel operation	Hearing damage	Minor	Wear appropriate hearing protection (PPE). Limit exposure where possible and have breaks between each test run. Shut workshop door to prevent area access during operation. Make sure enclosed footwear and safety glasses are wear throughout tests	Unlikely	Low
Wind tunnel operation	Electric Shock	Moderate	Ensure three-phase cables are correctly in-place before switching machine on	Rare	Low
Airflow from wind tunnel outlet	Impact from flying debris, eye or skin injuries	Minor	Have an exclusion area surrounding the outlet and do not walk within it during testing.	Unlikely	Low
Use of the smoke machine	Fire or oil spill. smoke inhalation, slip hazard, skin irritation, burns from wand tip	Minor	Use of a respirator if necessary. Ensure fire blanket or extinguisher is available close by. Follow start-up and shut down procedure shown in manual. Avoid touching the end of the wand or placing it on a combustible material.	Unlikely	Low

All of the identified risks were as low as reasonably possible (ALARP). Therefore no dedicated action plan for controls that are not already in place was required.

9.3 Appendix C – Resource analysis

The Safety Data Sheet (SDS) for the smoke machine oil (Propylene Glycol) purchased from Chem-Supply Pty Ltd can be found at the following link:

https://www.chemsupply.com.au/documents/PL0101CHBY.pdf

Last revision was April 2018.

9.4 Appendix D – Project timeline

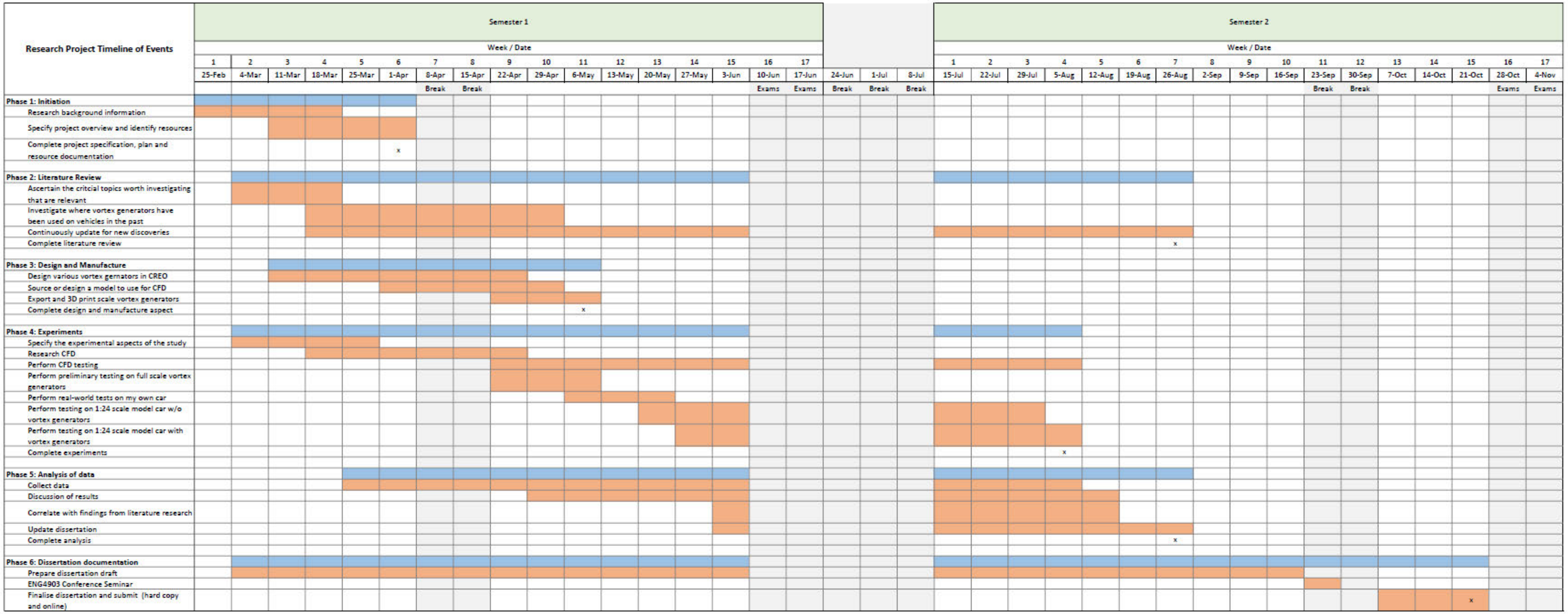

Figure D.1: Research Project Timeline

9.5 Appendix E – Full-scale tests

The full-scale tests were taken as an opportunity to gain a first-hand understanding of how boundary layer separation occurs and whether or not the inclusion of vortex generators would decrease the amount of turbulent air flowing over the rear section of a car. Figures E.1 and E.2 are additional photos not included in the main report but help to explain what the testing involved.

Figure E.1: Control test setup

Figure E.2: Secondary test showing the relative angle of the vortex generators (25°)

Please note the green painter's tape was used to protect the vehicle's paint from the double-sided tape.

Figure E.3: Side profile photo showing the flow field

9.6 Appendix F – Preliminary setup for the wind tunnel experiment

Figure F.1 displays the AutoCAD drawing drafted up and provided to the USQ Workshop for fabrication of the rod that positioned the model in the wind tunnel. This included the drilling location on the model that was close to the centre of gravity and principal axis to reduce any rotation.

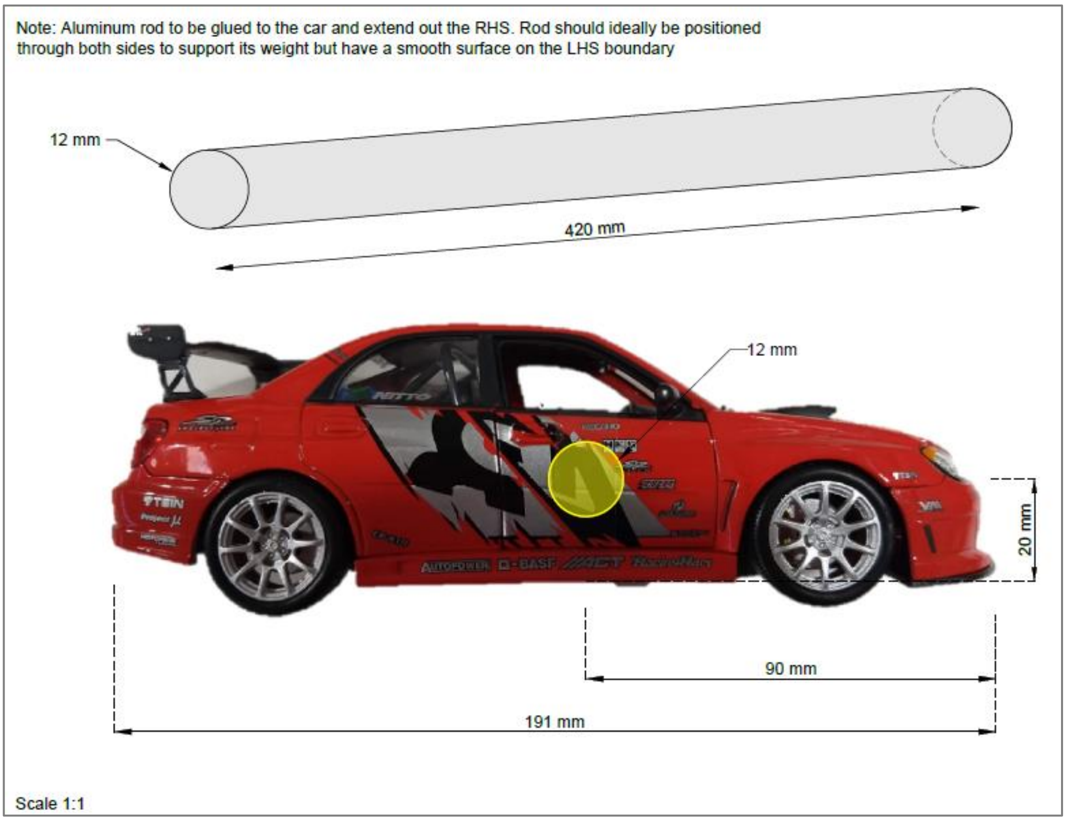

Figure F.1: Drawing for the workshop procedure

The workshop completed the task in a short time frame, allowing for testing to be undertaken when given the opportunity. Figure F.2 shows the final design that was used in the wind tunnel. This task was completed on two scale models to allow for ease of testing as there was a limited timeframe to perform these tests. One model had the vortex generators installed and the other did not as it was the control.

Figure F.2: Final piece ready for the wind tunnel arrangement

9.7 Appendix G – 3D scanning

Additional photos of the revisions made to the scale model to increase the 3D scanning accuracy are included in this section.

Figure G.1: First revision to 3D scanning setup

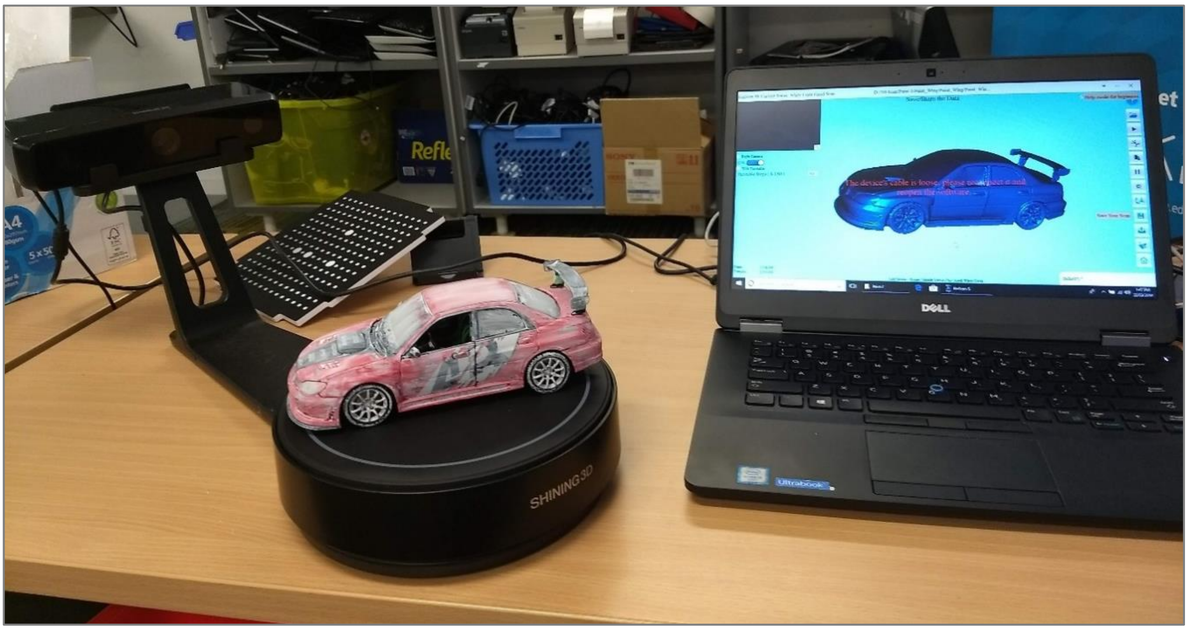

Figure G.2: Second revision to 3D scanning setup,
N.B. white acrylic paint

9.8 Appendix H – CAD models

Additional screenshots of the CAD models created from 3D scans are included in this section. Note the undercarriage is well designed with a flat section at the front to limit turbulent engine bay air travelling under the car. There is also an upswept section at the rear to help direct airflow.

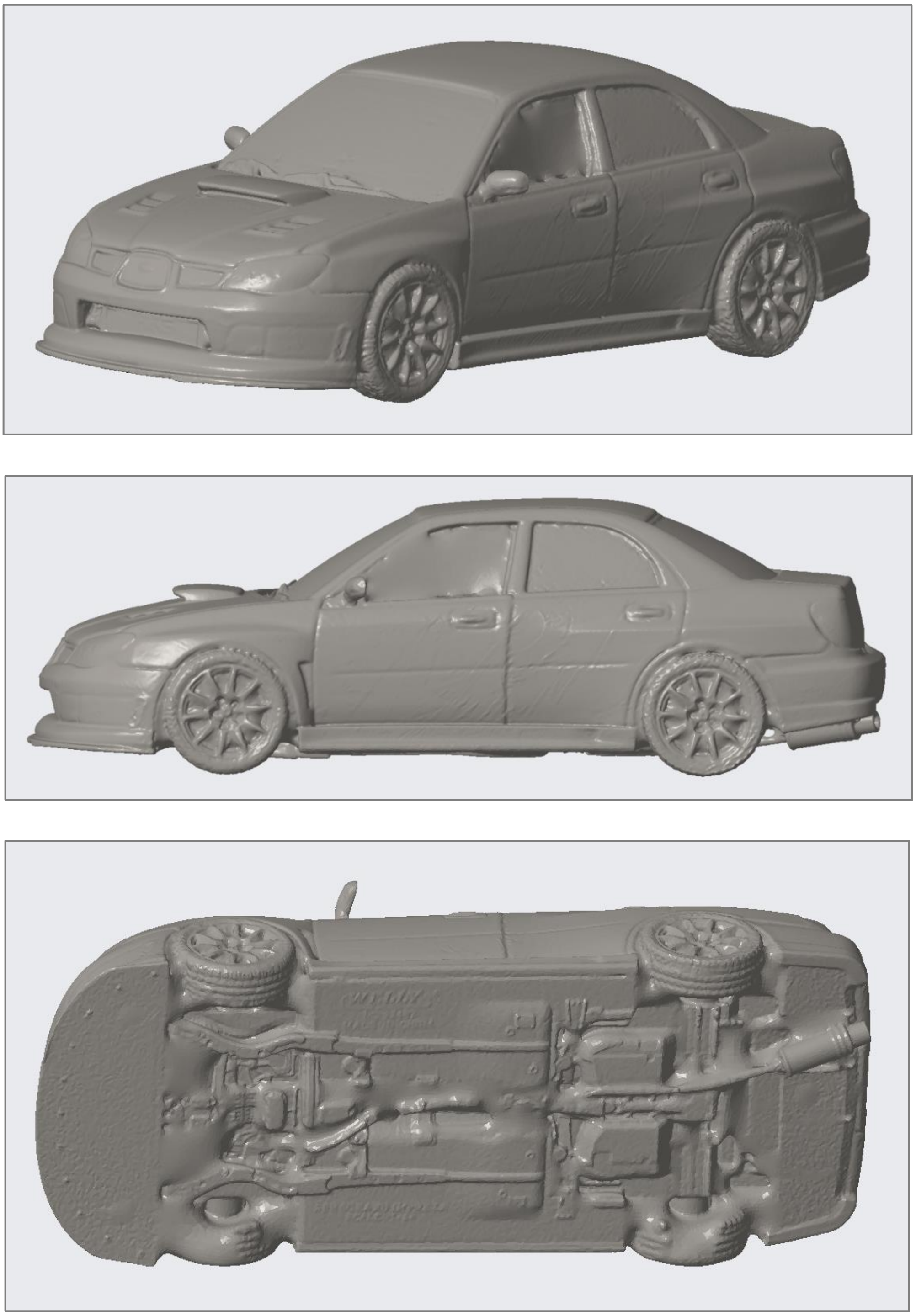

Figure H.1: 3D model without wing, angled view (top), side view (middle) and undercarriage view (bottom)

9.9 Appendix I – ANSYS mesh setup

The automatic setting was selected for the overall design as the in-built algorithm would select the most adequate meshing method. In this case the physics preference was setup for CFD analysis and solved via Fluent. There were several other changes made to the setup, including:

- The use of adaptive sizing,
- Increasing the resolution from a default baseline of 2 to 5 (any more than this returned errors as the education version had a resolution limit).

These alterations were to help add extra refinement to the mesh. In general the vehicle needed to have a finer mesh due to the detail in the object and would need a greater level of analysis.

Details of "Mesh"	
Display	
Display Style	Use Geometry Setting
Defaults	
Physics Preference	CFD
Solver Preference	Fluent
Element Order	Linear
Element Size	Default
Export Format	Standard
Export Preview Surface Mesh	No
Sizing	
Use Adaptive Sizing	Yes
Resolution	5
Mesh Defeaturing	Yes
Defeature Size	Default
Transition	Slow
Span Angle Center	Fine
Initial Size Seed	Assembly
Bounding Box Diagonal	1.7022 m
Average Surface Area	5.6079e-004 m^2
Minimum Edge Length	1.3209e-005 m
Quality	
Check Mesh Quality	Yes, Errors
Target Skewness	Default (0.900000)
Smoothing	Medium
Mesh Metric	None

Inflation	
Use Automatic Inflation	None
Inflation Option	Smooth Transition
Transition Ratio	0.272
Maximum Layers	5
Growth Rate	1.2
Inflation Algorithm	Pre
View Advanced Options	No
Assembly Meshing	
Method	None
Advanced	
Number of CPUs for Parallel Part Meshing	Program Controlled
Straight Sided Elements	
Rigid Body Behavior	Dimensionally Reduced
Triangle Surface Mesher	Program Controlled
Topology Checking	Yes
Pinch Tolerance	Please Define
Generate Pinch on Refresh	No
Statistics	
Nodes	75065
Elements	421765

Figure I.1: ANSYS Mesh details

Figure I.2 displays the mesh used for the wind tunnel, whereas Figure I.3 the mesh size of the vehicle. Note the smaller mesh used on this surface due to the higher detail of the object.

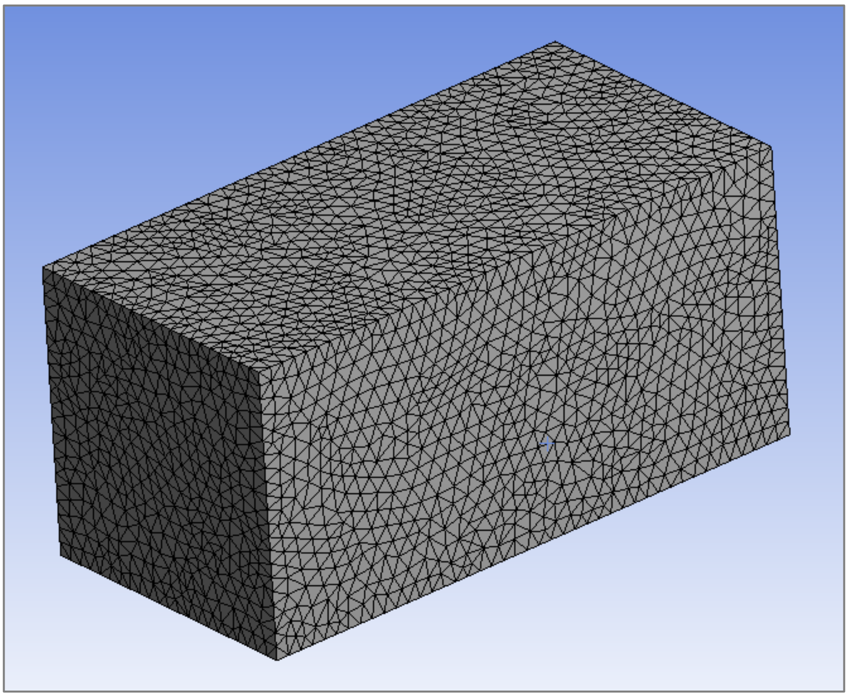

Figure I.2: Mesh used for the CFD wind tunnel enclosure

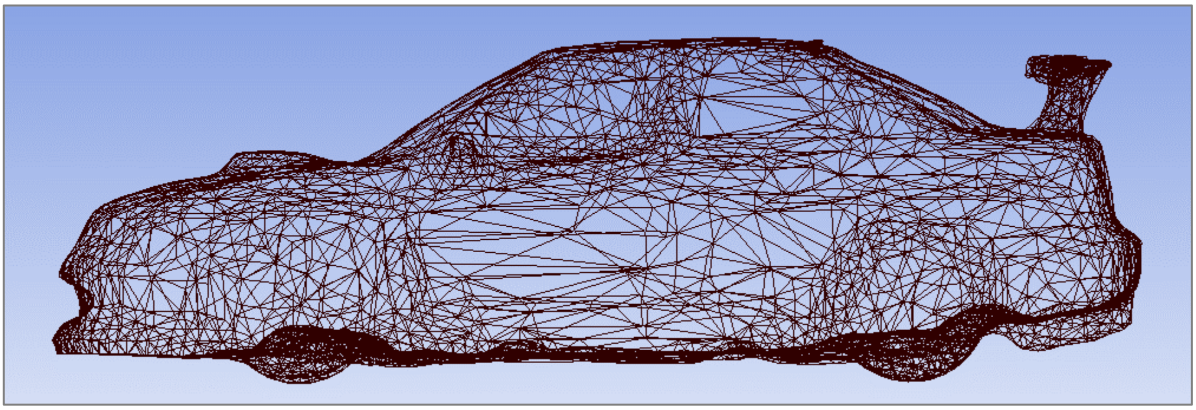

Figure I.3: Mesh used for the CFD vehicle.